

University of Louisville

## ThinkIR: The University of Louisville's Institutional Repository

---

Electronic Theses and Dissertations

---

5-2012

### Development of pituitary tumor-transforming gene (PTTG) transgenic mice for the treatment of ovarian cancer.

Miranda Y. Fong 1982-  
*University of Louisville*

Follow this and additional works at: <https://ir.library.louisville.edu/etd>

---

#### Recommended Citation

Fong, Miranda Y. 1982-, "Development of pituitary tumor-transforming gene (PTTG) transgenic mice for the treatment of ovarian cancer." (2012). *Electronic Theses and Dissertations*. Paper 448.  
<https://doi.org/10.18297/etd/448>

This Doctoral Dissertation is brought to you for free and open access by ThinkIR: The University of Louisville's Institutional Repository. It has been accepted for inclusion in Electronic Theses and Dissertations by an authorized administrator of ThinkIR: The University of Louisville's Institutional Repository. This title appears here courtesy of the author, who has retained all other copyrights. For more information, please contact [thinkir@louisville.edu](mailto:thinkir@louisville.edu).

DEVELOPMENT OF PITUITARY TUMOR-TRANSFORMING GENE (PTTG)  
TRANSGENIC MICE FOR THE TREATMENT OF OVARIAN CANCER

By

Miranda Y. Fong  
B.S., University of Nevada, Reno, 2004  
M.S., University of Louisville, 2009

A Dissertation  
Submitted to the Graduate Faculty of the  
School of Medicine of the University of Louisville  
in Partial Fulfillment of the Requirements  
for the Degree of

Doctor of Philosophy

Department of Physiology and Biophysics  
University of Louisville  
Louisville, Kentucky

May 2012

DEVELOPMENT OF PITUITARY TUMOR-TRANSFORMING GENE (PTTG)  
TRANSGENIC MICE FOR THE TREATMENT OF OVARIAN CANCER

By

Miranda Y. Fong  
B.S, University of Nevada, Reno, 2004  
M.S., University of Louisville, 2009

A Dissertation Approved on

March 22, 2012

by the following Dissertation Committee:

---

Sham Kakar, Dissertation Director

---

Jason Chesney

---

Stanley D'Souza

---

Madhavi Rane

---

Gary Anderson

## ACKNOWLEDGMENTS

I would like to thank my mentor, Sham Kakar, PhD, for his guidance and patience for the past four years. I would also like to thank my committee members for their valuable input: Jason Chesney, MD, PhD; Gary Anderson, PhD; Madhavi Rane, PhD; and Stanley D'Souza, PhD. I would also like to thank my family for their enduring support across the country, in particular my mother, Melissa Lamoureux, and father, George Fong, for their weekly phone calls and unwavering patience; my sister, Peng, who listened to all my problems; and my brothers, Bob and Bill, for their continued encouragement. This dissertation is dedicated to my loyal and kind dog, Rikki, who was my constant companion during the PhD program.

ABSTRACT  
TGPTTG FOR OVARIAN CANCER TREATMENT

Miranda Y. Fong

May 11, 2012

This dissertation is a hypothesis-driven research oriented study to determine the role of the pituitary-tumor transforming gene (PTTG) in ovarian cancer, specifically if it is involved in neoplastic transformation leading to tumorigenesis through oncogene activation and the involvement of tumor-suppressor gene, p53. Furthermore, generation of a useful ovarian cancer mouse model provides a platform technology to screen for ovarian cancer diagnosis and treatment options.

This dissertation is divided into four chapters covering the etiology of ovarian cancer and a novel treatment strategy for ovarian cancer. The first chapter reviews the related literature encompassing the etiology of ovarian cancer, mouse models of ovarian cancer, the biological function of PTTG, the role of PTTG in cancer and diabetes, and mouse models using PTTG as a transgene. The second chapter studies the role of PTTG in tumorigenesis *in vivo* through the generation of a PTTG transgenic (TgPTTG) mouse model observed at various ages, ranging from 4 to 10 months. The third chapter is a preliminary study investigating the signaling mechanisms affected by chemotherapy agent doxorubicin in combination with withaferin A *in vitro* and *in vivo* for the treatment of ovarian cancer. The fourth chapter is a discussion of the utility of ovarian cancer mouse models and the consequences of the lack of a working model.

## TABLE OF CONTENTS

	PAGE
ACKNOWLEDGMENTS.....	iii
ABSTRACT.....	iv
LIST OF TABLES.....	viii
LIST OF FIGURES.....	ix
INTRODUCTION.....	1
CHAPTER 1: Review of Relevant Literature.....	2
CHAPTER 2: PTTG Transgenic Mice as a Model for Ovarian Cancer.....	21-41
METHODS AND MATERIALS.....	21-23
Construction of CMV-PTTG-EGFP transgene.....	21
Animal housing.....	21
Generation of transgenic animals.....	22
p53 <sup>+/-</sup> mice.....	22
Genotyping and screening of transgenic and p53 <sup>+/-</sup> mice.....	23
RNA isolation and analysis of transgene expression via RT-PCR.....	23
Histological analysis and immunohistochemistry.....	23
RESULTS.....	23-35
Generation of CMV-PTTG-EGFP transgenic mice.....	23
PTTG expression in CMV-PTTG-EGFP mice.....	25
Histology of CMV-PTTG-EGFP transgenic animal tissues.....	26
Crossbreeding of TgPTTG with p53 <sup>+/-</sup> mice.....	30
DISCUSSION.....	36

CHAPTER 3: Withaferin A Enhances the Effect of Doxorubicin through Autophagy in Ovarian Cancer Cells.....	42-69
MATERIALS AND METHODS.....	45-48
Materials.....	45
Cell treatments.....	45
Cell proliferation assay.....	45
Flow cytometry.....	45
ROS assay.....	46
TUNEL assay.....	46
Western blots.....	46
Tumor Formation in Nude Mice.....	47
Immunohistochemistry.....	47
3D <i>in vitro</i> tumor growth.....	47
MTT assay for 3D tumors.....	48
Microscopy of 3D tumors.....	48
RESULTS.....	48-62
WFA enhances the killing effect of doxorubicin of ovarian cancer cells.....	48
Dox enhances WFA-induced inactivation of Akt pathway.....	51
ROS-induced cell death.....	54
Dox and WFA induce cell death by autophagy.....	59
Effect of Dox + WFA on xenograft tumorigenesis.....	61
Effect of Dox + WFA on 3-D tumors <i>in vitro</i> .....	63
DISCUSSION.....	63
CHAPTER 4: Conclusions.....	70
REFERENCES.....	73
APPENDIX.....	87

CURRICULUM VITAE.....92



## LIST OF TABLES

TABLE	PAGE
1. Summary of promoter and targeted gene in epithelial ovarian cancer.....	87
2. Breeding summary of TgPTTG founders.....	87
3. Group assignments for TgPTTG mice with summary of results.....	88
4. Group assignments for p53 <sup>mut</sup> mice with summary of results.....	88
5. Group assignments for TgPTTG <sup>f</sup> p53 <sup>mut</sup> mice with summary of results.....	88
6. Oncogenes involved in the pathogenesis of ovarian cancer.....	89
7. Tumor suppressor genes dysregulated in ovarian cancer.....	90

## LIST OF FIGURES

FIGURE	PAGE
1. Comprehensive diagram of the etiology theories of ovarian cancer.....	4
2. Hierarchical model of tumorigenesis.....	5
3. CMV-PTTG-EGFP transgene structure.....	24
4. Genotype of 34 F <sub>0</sub> mice by PCR.....	24
5. Genotype of F <sub>1</sub> mice from TgPTTG founders.....	25
6. RT-PCR of TgPTTG tissue for RNA expression.....	26
7. Immunofluorescence of PTTG-EGFP protein expression in 4 months TgPTTG mice.....	27
8. Immunofluorescence of PTTG-EGFP protein expression in 8 months TgPTTG mice.....	29
9. Histology of pre-cancer condition in 8 months TgPTTG female.....	30
10. Immunohistochemistry of 8 months TgPTTG tissues pre-cancer.....	31
11. Immunohistochemistry of 8 months TgPTTG tissues with cancer.....	32
12. Immunofluorescence of PTTG-EGFP protein expression in 10 months TgPTTG mice.....	33
13. Immunohistochemistry of 10 months TgPTTG tissues .....	34
14. Transgene copy number analysis of TgPTTG mice.....	35
15. Identification of TgPTTG/p53 <sup>mut</sup> offspring.....	36
16. Immunofluorescence of PTTG-EGFP protein expression in TgPTTG/p53 <sup>mut</sup> .....	37
17. Immunohistochemistry of TgPTTG/p53 <sup>mut</sup> tissues .....	38
18. Timeline of tumor development in p53 <sup>mut</sup> and TgPTTG/p53 <sup>mut</sup> mice.....	41
19. 24 hr cell proliferation of Dox + WFA treated cells.....	50
20. 48 hr cell proliferation of Dox + WFA treated cells.....	51

21. 72 hr cell proliferation of Dox + WFA treated cells.....	52
22. Annexin V flow cytometry of UV treated cells.....	52
23. Annexin V flow cytometry of Dox + WFA treated cells.....	53
24. Western blot analysis of signaling mechanism.....	54
25. ROS production after 6 hr of treatment.....	55
26. ROS production after 24 hr of treatment.....	56
27. Blockage of treatment-induced ROS using NAC for 24 hr.....	57
28. Blockage of treatment-induced ROS using NAC for 48 hr.....	57
29. ROS identification using SOD for 48 hr.....	58
30. TUNEL assay of A2780 cells.....	58
31. Electron microscopy of A2780 cells.....	60
32. Western blot analysis of autophagy marker LC3B and cell death marker caspase 3.....	61
33. Xenograft A2780 tumor growth in nu/nu mice.....	62
34. Immunohistochemistry of xenograft A2780 tumors.....	64
35. 3D <i>in vitro</i> tumor growth.....	65

## INTRODUCTION

The ovary is surrounded by a single cell epithelial layer derived from the coelomic mesothelium during development. The coelomic mesothelium has the potential to undergo neoplastic transformation to a malignant phenotype and differentiate towards many different cells types found in the Mullerian tract, including the ovarian stroma, fallopian tube, uterus, and cervix [2].

The most common form of ovarian cancer is epithelial ovarian cancer (EOC) accounting for approximately 90% of cases. Other tumor types include germ cell tumors (5%) [3] and sex cord-stromal cell tumors (< 5%) [4]. EOC is further sub-divided into distinct histotypes: serous (70%), mucinous (5-10%), clear cell (5-10%), and endometrioid (20%) [5]. Furthermore, serous carcinomas can be divided into high-grade and low-grade lesions, with the former being the most common [6].

Ovarian cancer is the most lethal malignancy of the female genital tract, being the 5<sup>th</sup> cause of cancer death in women and 8<sup>th</sup> most common cancer. If ovarian cancer is diagnosed at Stage I, the five year survival rate is 93.5% but drops to 27.6% at Stage IV where a majority of cases are diagnosed [7], mainly due to a lack of symptoms and unreliable detection methods. Current detection methods include transvaginal ultrasound and serum CA-125 levels. However, with transvaginal ultrasound, ovarian cancer can be mistaken for functional cysts in premenopausal women, while CA-125 has a high false positive rate [5]. Over the past four decades, the incidence of ovarian cancer has slightly decreased but the mortality remains relatively unchanged [7]. This is in part due to a lack of understanding of the etiology of ovarian cancer and the heterogeneity found across patient tumors, which has made it difficult to produce a reliable animal model that represents human EOC.

## CHAPTER 1

### A REVIEW OF THE RELATED LITERATURE

#### **Etiology of Ovarian Cancer**

Ovarian cancer can be subdivided into three groups based on tissue of origin. Most cases are believed to originate from the ovarian surface epithelium (OSE), while stromal cell tumors and germ cell tumors are relatively rare [8]. However, recently some debate has arisen that serous ovarian cancer originates in the fallopian tube and migrates to the ovary [9] as tubal ligation provides a measure of protection against ovarian cancer [10]. Despite some progress to define the mechanism of the etiology of ovarian cancer, the link between normal to neoplastic transformation has not been clearly established, in part due to a lack of a representative model. Despite this most animal studies focus on oncogenic activation or tumor repressor gene silencing to find the switch from normal healthy cells to transformed tumorigenic cells. Several theories have been suggested: the Gonadotropin Theory, chronic inflammation, and cancer stem cells (CSCs) all of which will be discussed in detail (Fig. 1). Another theory states that the OSE can invaginate and form inclusion cysts, which can undergo neoplastic transformation either through stromally-derived growth factors or cytokines that would normally be restricted to the tunica albuginea [11]. It has also been suggested that incessant ovulation damages the OSE and the requisite repairs can lead to genetic mutations, as a reduction in ovulation reduces the risk for developing ovarian cancer from conditions such as oral contraception, pregnancy, and lactation [2] which ties into inflammation pathways.

#### *The Gonadotropin Theory*

Coined by Chinmoy K. Bose [12], the Gonadotropin Theory suggest that constant excessive exposure to gonadotropins, particularly follicle stimulating hormone (FSH), over-

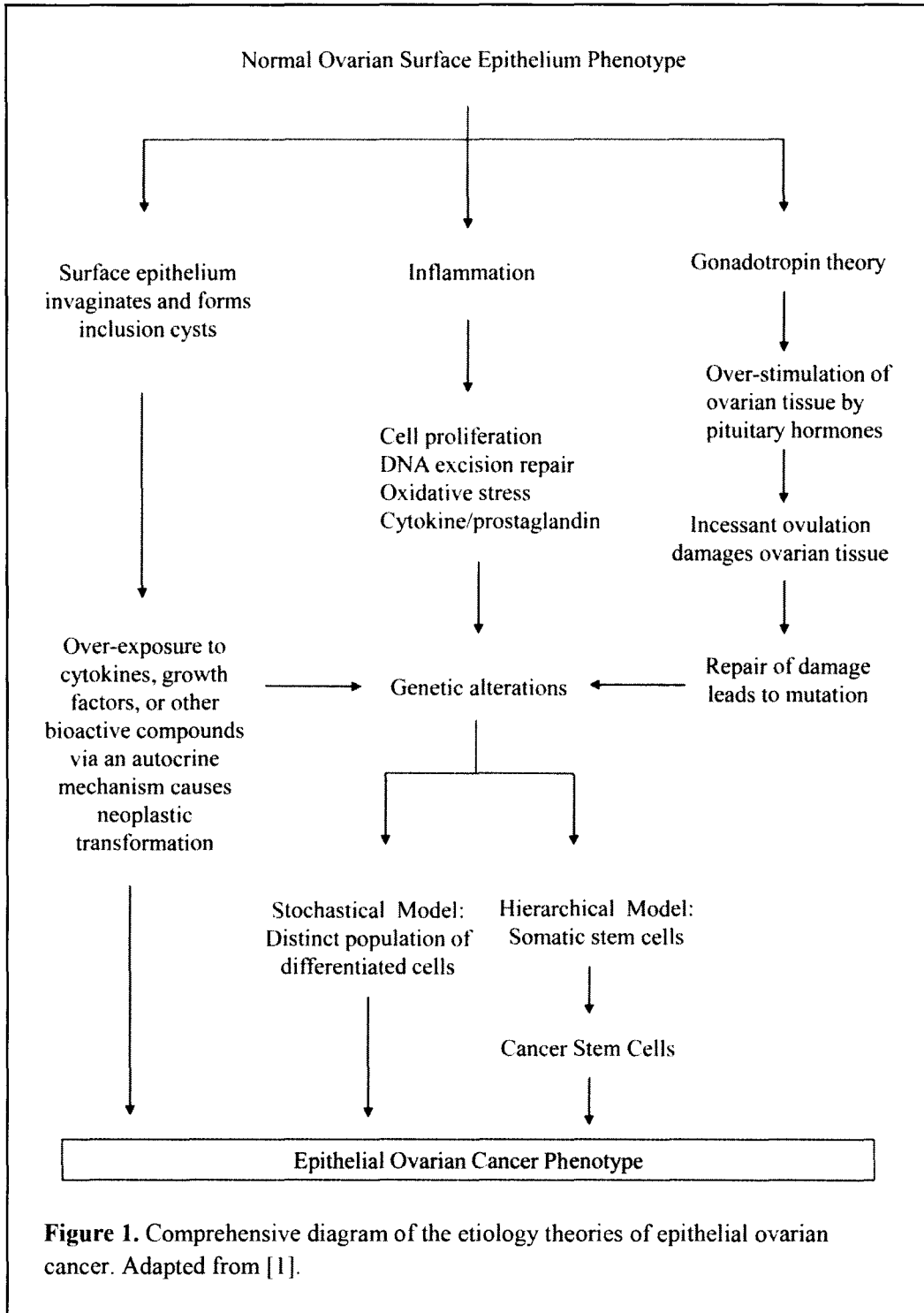
stimulate the ovary to cause excessive ovulation resulting in tissue damage. Experiments related to this theory have provided conflicting results. One study found that FSH reduced the ability of the surface epithelial cells to proliferate [13] while another study showed that FSH increased cell proliferation in a cell culture derived from an omental metastasis of epithelial ovarian cancer (EOC) [14]. To clarify this issue, serum LH and FSH levels were measured in the serum and cystic fluid of patients with ovarian epithelial neoplasms [15]. There was a significant difference between malignant neoplasms and borderline or benign neoplasms. While FSH receptors (FSHR) are found in 80% of EOC [16, 17], no experiments have been performed to show that FSH can promote anchorage-independent colony formation to demonstrate cellular transformation *in vitro*.

#### *Inflammation in cancer*

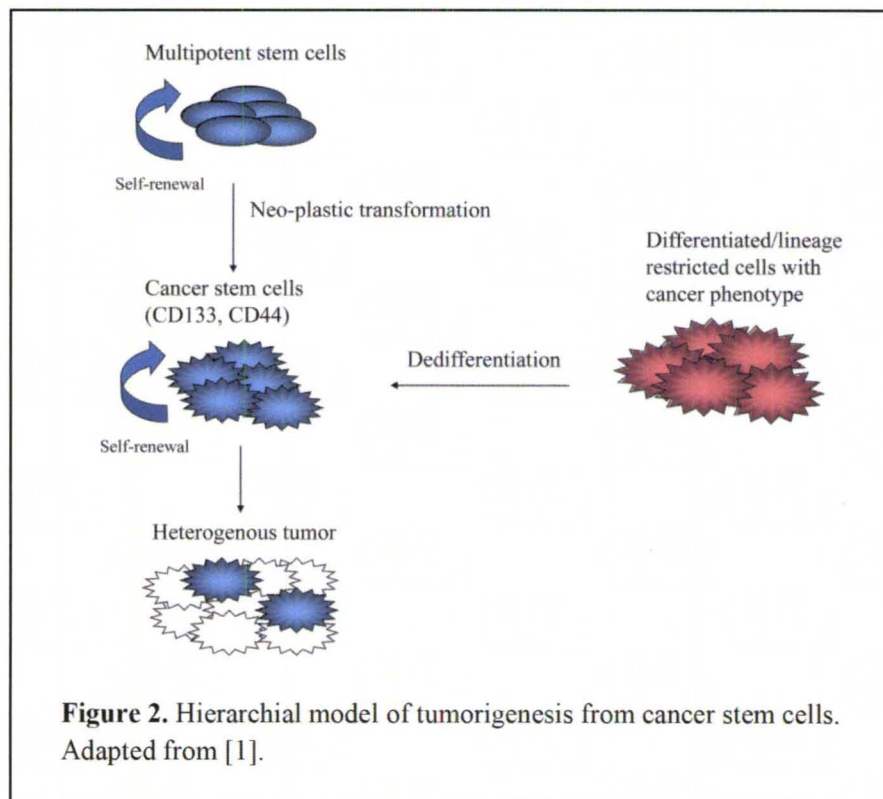
While bacterial and viral agents have been linked to gastric, liver, and cervical cancer [18, 19], several types of inflammation can promote tumor development, although the mechanism varies depending on the source of inflammation (reviewed in [20]). With chronic inflammation, reactive oxygen species (ROS) are produced, which alters the extracellular matrix by altering the MMP:TIMP ratio and promote metastasis [18]. In addition, inflammation is known to promote cell proliferation, DNA excision and repair, oxidative stress, and a high concentration of cytokines and prostaglandins [21]. Pelvic inflammatory disease has also been linked with EOC development [18]. With tumor-associated inflammation, the tumor microenvironment provides a niche for immune cells such as tumor-associated macrophages (TAMs), neutrophils, mast cells, myeloid-derived suppressor cells, and natural killer T cells which have autocrine and paracrine functions to promote tumor growth through the production of cytokines and chemokines [20]. TAMs are the frequently found immune cell in the tumor microenvironment and may be necessary for angiogenesis, invasion, and metastasis [22].

#### *Cancer stem cells (CSCs)*

Cancer stem cells (CSCs) are described as “multipotent cells capable of forming heterogeneous tumors in immunodeficient mice at high efficiency” [23]. Five characteristics are



used to identify CSCs: 1) self-renewal, 2) restriction to a small percentage of the tumor population, 3) ability to reproduce the heterogenous tumor phenotype, 4) multipotent differentiation into non-tumorigenic cells, and 5) expression of distinctive cells markers [24-28]. As such, CSCs have also been referred to as cancer-initiating cells [28] or tumor-initiating cells [24]. The origin of CSCs are thought to come from somatic stem cells that have undergone mutations transforming them into a cancer phenotype [29], and while evidence has suggested the presence of ovarian somatic stem cells, their source differs [30, 31]. Others have suggested that CSCs are formed from differentiated cells with a cancer phenotype that dedifferentiate into CSCs [32], a phenomenon that has been seen in cell culture with the epithelio-mesenchymal transition (EMT) [30], which lends credence to this theory (Fig. 2). CSCs were first identified in acute myeloid leukemia [33] and have since been identified in many types of solid tumors including ovarian, breast, prostate, liver, brain, lung, melanoma, colon, and pancreas [26, 28, 34-43].





In an effort to identify CSCs, two markers have been proposed: CD133 and CD44. CD133<sup>+/+</sup> have been found in the EOC cell lines OVCAR-8, while CD133<sup>+/-</sup> has been found in the EOC cell lines A2780, PEO1, OVCA432, OVCAR-2, and OV90 [44]. A single CD133<sup>-</sup> cell from A2780 or PEO1 was only able to produce cells of the same phenotype. In contrast, a single CD133<sup>+</sup> cell from the same cell lines was able to undergo asymmetric division and produce CD133<sup>+</sup> and CD133<sup>-</sup> cells. Since a characteristic of CSCs is to form xenograft tumors, CD133<sup>+</sup> and CD133<sup>-</sup> cells isolated from A2780 were injected into nude mice. CD133<sup>+</sup> cells formed larger, more aggressive tumors with a shorter latency. Immunohistochemistry of the ectopic tumors showed that the tumors derived from CD133<sup>+</sup> cells contained both positive and negative staining, showing not only self-renewal but capability to produce a heterogeneous phenotype. Tumors derived from CD133<sup>-</sup> cells showed none to extremely low staining for CD133. CD133<sup>+</sup> cells have been isolated from primary ovarian carcinomas [45] and represented less than 1% of the total population, a defining characteristic of CSCs. The CD133<sup>+</sup> cells showed anchorage independent growth by forming colonies in soft agar as indicative of tumorigenic properties and also had a higher proliferation rate than CD133<sup>-</sup> cells. Upon comparing the percentage of CD133<sup>+</sup> in 8 normal ovaries, 5 benign ovarian tumors, 16 primary ovarian carcinomas, and 25 omental metastases, ovarian carcinomas have a significantly higher percentage than all the other groups [45].

The other marker CD44<sup>+</sup> has been identified in human EOC [28, 29, 36, 37, 46]. CSCs derived from primary stage III serous adenocarcinomas showed anchorage-independent growth, which clustered into spheres and expressed Oct-4, nestin, Nanog, SCF, Notch-1, and Bmi-1, suggesting an undifferentiated phenotype, which were able to differentiate into an epithelial morphology [28]. When the spheroids were injected into nude mice, they were able to reconstitute the tumor, as hence were designated as CSCs. CD44<sup>+</sup>/CD117<sup>+</sup> cells were highly tumorigenic and formed heterogeneous tumors reconstituting the original tumor phenotype compared to CD44<sup>-</sup>/CD117<sup>-</sup>. As few as 100 CD44<sup>+</sup>/CD117<sup>+</sup> cells resulted in tumor formation

with a shorter latency. CD44<sup>+</sup> cells isolated from malignant ovarian ascites samples obtained from patients with stage III/IV ovarian cancer formed spheroids and maintained this phenotype over 20 passages, suggesting that they have the ability to self-renew [47]. Furthermore, CD44<sup>+</sup> cells were injected into nude mice to determine their tumorigenicity. Purified CD44<sup>+</sup> cells formed tumors that were 10% CD44<sup>+</sup> and 90% CD44<sup>-</sup>, which was representative of the original tumor phenotype. A differential global gene expression profile of CD44<sup>+</sup> cells and CD44<sup>-</sup> cells showed that there was difference in genes belonging to families associated with control of cell death and apoptosis, signal transduction, transcription regulation, and control of cell differentiation. In a different study, 19 of 65 clones isolated from the ascite sample of a malignant grade IV serous adenocarcinoma were immortalized and showed variations in morphology and growth rates [36]. Of the 19, 10 representative clones were selected and showed an up-regulation CD44, c-met, epidermal growth factor receptor (EGFR), E-cadherin (9 of 10), Snail (2 of 10), and Slug. E-cadherin, Snail, and Slug are known mediators of the EMT [48]. Two selected clones underwent transformation, evinced by an increased proliferation rate and ability to form organized spheroids. These clones also showed the stem cell markers Nestin, Oct4, and Nanog, which was reduced upon tumor formation in nude mice [36]. Mice given intraperitoneal injections of EOC cell line SKOV3 formed tumors with a higher proliferation rate through the interaction of hyaluronan and CD44 to recruit Nanog into the complex, which functionally coupled to Stat-3 to induce transcription of cell proliferation proteins [46].

#### *Genetic contribution to ovarian cancer*

Only about 9% of EOC cases are hereditarily linked to *BRCA1* or *BRCA2* mutations [2]. Part of what makes the etiology of ovarian cancer hard to elucidate is the heterogeneity that exists between tumor types. For example, ovarian cancer can be sub-classified as serous, mucinous, endometrioid, and clear cell carcinomas depending on histology. Furthermore, the malignancies can be classified as high-grade or low-grade, each with its own molecular signals. High-grade tumors grow rapidly without a definite precursor lesion and are relative sensitive to

chemotherapy. p53 mutations as well as Akt and Her2 overexpression are more common in high-grade malignancies found in 50-90%, 12-30%, and 20-66% respectively, but are rarely found in low-grade malignancies [2]. In contrast, low-grade tumors grow more slowly, are relatively insensitive to chemotherapy, and share molecular characteristic with low-malignant neoplasms [2]. K-Ras, B-Raf, and PTEN mutations are more commonly found in low-grade neoplasms found in 30-50% for both K-Ras and B-Raf and 20% for PTEN [2]. Due to stage of the tissue at collection, it is imperative to differentiate between pathways that initiate and/or contribute to tumorigenesis from those that trigger metastasis.

### **Mouse Models of Ovarian Cancer**

Animal models have allowed us to study gene contribution to tumorigenesis through overexpression of potential oncogenes or conditional deletion of tumor suppressor genes. There have been many different techniques to develop an ovarian tumor model that adequately represents human ovarian cancer with variable success.

#### *Syngeneic mouse models*

Syngeneic models combine *in vitro* and *in vivo* methods to generate a tumor model. This technique was first used in rats by Godwin *et al.* [49] and Testa *et al.* [50] on the spontaneous transformation of surface epithelial cells isolated from rats, a technique which has been used by numerous investigators for subsequent studies [51-56]. As such, mouse OSE (MOSE) cells are isolated from the ovaries of virgin wildtype mice and cultured *in vitro* before transplantation into recipient mice [57]. Perhaps one of the most revealing MOSE studies was conducted by Roberts *et al.* [51], who compared the alterations of the actin cytoskeleton as well as expression of cellular adhesion proteins versus the number of passages to study the progression of ovarian carcinogenesis, showing that MOSE cells spontaneously transform with repeated passages. Late passage cells injected intraperitoneally into immunocompetent C57BL6 mice formed tumors in numerous organs, showing the transformation from premalignant to highly malignant phenotype with downregulation of E-cadherin and connexin-43. In another example, Greenaway *et al.* [52]

injected a spontaneously tumorigenic MOSE cell line named ID8 into the ovarian bursal cavity of C57Bl6 mice. The ID8 cells formed direct contact with the ovarian stroma, resulting in primary tumor formation, secondary peritoneal carcinomatosis, and extensive ascites fluid production between 80 to 90 days post-exposure. The cytological and architectural features resembled serous carcinoma. Interaction between ID8 cells and the ovarian stroma resulted in increased expression of proliferative and survival markers, including phosphorylated Akt (p-Akt), proliferating cell nuclear antigen (PCNA), and Bcl-2. Vascular endothelial growth factor (VEGF) levels were also increased in the serum and ascitic fluid. In conjunction, the pro-apoptotic factor Bax was decreased. The study supports the theory that the OSE can undergo invaginations and form inclusion cysts capable of undergoing neoplastic transformation [11].

ID8 cells have further been used to test the protective effects of a transgene. Transgenic mice overexpressing apolipoprotein A-I (apoA-I) were intraperitoneally (i.p.) injected with ID8 cells and showed an enhanced survival compared to wildtype animals as the median time of death in wildtype animals was 86 days vs. 106 days in apoA-I mice. ApoA-I mice also showed decreased tumor burden whether injected i.p. or subcutaneously [58]

#### *Genetically induced mouse models*

One of the first reports to test genetic changes was made by Orsulic *et al.* [59], who used an avian retroviral delivery system. Transgenic mice were established to express the TVA virus receptor making them susceptible to infection to a subgroup of replication-competent avian leukosis viral-derived vectors (RCAS), thus allowing for the introduction of oncogenes that would integrate newly reverse-transcribed DNA into the host genome and allow long-term expression. The TVA receptor was placed under control of the keratin 5 promoter to direct expression to the ovarian epithelium or alternatively under control of the  $\beta$ -actin promoter to direct expression to all cells of the ovary. TVA-transgenic mice were crossbred with p53<sup>-/-</sup> mice to generate TVA/p53<sup>-/-</sup>, which were used to study the oncogenes *c-Myc*, *K-Ras*, and *Akt* individually and in combination. However, the keratin 5 promoter is constitutively active in the basal layer of

stratified and simple epithelia in several organs [60], therefore, it was necessary to isolate the expression of the virally delivered oncogenes. The ovaries were removed from the TVA/p53<sup>-/-</sup> mice, cultured, and infected *in vitro* before introduction into recipient mice either by subcutaneous or i.p. injection or by transplantation under the ovarian bursa. Once infected, the mammalian cells would not produce detectable levels of infectious viral particles, which limited spreading to the surrounding tissue. Introduction of any two oncogenes in keratin 5-TVA/p53<sup>-/-</sup> ovarian cells was sufficient to drive tumorigenesis. However, p53<sup>-/-</sup> mice develop tumors, usually lymphomas and sarcomas, at approximately 3 months of age, making cross-breeding cumbersome as they only produce 1 litter.

Using a novel approach, Connolly *et al.* [61] targeted simian virus 40 T antigen (SV40 TAg) to the epithelial ovarian surface by using the Müllerian Inhibitory Substance Type II Receptor (MISIIR) promoter for the production of transgenic animals. While 18 of 36 (50%) transgenic mice developed bilateral ovarian tumors resembling serous carcinomas by 6 to 13 weeks of age, the aggressiveness of the formation of the tumors inhibited reproduction, making it extremely difficult to establish a transgenic line via the female founders. One transgenic mice also developed a uterine mass and while another developed enlarged polycystic kidneys, possibly due to recombination events during transgenic mouse production. Not unexpectedly, 7 of 25 (28%) transgenic animals developed testicular cancer. Intrapleural invasion of tumors into the omentum, the mesentery, and visceral and parietal pleura was also observed, possibly due to the invasiveness of the ovarian tumors. However, SV40 TAg is not known to be a genetic contributor to ovarian carcinogenesis [2, 62, 63]. Yet despite these limitations, this model has been used for further experiments by establishing a transgenic line through the male founder [64, 65].

Based off of the MISIIR-SV40TAg transgenic mice, Quinn *et al.* produced a syngeneic mouse model of high-grade serous ovarian cancer [66] by removing the ovarian carcinomas from donor transgenic mice and xenografting them into recipient immunodeficient and wildtype C57BL/6 mice. The murine ovarian carcinomas cells (MOVCAR) grew only in immunodeficient

mice and resulted in consistent SV40 TAg protein production. As p53 is bound to TAg, it results in p53 stabilization. Similar to MISIIR-SV40TAg transgenic mice, xenografted MOVCAR resulting in rapid tumor growth with euthanasia necessary within 4-6 weeks as a result of VEGF expression. In order to develop a more suitable recipient strain, tumor prone MISIIR-SV40TAg transgenic mice were subjected to three different surgical manipulations: 1) bilateral oophorectomy, 2) bilateral oophorectomy and salpingectomy, and 3) bilateral oophorectomy and salpingectomy with removal of the ovarian bursa. Tumor formation occurred in most mice, with mice in the third group developing primary peritoneal carcinomatosis of uncertain origin. While this tumor development made these mice unsuitable as MOVCAR recipients, MISIIR-SV40TAg transgenic mice expressing a low amount of TAg are not tumor prone and hence can serve as immunocompetent syngeneic recipients for MOVCAR.

Models that require either *ex vivo* manipulation or expression of a transgene during embryonic development do not accurately represent human EOC, which tends to be spontaneous in post-menopausal women. In an effort to mimic spontaneous EOC development, Flesken-Nikitin et al. [67] obtained mice from Anton Berns [68, 69] with LoxP sites containing p53 and Rb alleles to assess gene inactivation in the initiation of EOC. Mice were homozygous for the mutation and crossbred to generate  $p53^{loxP/loxP}Rb1^{loxP/loxP}$ . To assess the efficiency of Cre recombinase (Cre) expression derived by the cytomegalovirus (CMV) promoter, the ovaries were removed and cultured prior to exposure to adenovirus infection. Adenoviruses carrying *CMV-enhanced fluorescent green protein* (AdCMVEGFP) were used as a control against adenoviruses carrying *CMV-Cre* (AdCMVCre). Administration of AdCMVCre resulted in increased cell proliferation assessed by BrdU incorporation. To detect the feasibility in targeting the ovarian bursal cavity in the mouse, AdCMVEGFP was administered. It was detected only in the OSE for 21 days, as expected with a transient adenovirus infection. As a result of both p53 and Rb inactivation, 33 of 34 mice succumbed to ovarian tumors at a median of 227 days. However, administration of an adenovirus to achieve the desired results is cumbersome without generating a

reproductive line that would spontaneously form tumors. Targeting the ovarian bursal cavity is difficult at best, making this model not a feasible choice for large-scale applications.

While the previous models developed tumors resembling human serous adenomas, Dinulescu et al. [70] generated mice that have a transcriptionally silent oncogenic allele of *K-Ras* (*LSL-K-Ras<sup>G12D/+</sup>*) as first developed by Tyler Jacks [71-73], which can be conditionally expressed through administration of an adenovirus containing Cre. While the *LSL-K-Ras<sup>G12D/+</sup>* mice formed benign endometriosis-like lesions and benign lesion within the OSE upon *K-Ras* activation, the mice did not form ovarian carcinomas. However, when the *LSL-K-Ras<sup>G12D/+</sup>* mice were crossed with *PTEN<sup>loxP/loxP</sup>* mice, they developed invasive primary ovarian endometrioid adenocarcinomas, a subtype of EOC, suggesting that phosphate and tensin homologue deletion on chromosome 10 (*PTEN*) plays a role in tumorigenesis when combined with other oncogenes. This finding is consistent with *PTEN* deletion or mutation in other cancer types including endometrium, breast, thyroid, intestines, prostate, lung, liver, and T-cell lymphomas [74-78]. Concurrent *K-Ras* and *PTEN* mutations have also been found in complex endometrial hyperplasias, the precursor type of uterine endometrioid adenocarcinomas [79]. *PTEN* and adenomatous polyposis coli (*APC*) tumor suppressor genes were similarly conditionally deleted upon administration of an adenovirus carrying *Cre* to create *PTEN<sup>loxP/loxP</sup>* mice [80]. *APC* has been shown to regulate Wnt/ $\beta$ -catenin signaling [81]. *PTEN<sup>loxP/loxP</sup>* mice were cross-bred with *APC<sup>loxP/loxP</sup>* transgenic mice to determine if there was an interaction between the two pathways. The *PTEN<sup>-/-</sup>APC<sup>-/-</sup>* animals developed tumors within 6 weeks upon inactivation, with death occurring at 19 weeks. These tumors resembled human OEA, with increased signaling through Akt. Loss of E-cadherin and cytokeratins indicated that these tumors were undergoing epithelial-mesenchymal transition (EMT), which is consistent with Wnt/ $\beta$ -catenin and PI3K/Akt activation [82, 83].

Clark-Knowles et al. [84] used *Brcal<sup>loxP/loxP</sup>* mice, which upon administration of AdCre would remove introns 5 through 13 (*Brcal <sup>$\Delta$ 5-13</sup>*). Conditional deletion of *Brcal* resulted in

morphological changes, such as surface epithelium hyperplasia and formation of inclusion cysts, which was not due to increased proliferation. The incidence of these changes increased over time as observed from 60 days post-infection to 240 days. Interestingly, the genes involved in cancer initiation and progression p53 [85], E-cadherin [86], and collagen IV [87] were altered in *Brcal*<sup>Δ5-13</sup> ovaries compared to other tumor models. In *Brcal*<sup>Δ5-13</sup> ovaries, p53 was absent compared to SV40-induced tumors. E-cadherin was also downregulated, consistent with pre-neoplastic transformation. Collagen IV expression was found in the basement membrane, regardless of morphological changes of the OSE.

More recently, Liang et al. [88] used the MISIR promoter to drive expression of murine phosphatidylinositol 3-kinase catalytic subunit p110-alpha (*PIK3CA*) in transgenic mice. Although over-expression of *PIK3CA* resulted in increased phosphorylated Akt as its downstream target and in OSE hyperplasia, after 18 months post-birth of the F1 generation, tumorigenesis did not occur. Interestingly, the authors cultured isolated ovaries from non-transgenic mice and co-transfected them with both *PIK3CA* and mutant *K-Ras* or *c-Myc* to assess OSE transformation *in vitro*. Concurrent overexpression of *PIK3CA* and mutant *K-Ras* led to increased anchorage-independent growth of cultured OSE cells. Liang et al. [88] acknowledged that producing a “bigenic” animal by crossbreeding the transgenic *PIK3CA* mouse with a transgenic mutant *K-Ras* remains a technical challenge because mutant *K-Ras* animals develop tumors that inhibit reproduction. However, they suggested that a Cre-lox system of *K-Ras* expression may provide an alternative method of generation.

A summary of promoters and targeted genes in epithelial ovarian tumorigenesis can be found in Appendix I, Table I.

### **PTTG Expression and Biological Function**

Under normal physiological conditions, the pituitary tumor transforming gene (PTTG) is robustly expressed in the adult testes and thymus, with weaker expression in the colon, small intestine, brain, lung, pancreas, placenta, and in the embryonic liver [89-91]. PTTG cDNA has



been cloned from adult testes and embryonic liver [92, 93]. PTTG earned its name from being first cloned from rat pituitary tumor cells as a 974bp mRNA that yielded a 199 amino acid protein, which was not expressed in the normal pituitary [90]. Structural homology identified that PTTG was identical to human securin [94]. The C-terminal domain of securin binds to the N-terminal domain of separase to inhibit it and thus chromosome separation [94, 95]. Through immunoprecipitation, the N-terminal domain of PTTG binds to Ku70, the regulatory subunit of the Hu70:Ku80 heterodimer that composes the DNA-dependent protein kinase (DNA-PK). In the presence of a double strand break, Ku80 phosphorylates PTTG to release it from the DNA-PK complex and allows for PTTG to block separase, and thus couple DNA damage repair with the delay of mitosis [96].

*Downstream signaling/transactivation activity*

PTTG overexpression induced transcription of p53 by binding to c-myc to activate the p53 promoter through its c-myc binding domain and leads to the expression of Bax, a pro-apoptotic protein [97]. Hence in the presence of DNA damage, PTTG induces apoptosis in a p53-dependent and -independent manner. Cells can evade apoptosis through the continuous degradation of PTTG [98]. p53 is a known activator of p21, a cyclin-dependent kinase inhibitor, to arrest the cell cycle. In the case of PTTG deletion, p53 levels were not altered, but p21 expression increased dramatically through promoter activation in a dose-dependent manner [99]. In PTTG null pituitary tumors and pancreatic  $\beta$ -cell islets, the ARF/p53/p21 pathway is frequently activated to induce pituitary senescence, in part by induction of p19 which prevents p53 degradation by restraining MDM2 [100, 101]. Reports have been conflicting whether PTTG deletion promotes or prevents apoptosis [99, 100].

PTTG overexpression has been correlated with the promotion of angiogenesis and metastasis through increased expression and secretion of several growth factors and stimulators, including basic fibroblast growth factor (bFGF), vascular endothelial growth factor (VEGF), and interleukin 8 (IL-8) [102-104]. PTTG null mice show decreased vascular invasion by reducing

FGF2, its receptor FGF1, and VEGF and reducing metastases by decreasing cell motility [105], while PTTG overexpression correlates with increased VEGF and number of blood vessels formed [106]. An important signaling molecule downstream of VEGF is inhibitor of DNA binding 3 (ID3) transcription factor. ID3 is upregulated by the SH3 binding domain of PTTG via kinase insert domain receptor (KDR) expression and phosphorylation, leading to MAPK mitogenic pathway activation and promotion of angiogenesis [107, 108]. However, PTTG decreases expression of thrombospondin-1 (TSP-1), which associates with the extracellular matrix to promote angiogenesis, possibly through p53 as it is a positive regulator of TSP-1 [108, 109]. In the case of metastasis, PTTG overexpression increases matrix metalloproteinase-2 (MMP-2) expression and secretion, resulting in increases in cell migration and invasion to promote metastasis [110].

### **Tumorigenic Potential of PTTG and PTTG Transgenic Mice**

#### *PTTG in cancer*

As PTTG functions as securin, it is not surprising that PTTG has tumorigenic potential, as missegregation is predicted to be a major cause of genomic instability with drastic consequences in cancer development [111]. Furthermore, PTTG overexpression in a follicular thyroid cancer cell line correlated with genomic instability [112] and aneuploidy which included the presence of micronuclei and multiple nuclei in the absence of p53 [98].

PTTG is overexpressed in a variety of cancers including renal clear cell carcinoma, ovary, uterine, pituitary, thyroid, lung, colon, liver, and brain [91, 99, 113-118]. Interestingly, PTTG overexpression was detected in several tumor cell lines including promyelocytic leukemia HL60, cervical adenocarcinoma HeLa cell S3, chronic myelogenous leukemia K562, lymphoblastic leukemia MOLT-4, Burkitt's lymphoma Raji, colorectal adenocarcinoma SW480, lung carcinoma A549, melanoma G361, multiple hepatoma cell lines (SH-J1, SK-Hep1, and Huh7), and multiple astrocytoma cell lines (U87MG, U138MG, and LN405). Although PTTG is overexpressed in pituitary tumors, a mutational study revealed that PTTG overexpression was not

due to promoter mutations [119]. PTTG overexpression, either as a result of degradation failure or enhanced accumulation, has induced aneuploidy in the lung cancer cell line H1299 by inhibiting mitotic progression and chromosome segregation. Furthermore, PTTG is capable of inducing transformation in mouse fibroblast NIH3T3 cells when analyzed using anchorage-independent growth shown by forming larger colonies than control cells [91]. When PTTG overexpressing cells were injected into athymic nude mice, all 5 mice developed tumors within 2 weeks. Mutations in the structure of PTTG resulted in no tumors after 3 weeks of injection [91]. This was followed by a similar study using HEK 293 cells to see if PTTG could induce transformation in human cells without necessitating a partner oncogene [102]. HEK 293 cells stably transfected with PTTG (HEK-PTTG) showed increased cell proliferation, whereas mutations in the proline rich region of the sequence (HEK-mPTTG) did not. Soft agar colony formation also increased 30% in HEK-PTTG compared to vector only at 2%. HEK-PTTG formed poorly differentiated tumors upon subcutaneous injection into athymic mice, suggesting that PTTG is a potent oncogene that does not require co-expression of other oncogenes to achieve its tumorigenic function. Furthermore, cloning and sequencing of PTTG isolated from tumors shares the same sequence homology as that isolated from human testes cDNA suggests that it is overexpression and not mutation that contributes to its oncogenic properties [94].

To explore the role of PTTG in tumor growth and progression, siRNA against PTTG was utilized. In the lung cancer cell line H1299 [120], a 60% reduction in PTTG protein resulted in reduced colony formation in soft agar showing that PTTG suppress tumor growth *in vitro*. Untransfected H1299 cells and cells transfected with control siRNA formed tumors upon injection into nu/nu mice after 2 weeks. Tumor mass at the end of 4 weeks was 232.12±102.78 mg from untransfected cells and 231.57±83.76 mg from control siRNA cells. However, cells transfected with PTTG siRNA suppressed tumor growth only formed small tumors (67.85±45.87 mg) in 3 out of the 5 animals. No tumor growth was evident from PTTG siRNA cells before 2 weeks. A similar study was carried out using an ovarian cancer cell line A2780 with similar

results [116]. PTTG deletion resulted in reduced cell proliferation, decreased colony formation *in vitro*, and reduced tumor growth and development *in vivo*. In the invasive sarcoma SH-J1 hepatoma cell line, PTTG silencing resulted in reduced cell proliferation and apoptosis *in vitro* and reduced tumor formation *in vivo* [99]. Huh-7 or SH-J1 hepatoma cells were injected subcutaneously into nude mice. Huh-7 cells mock injected with PBS formed large tumors over 2cm<sup>2</sup> in 2 weeks while growth was inhibited in Huh-7 PTTG siRNA cells. SH-J1 injected into nude mice had similar results with 1 mouse in 7 injected with SH-J1 PTTG siRNA cells being tumor free.

#### *Influence on cell proliferation in diabetes and cancer*

PTTG null mice were first generated by Wang *et al.* [121] and showed significant metabolic changes resulting from reduced pancreatic  $\beta$ -cell proliferation with pleiotropic nuclei leading to decreased insulin production and elevated blood glucose levels ranging between 150 – 650 mg/dl.  $\beta$ -cell mass is controlled through several cellular mechanisms: expansion occurs from proliferation of existing  $\beta$ -cells, increase in  $\beta$ -cell size, and neogenesis from ductal progenitor cells. Upon further exploration, the pancreatic  $\beta$ -cells from PTTG null mice showed reduced proliferation measured by PCNA labeling and increased apoptosis by TUNEL assay [101]. PTTG null males can be rescued from diabetes development by undergoing surgical gonadectomy followed by estradiol treatment through increased serum adiponectin levels resulting in increased insulin sensitivity [122]. As a follow-up study, the mechanism of reduced pancreatic  $\beta$ -cells proliferation by PTTG deletion was determined [123]. Staining for insulin and the transcription factor pancreatic duodenal homeobox 1 (PDX-1) as markers for neogenesis were positive in both WT and PTTG null mice indicating that it is defective replication, not differentiation, that is responsible for the decreased  $\beta$ -cells mass. In order to further study this mechanism, murine PTTG (mrPTTG) was linked to EGFP (mrPTTG-EGFP) and expression driven using the CMV promoter. This constructed was transfected into MIN6 cells. Microscopy was utilized to determine localization of mrPTTG-EGFP at interphase in the nuclei and cytoplasm and at

anaphase in the cytoplasm only as the nuclear envelope was dissolved. The duration of mitosis was directly related to level of mrPTTG-EGFP expression: low expression levels doubled the duration, medium expression levels prolonged mitosis 4- to 5-fold, and high expression levels blocked mitosis for at least 2 hrs. Cells did not undergo division until all the mrPTTG-EGFP was degraded. EGFP alone was indistinguishable from untransfected cells. Furthermore, mrPTTG-EGFP co-immunoprecipitated with V5-separase. These results indicate that mrPTTG functions as securin to regulate cell division in pancreatic  $\beta$ -cells. Intracellular insulin levels did not differ between groups, suggesting that insulin production was not affected by mrPTTG.

$Rb^{+/-}$  mice develop pituitary tumors with almost complete penetrance [124, 125]. In order to investigate whether PTTG deletion could abrogate tumor development,  $Rb^{+/-}PTTG^{+/-}$  mice were crossbred to obtain  $Rb^{+/-}PTTG^{-/-}$  animals.  $Rb^{+/-}PTTG^{-/-}$  animals had lower spleen, pancreas, testes, and pituitary weights compared to  $Rb^{+/-}PTTG^{+/+}$  mice. As a result of PTTG deletion, either genetically or using shRNA, pituitary corticotroph cells displayed decreased cell proliferation due to an increase in p21 mRNA and protein, and resulted in reduced incidence of tumor development and increased survival time [126].

Mice with mutations in the thyroid hormone  $\beta$  receptor gene ( $TR\beta^{PV/PV}$ ) exhibit severe dysfunction of the pituitary-thyroid axis, impaired weight gains, and abnormal bone development consistent with the human syndrome resistance to thyroid hormone (RTH). These mice differed from mice with a null phenotype for  $TR\beta$  [127]. However, when  $TR\beta^{PV/PV}$  mice were crossbred with  $PTTG^{-/-}$  to create doubly-mutant mice, they displayed decreased thyrocyte proliferation resulting in decreased thyroid growth and ablation of goiter development as seen with  $TR\beta^{PV/PV}$  mice.  $TR\beta^{PV/PV}PTTG^{-/-}$  mice did not have altered pituitary-thyroid dysregulation. While PTTG deletion did not alter follicular thyroid cancer development in  $TR\beta^{PV/PV}$  mice, there was decreased vascular invasion trending towards decreased lung metastasis [105].

### *PTTG transgenic mice*

Abbud *et al.* [128] produced transgenic mice using the common  $\alpha$ -subunit of the glycoprotein hormones promoter, referred to as the  $\alpha$ -subunit of glycoprotein hormone ( $\alpha$ -GSU) to drive expression of PTTG and enhanced green fluorescent protein (EGFP) to target expression to the gonadotrope and thyrotrope cells of the pituitary. Transgenic mice developed enlarged pituitaries along with increased serum IGF-1 and testosterone. Using scanning confocal microscopy to detect EGFP expression on the surface and 100 $\mu$ m deep, the authors found that EGFP-positive cells in transgenic mice were arranged in two bilateral streaks. These streaks were arranged next to blood vessels. Some of the transgenic animals with focal PTTG expression showed loss of the reticulin network, indicating microadenoma rather than hyperplasia. However, the most striking phenotype in transgenic males was urinary tract obstruction secondary to prostate hyperplasia at 8-12 months of age with enlargement of the seminal vesicle and showed fibromuscular stromal thickening upon histological examination.

As  $Rb^{+/-}$  were known to develop pituitary tumors, Donangelo *et al.* [129] crossbred  $\alpha$ -GSU-PTTG-EGFP transgenic mice with  $Rb^{+/-}$  transgenic mice to develop a bitransgenic animal to further understand the role of PTTG in pituitary tumor development.  $\alpha$ -GSU-PTTG mice displayed normal pituitary cells with the exception of gonadotrophs cells, which showed abundant secretory vesicles and very active Golgi complexes. However,  $\alpha$ -GSU-PTTG/ $Rb^{+/-}$  had more diverse cell morphology, ranging from minute secretory granules similar to  $\alpha$ -GSU-PTTG pituitaries to massive gonadotroph hyperplasia showing several small and large secretory granules. Glycogen  $\beta$ -particles were also present in cytoplasm. Three  $\alpha$ -GSU-PTTG/ $Rb^{+/-}$  mice also developed pituitary tumors. One 5-month old male developed one tumor of gonadotroph origin and another derived from a thyrotroph cell. Two females (12- and 13-months old) developed gonadotroph neoplasms. Using confocal microscopy, 88% (192 of 217) of  $\alpha$ -GSU-PTTG mice expressing EGFP and 95% (97 of 102) of  $\alpha$ -GSU-PTTG/ $Rb^{+/-}$  displayed altered nuclei as a result of chromatin reorganization.  $\alpha$ -GSU-PTTG/ $Rb^{+/-}$  also exhibited large nuclear

vacuoles. The altered nuclei were compared to wildtype (9%, 19 of 213), monotransgenic  $Rb^{+/-}$  (28%, 62 of 222), EGFP negative monotransgenic  $\alpha$ -GSU-PTTG (23%, 10 out of 43), and EGFP negative bitransgenic  $\alpha$ -GSU-PTTG/ $Rb^{+/-}$  (14%, 13 out of 93) animals. The age of tumor development was not significantly different between  $Rb^{+/-}$  and  $\alpha$ -GSU-PTTG/ $Rb^{+/-}$ . However, 80% (16 out of 20)  $Rb^{+/-}$  pituitary tumors originated from the intermediate lobe, 10% (2 out of 20) from the anterior lobe, and 10% (2 out of 20) from both lobes. In  $\alpha$ -GSU-PTTG/ $Rb^{+/-}$  only 36% (6 out of 20) arose from the intermediate lobe, 25% (5 out of 20) originating from the anterior lobe, and 45% (9 out of 20) from both lobes.

In a previous experiment through our lab, the construct for targeting PTTG to the ovary epithelium used the promoter reported by Connolly *et al.* [61], MISIIR, to produce MISIIR-PTTG transgenic mice [130]. Transgenic ovaries showed an increase in the corpus luteum mass accompanied by the increase in serum luteinizing hormone (LH) and testosterone levels. The transgenic females also displayed a generalized hypertrophy of the endometrium. This study showed that by using the MISIIR promoter, 3 different tissues could be targeted: OSE, granulosa cells, and pituitary. However, possibly due to the weak expression of PTTG, the animals failed to generate any visible tumors, as the amount of expression is critical in ectopic tumor progression [116].

## CHAPTER 2

### PTTG TRANSGENIC MICE AS A MODEL FOR OVARIAN CANCER

PTTG can function as an oncogene when overexpressed and trigger ectopic tumorigenesis in nude mice [91, 94], suggesting that it does not require a partner gene in order to achieve its tumorigenic potential. As PTTG has also been identified in ovarian cancer taken from patients at the time of surgical resectioning [116], we wanted to identify the *in vivo* tumorigenic potential of PTTG through the development of a transgenic mouse model that could faithfully represent spontaneous EOC found in patients through the strong, non-specific overexpression of PTTG using the CMV promoter.

#### Materials and Methods

##### *Construction of CMV-PTTG-EGFP transgene*

Human PTTG (PTTG) cDNA was subcloned into the pEGFP-N3 vector at the multiple cloning site between the CMV promoter and downstream enhanced GFP (EGFP) reporter gene. Subsequently, the vector was cut using restriction enzymes Ase I and Afl II by incubating each restriction enzyme individually with the vector for 2 hrs at 37°C to reduce the transgene size and eliminate unwanted genes. The first restriction enzyme was neutralized with phenol/chloroform and DNA was purified before addition of the second restriction enzyme. The restricted vector was run on a 0.7% agarose gel to isolate the transgene fragment, CMV-PTTG-EGFP (2.3kb; Fig. 1). CMV-PTTG-EGFP was excised from the gel and purified using a gel extraction kit (Qiagen). CMV-PTTG-GFP was then sent for sequencing to ensure mutation of PTTG had not occurred.

##### *Animal housing*

Mice were housed in a conventional facility with a 12 hr light: 12 hr darkness cycle. All animals were treated in accordance with National Institutes of Health Guidelines for the Care and Use of



Laboratory Animals and approved by Animal Use and Care Committee at the University of Louisville.

#### *Generation of transgenic animals*

Purified CMV-PTTG-GFP transgene was sent to the University of Cincinnati, Transgenic Mouse Core, where microinjection was performed into the male pronucleus of FVB 0.5 day old embryos. Embryos were then transplanted into a pseudo-pregnant female to generate founders. Wildtype males were bred to positive TgPTTG female founders. TgPTTG F<sub>1</sub> males were bred to wildtype females to establish a colony line.

#### *P53<sup>+/-</sup> Mice*

P53<sup>+/-</sup> mice on an FVB background were obtained from Jackson Laboratory. A male p53<sup>+/-</sup> mouse was used to crossbreed with founder 71305 (♀). Female p53<sup>+/-</sup> were crossbred with a transgenic male to create TgPTTG/p53<sup>+/-</sup> mice.

#### *Genotyping and screening of transgenic and p53<sup>+/-</sup> mice*

Mice were tail clipped between 21-28 days of age and ear tagged or toe tattooed with an ID number. DNA from tail clips was extracted using PCR Extract-N-Amp kit (Sigma). hPTTG-GFP (PTTG<sup>t</sup>) genotype was identified via PCR using the specific primer: hPTTG 16182: sense 5'-ACT GAG AAG ACT GTT AAA GC-3' or hPTTG 16207: sense 5'-ACG AAT TCA TGG CTA CTC TGA TCT ATG T-3', and GFP antisense 23759: 5'-AGA TGA ACT TCA GGG TCA GC-3' that specifically amplified the transgene sequence. PCR conditions were 1) 94°C for 5 min, 2) 94°C for 30 sec, 3) 58°C for 30 sec, 4) 72°C for 1 min, 5) Steps 2-4 repeated for 30 cycles, 6) 72°C for 7 min. P53<sup>+/-</sup> were genotyped via PCR using the specific primers according to Jackson Laboratory Protocol: Wildtype: sense 5'-ACA GCG TGG TAC CTT AT-3', Common: sense 5'-TAT ACT CAG AGC CGG CCT -3', and Mutant: 5'-CTA TCA GGA CAT AGC GTT GG-3'. PCR conditions were 1) 94°C for 3 min, 2) 94°C for 30 sec, 3) 64°C for 1 min, 4) 72°C for 1.5 min, 5) Steps 2-4 repeated for 35 cycles, 6) 72°C for 2 min.

#### *RNA isolation and analysis of transgene expression via RT-PCR*

Total RNA was isolated from tissues by preserving tissue in RNALater (Sigma) at the time of sacrifice. Tissues were homogenized in 1 ml Trizol (Sigma) and isolated via standard procedure. 1 µg of total RNA was converted to cDNA using a reverse transcription kit (BioRad). Total cDNA was then subjected to PCR as described above for PTTG-EGFP expression.

#### *Histological analysis and immunohistochemistry*

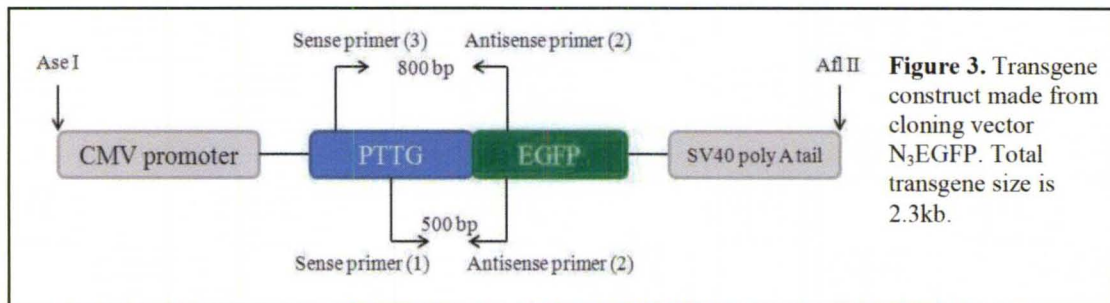
Tissues samples were fixed in 10% formalin buffer (Fisher Scientific) overnight at RT. After 24 hr formalin was replaced with 70% ethanol and stored at 4°C until processing. Tissues were imbedded in paraffin using standard technique. Six micrometer sections were stained with H&E by the Pathology Core Research Laboratory, University of Louisville and evaluated by a licensed human pathologist, Hanan I. Farghaly, MD. For immunohistochemistry, sections were deparaffinized in fresh xylene and rehydrated in a graded series of ethanol. Antigen retrieval was conducted by incubating the slides in 10 mM Sodium Citrate (pH 6.0) at 95°C for 20 min then rinsed twice with PBS. Slides were incubated in 4 drops per section of Image-It FX Signal Enhancer (Invitrogen) for 30 min with humidity then rinsed with PBS. Slides were blocked with 10% goat serum (Sigma) in PBS for 1 hr followed by anti-PTTG 1:1,500 dilution in PBS and incubated at 4°C overnight. Slides were then washed in PBS before application of secondary antibody Alexa 594 anti-rabbit (Invitrogen) 1:500 with 1 drop of goat serum per 5 mL and incubated 45 min at RT in the dark, then washed with PBS. Slides were dehydrated in a graded series of ethanol, treated with xylene, and mounted with Clarion mount (Sigma). Images were acquired on Nikon Eclipse E400 and ACT-1.1 imaging software (Huntley, IL, USA).

## **Results**

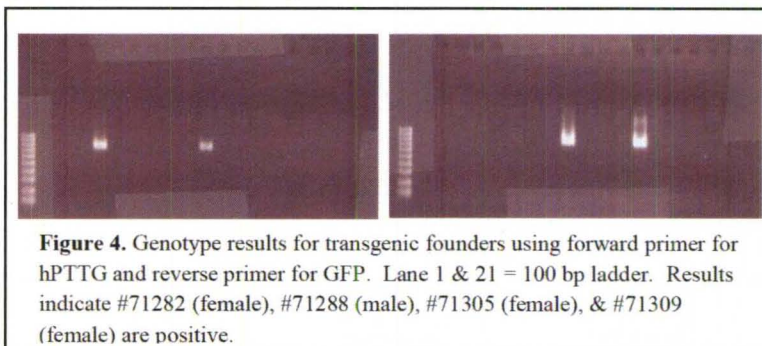
#### *Generation of CMV-PTTG-EGFP transgenic mice*

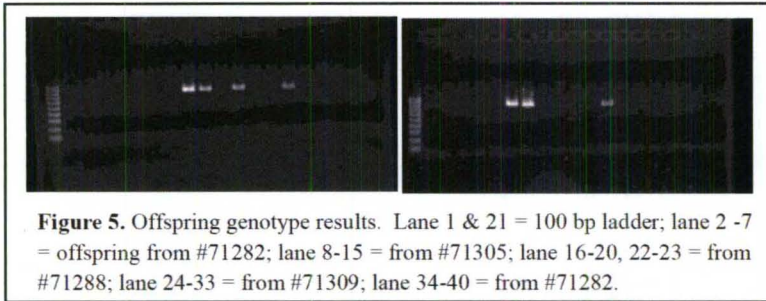
As a previous attempt to generate PTTG transgenic (TgPTTG) mice did not result in tumorigenesis, we asked whether the level of PTTG expression was sufficient. To this end we selected the non-specific strong CMV promoter to drive PTTG expression. Human PTTG

(PTTG) was subcloned into the N3 expression vector containing the CMV promoter, a multiple cloning site where *PTTG* cDNA was inserted, and a downstream *enhanced GFP (EGFP)* marker gene (Fig. 3). To test promoter activity, African green monkey kidney fibroblast-like cells (COS7) were transfected and GFP fluorescence observed with a fluorescent microscope. In order to reduce the transgene fragment size for ideal transgenic mouse production, the N3 vector was cut with two restriction enzymes, *Ase* I and *Afl* II, that did not impact *hPTTG* cDNA resulting in



the fragment CMV-PTTG-EGFP (Fig. 3). This purified fragment was also transfected into COS7 cells to determine recombination and then microinjected into the male pronuclei of 0.5 day old Friend Virus B-Type (FVB) embryos. Transgenic founders were identified by PCR screening of DNA extracted from the tail clip of 34 F<sub>0</sub> mice using two different sense primers located in PTTG and one antisense primers located in EGFP (Fig. 3). This resulted in the identification of 1 male (#71288) and 3 female TgPTTG founders (#71282, 71305, and 71309; Fig. 4). The founders were





cross-bred with wildtype FVB mice and resultant  $F_1$  offspring were genotyped by PCR (Fig. 5). All founders were fertile and produced an average litter size (Appendix 1, Table 2). However, the male and 1 female founder failed to transmit the transgene to their offspring ( $F_1$ ), suggesting that the transgene did not integrate in the germ line during homologous recombination events during embryo development. TgPTTG males from a single line (founder #71309) were cross-bred to wildtype females through multiple generations to create  $F_2$ - $F_4$  to generate a sufficient number to TgPTTG mice. Transgenic males were often aggressive by 6 months of age and had to be maintained in separate cages. All mice demonstrated hyperactivity during housing.

#### *PTTG expression in CMV-PTTG-EGFP mice*

TgPTTG mice were sacrificed at 4, 6, 8, 10, and 12 months of age along with the age-matched controls and tissue harvested for RNA isolation and immunohistochemistry. Tissue distribution was determined by promoter expression [131] and examined by reverse transcription PCR of RNA samples isolated from the ovary, fallopian tube, uterus, testes, seminal vesicle, lung, liver, spleen, kidney, and pituitary (Fig. 6). As expected, PTTG expression was detected in all of the tissues with the exception of the pituitary. The strongest expression was seen in the testes, with weaker expression in the remaining tissues.

Specificity of the PTTG antibody to PTTG vs. murine PTTG has been addressed [130]. Immunohistochemistry of the ovary, fallopian tube, uterus, and seminal vesicle showed staining in the epithelium, while the testes PTTG expression was localized to the seminiferous tubules (Fig. 7) in 4 months old animals.

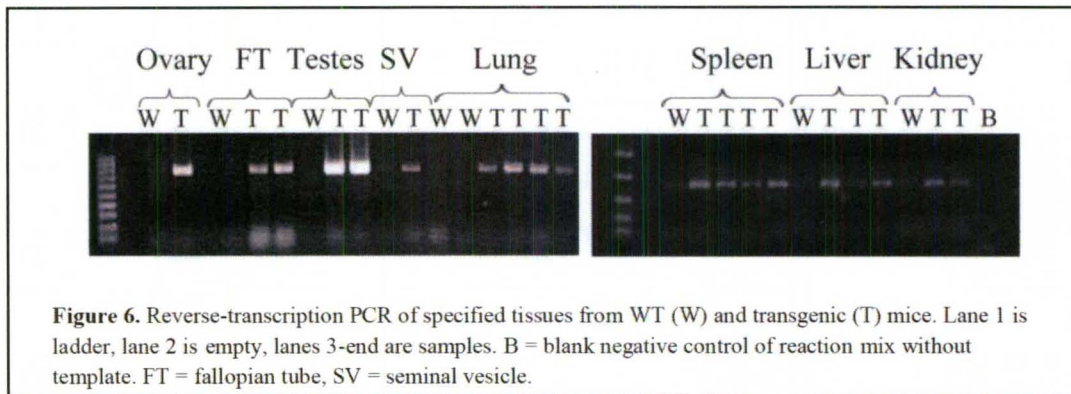


**Figure 6.** Reverse-transcription PCR of specified tissues from WT (W) and transgenic (T) mice. Lane 1 is ladder, lane 2 is empty, lanes 3-end are samples. B = blank negative control of reaction mix without template. FT = fallopian tube, SV = seminal vesicle.

#### *Histology of CMV-hPTTG-EGFP transgenic animal tissues*

Formalin-fixed paraffin imbedded tissues were sectioned and stained with hematoxylin and counterstained with eosin (H&E). Evaluation of the histology was performed by a licensed pathologist. Tissues were selected based on CMV promoter expression [131] and was as additional tissues of interest including ovary, fallopian tube, uterus, and pituitary. While all tissues were normal in 4 months old TgPTTG mice, pre-cancer conditions (4 out of 15, 27%) and carcinomas (2 out of 15, 13.3%) were observed as early as 8 months of age. A total of 15 females and 9 males were included in the transgenic 8 months old group and were compared to 11 wildtype age-matched controls. PTTG-EGFP expression was confirmed using immunofluorescence (Fig. 8). Pronounced follicular cysts and corpus luteum were observed in 6 out of 15 (40%) of TgPTTG females. Pre-cancer conditions included one female (#31) developed a leiomyoma (Fig. 9a) with chronic inflammation (Fig. 9b). A second female (#286) had squamous dysplasia with extensive keratinization at the transformation zone between the uterus and the cervix (Fig. 10), while a third female (#436) developed low grade dysplasia with acute cervicitis (Fig. 10). PCNA analysis was performed to verify hyperplastic conditions. TgPTTG #286 revealed 25% positive cells with reverse maturation of the squamous epithelium of the cervix, while TgPTTG #436 was 5-10% positive, localizing to the basal cells and also showed a pattern of reverse maturation (Fig. 10). These were compared to WT 8 month old cervix (Fig. 10). Negative controls with no primary antibody were included in the analysis. An additional female

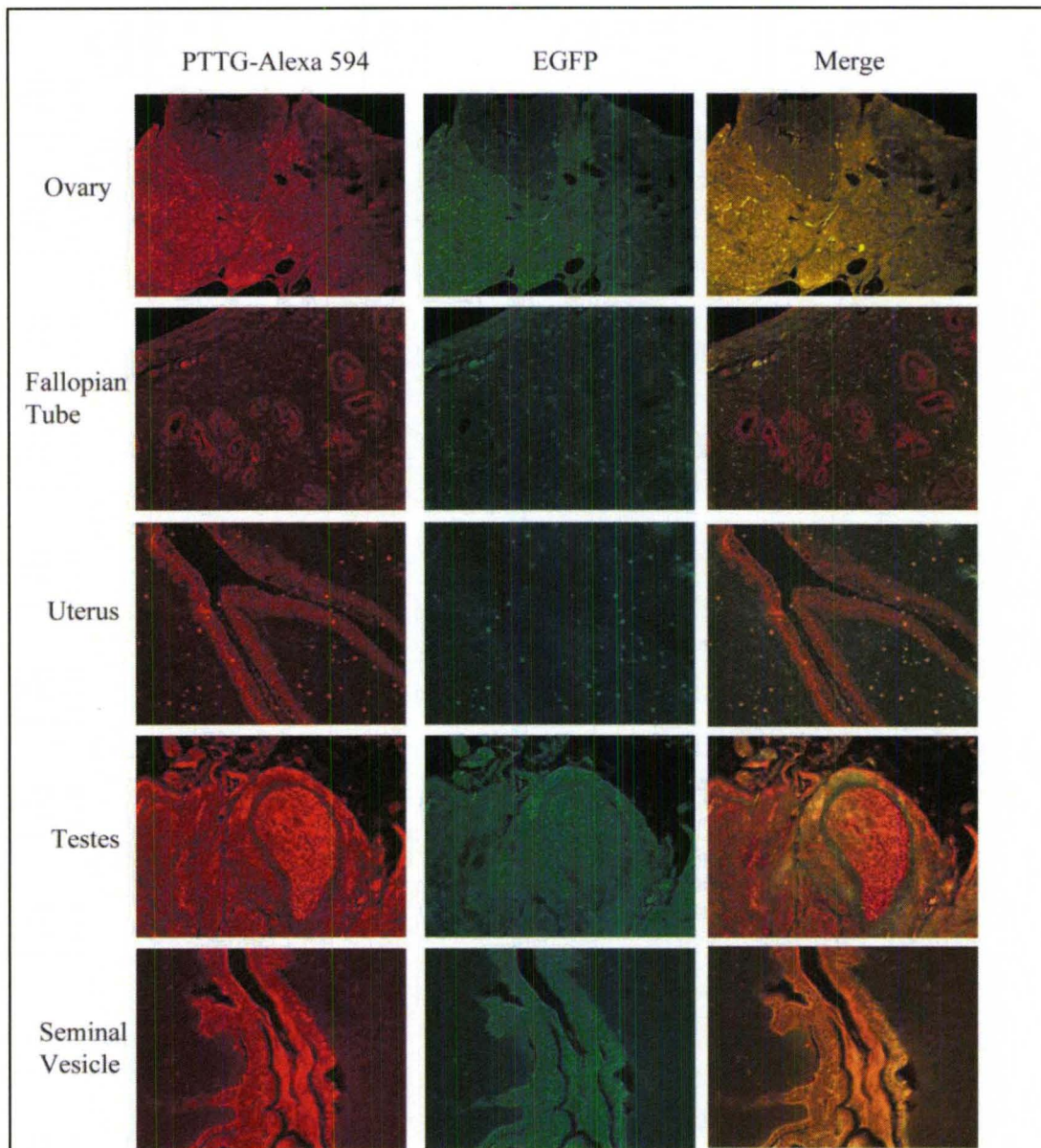
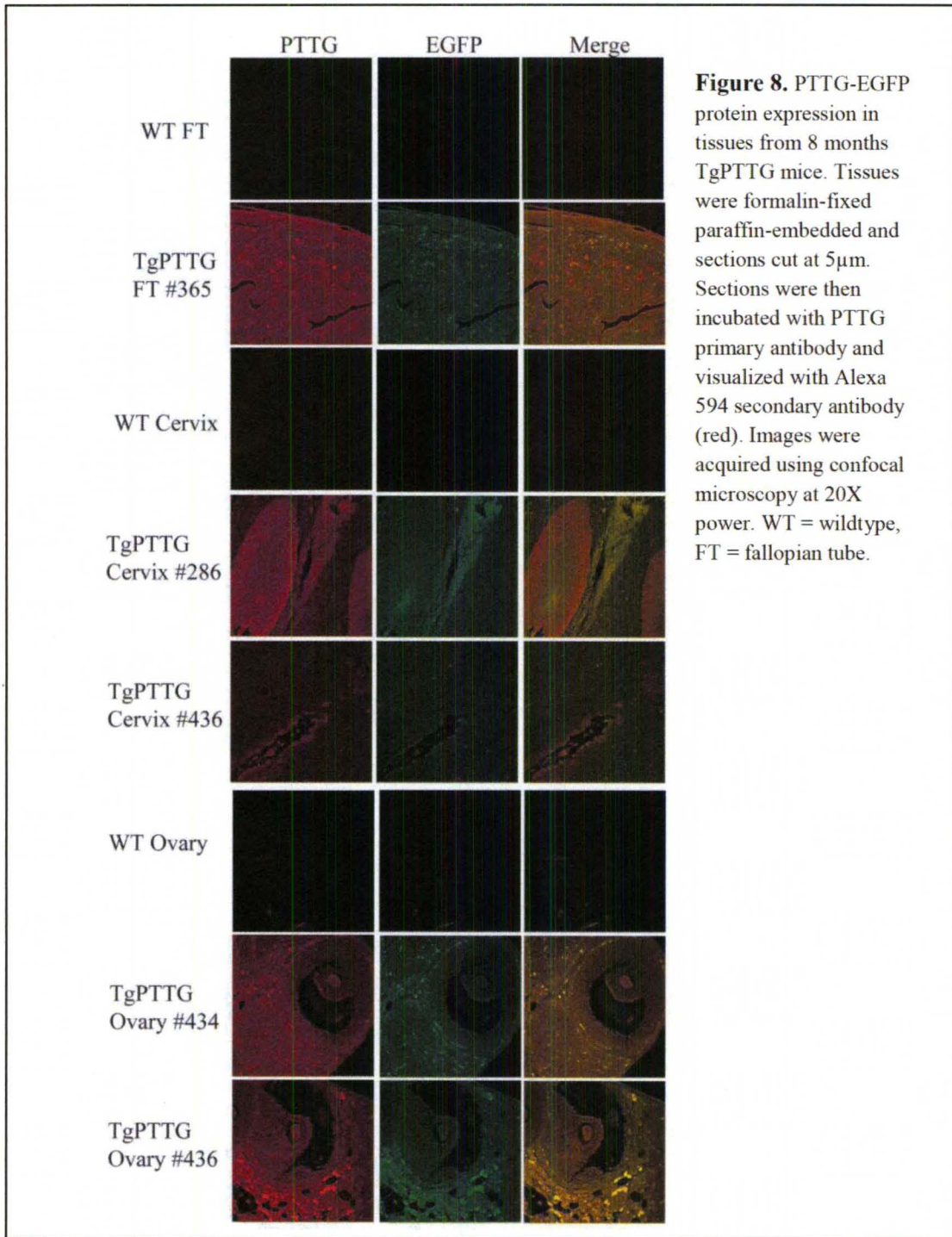


**Figure 7.** PTTG-EGFP protein expression in tissues from 4 months TgPTTG mice. Tissues were formalin-fixed paraffin-embedded and sections cut at 5 $\mu$ m. Sections were then incubated with PTTG primary antibody and visualized with Alexa 594 secondary antibody (red, column 1). EGFP expression was visualized using the FITC filter (column 2). Column 3 shows the merging of column 1 and 2.

(#365) developed hyperplasia of the fallopian tube with endothelial atypia (Fig. 10). PCNA analysis of #365 fallopian tube was compared to WT fallopian tube and showed 25% positive cells that were localized to the epithelial glands (Fig. 10). Three females (#269, 366, and 368; 20%) had adenomyosis of the uterus. Two females (13.3%) developed ovarian cancer (Fig. 10). We decided to use the plus rating system for CD31 staining, where 1+ means < 25% of tissues was stained, 2+ means 25-75% of tissue was stained, and 3+ means > 75% of tissue was stained. TgPTTG #434 developed ovarian serous adenocarcinoma with PCNA staining showed 35% positivity and CD31 was 2+ (Fig. 11). TgPTTG #436 developed a granulosa tumor and a follicular cyst with mitotic figures. In this female, PCNA staining was 5% and CD31 2+ (Fig. 11). Comparatively, age-matched WT animals showed 1% PCNA staining of the ovary, which was localized to the granulosa cells of the follicle as would be expected, while CD31 was 1+ (Fig. 11).

TgPTTG 10 month old group included 10 females and was compared to 13 WT age-matched controls. PTTG-EGFP expression was confirmed by immunofluorescence (Fig. 12). One female developed a pre-cancerous serous cyst adenoma of the ovary. Another developed serous adenocarcinoma of the ovary and fallopian tube (#381, Fig. 13), while an additional female developed a tumor of ovarian follicular cells (#383, Fig. 13). PCNA staining was 5-10% in both TgPTTG ovaries and 15% in age-matched WT controls which was localized to the follicles (Fig. 13). CD31 was similar between WT ovaries and TgPTTG ovaries (1+, Fig. 13). Interestingly, PTTG expression was higher in the female that developed serous adenocarcinoma vs. the female with the follicular cells tumor (Fig. 12). Additionally, 1 out of 20 (5%) developed an ectopic tumors diagnosed as a papillary serous adenocarcinoma that was 75% positive for PCNA and had significant (3+) angiogenesis (Fig. 13). Two other females (20%) showed atypia of epithelial cells of the fallopian tube.



TgPTTG 12 months old group included 11 females and 10 males, which was compared to 20 wildtype age-matched controls. One female (#185) developed a papillary serous carcinoma of



peritoneal origin along with uterine focal hyperplasia. The ovarian cells appeared luteinized, which is an indication of hyperactivity. This was coupled with a reduction in stromal tissue.

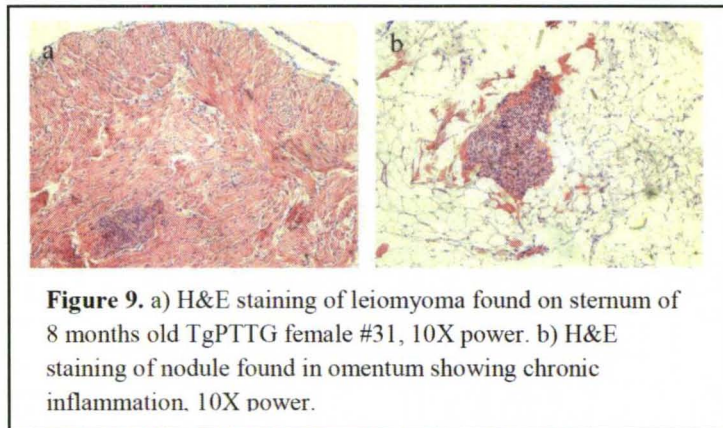


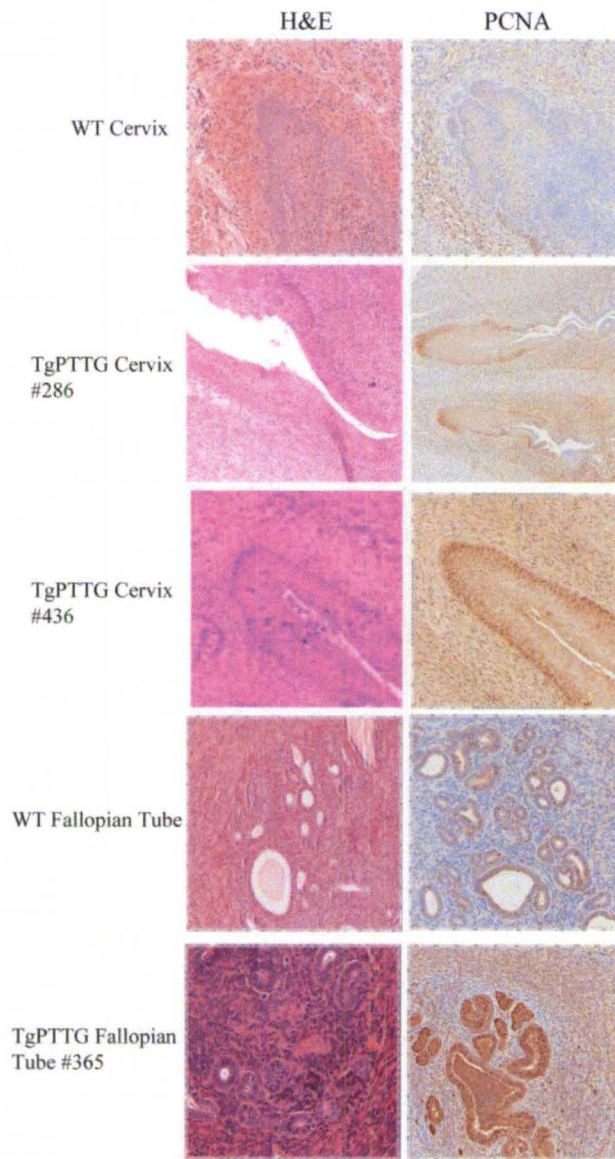
**Figure 9.** a) H&E staining of leiomyoma found on sternum of 8 months old TgPTTG female #31, 10X power. b) H&E staining of nodule found in omentum showing chronic inflammation. 10X power.

Group assignments along with a summary of results can be found in appendix 1, Table 3.

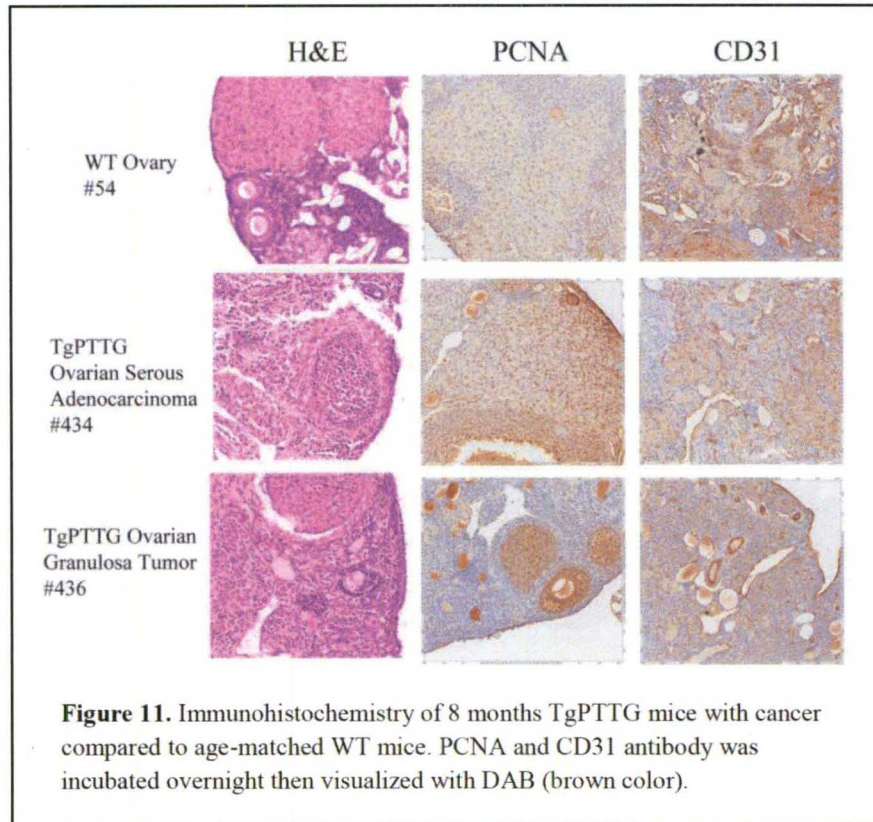
Transgene copy number was assessed to analyze differences between TgPTTG that developed cancer and those that did not. A standard curve was generated using the N<sub>3</sub> vector containing PTTG (Fig. 14a) using real-time PCR. By calculating the kb size of the vector, a copy number could be assessed to the standard curve. Then by taking 100 ng of genomic DNA isolated for the tail clip, the gene copy number was extrapolated from the standard curve (Fig. 14b) as 100 ng of DNA was reported to yield  $1.67 \times 10^4$  diploid cells [132]. We found no difference in transgene copy number between TgPTTG mice that developed cancer and those that did not.

#### *Crossbreeding of TgPTTG with p53<sup>+/-</sup> mice and histology*

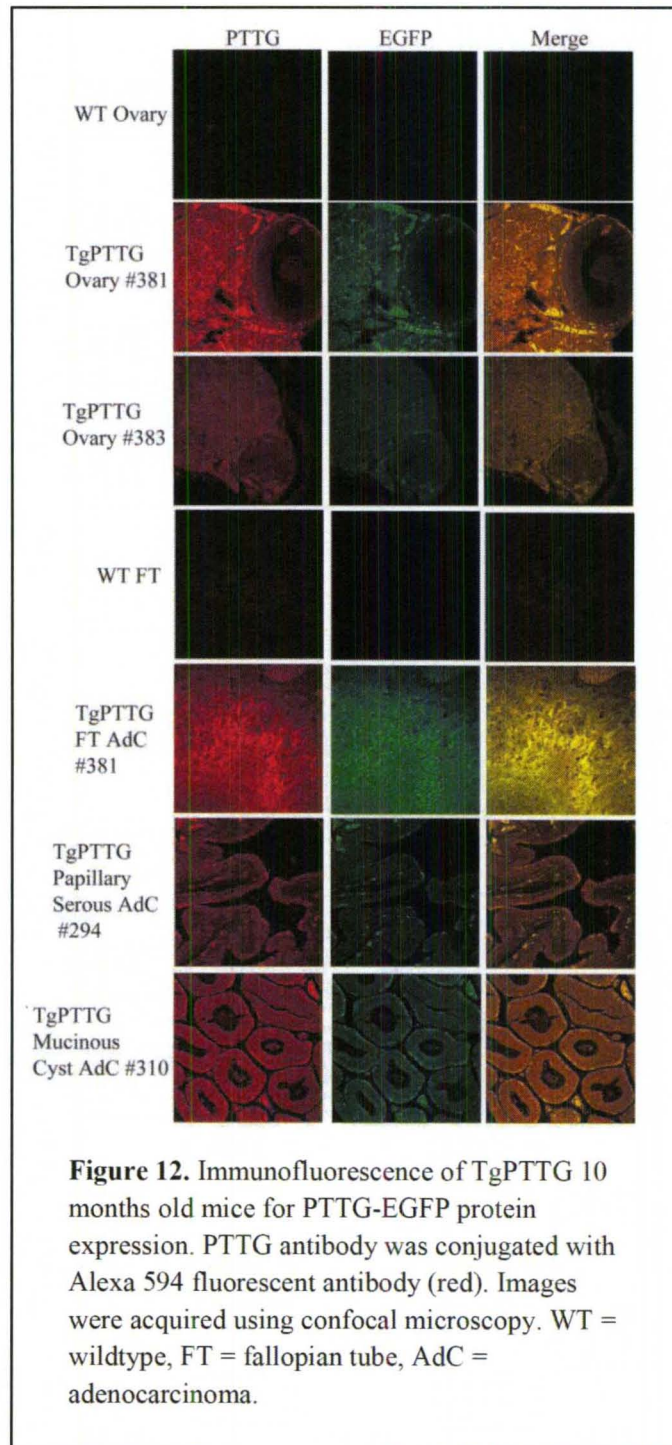
P53 mutant (p53<sup>mut</sup>) mice were produced by a targeted neo cassette insertion into the p53 locus in the laboratory of Dr. Tyler Jacks at the Center for Cancer Research at the Massachusetts Institute of Technology [133] and are available through the Jackson Laboratory. These mice have an 18% incidence of adenocarcinomas and a 56% incidence of sarcomas [134]. Based on the 56 mice observed (45 p53<sup>+/-</sup> and 11 p53<sup>-/-</sup>, appendix 1, Table 4), four p53<sup>+/-</sup> mice (8.9%) developed sarcomas at between 3 and 11 months, while nine p53<sup>-/-</sup> (81.8%) develop lymphoma and sarcomas between 9 and 12 weeks.

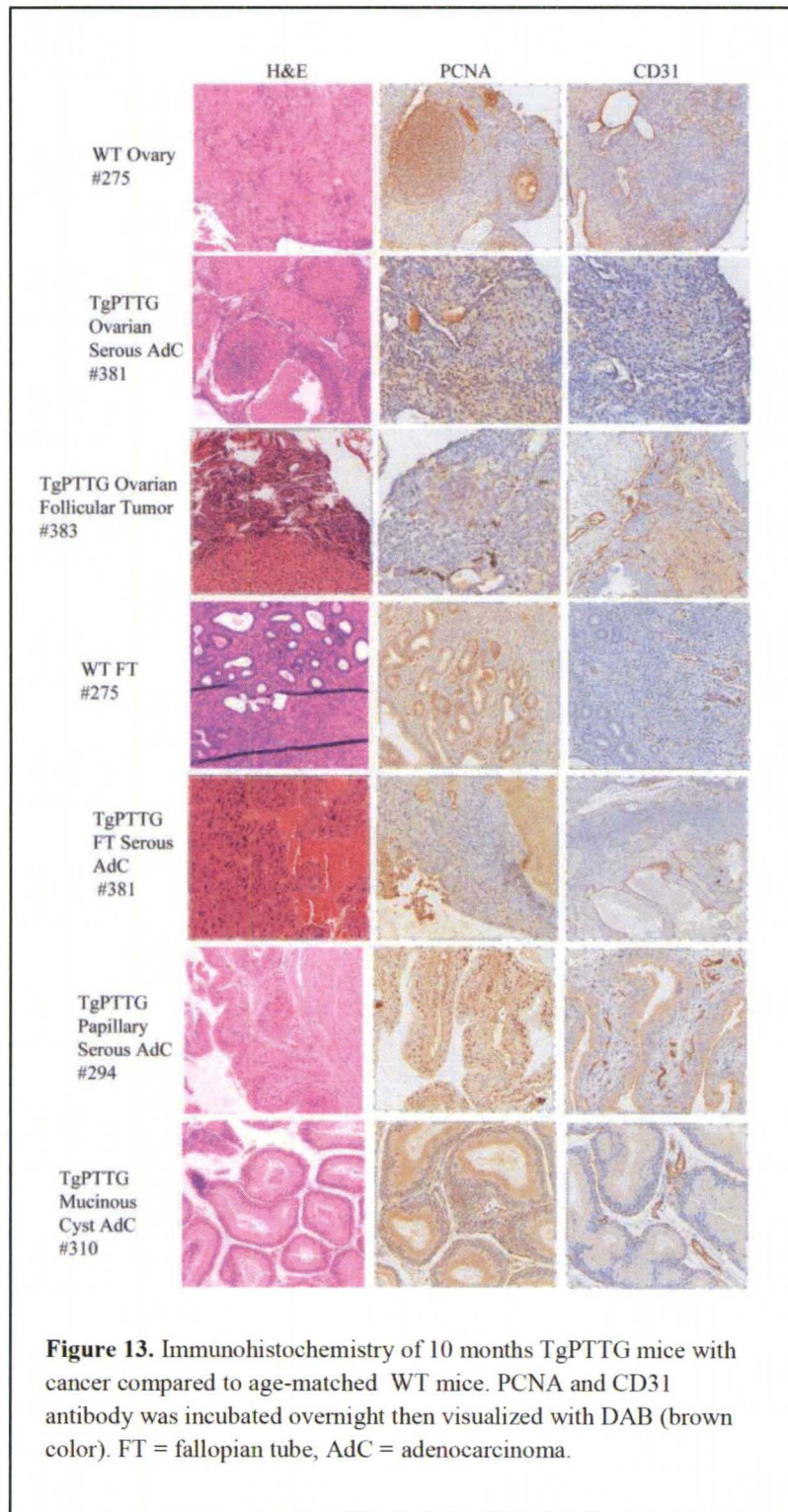


**Figure 10.** Immunohistochemistry of TgPTTG 8 month old mice with pre-cancer conditions compared to age-matched WT mice. PCNA antibody was incubated overnight then visualized with DAB (brown color).



Due to the short lifespan of  $p53^{-/-}$  mice,  $p53^{+/-}$  mice were chosen for crossbreeding to increase the incidence, decrease the onset time, and/or possibly change the type of cancer in TgPTTG mice. Two male TgPTTG mice from line #71309 were crossbred to  $p53^{+/-}$  females to maximize offspring, resulting in generation  $F_2$  (Fig. 15). PTTG-EGFP expression was analyzed by immunofluorescence to determine the level of expression (Fig. 16). One TgPTTG/ $p53^{-/-}$  mouse developed two teratocarcinomas at 7 weeks of age, while another developed lymphoma and sarcomas at 12 weeks of age (Fig. 17). One TgPTTG/ $p53^{+/-}$  mouse developed adenocarcinoma of the fallopian tube and sarcomas at 7 months of age (Fig. 17). Group assignments along with a summary of results can be found in appendix 1, Table 5.

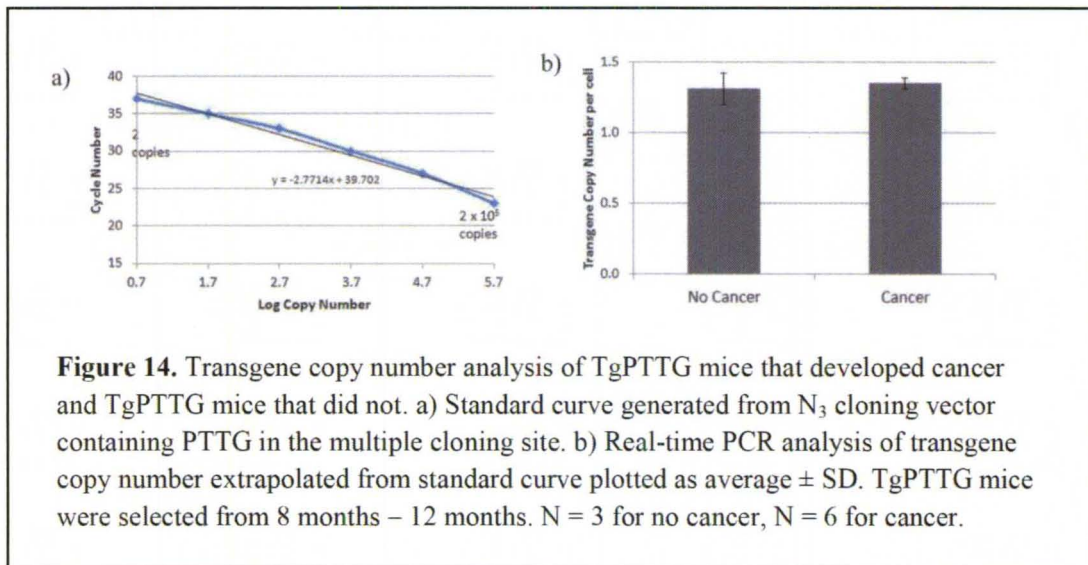


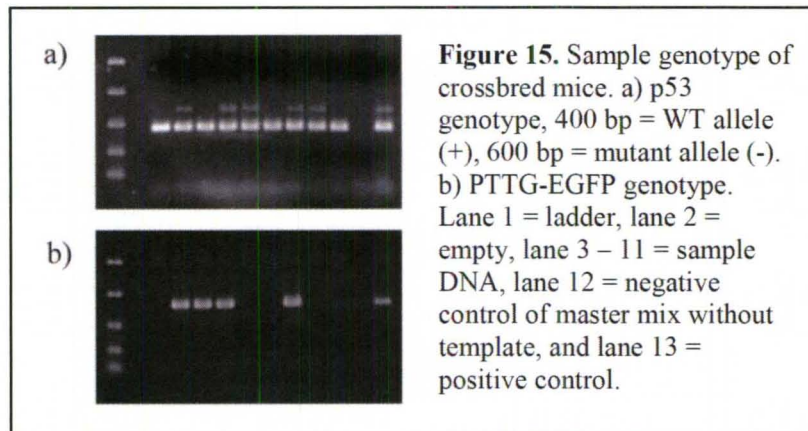


TgPTTGp53<sup>+/-</sup> mice aged to 8 months included 9 females and 8 males. Of the TgPTTGp53<sup>+/-</sup> females aged to 8 months, 4 of 9 (44%) had severe dysplasia of the cervix resulting in carcinomas *in situ* along with 1 of 17 (6%) developing a sarcoma. PCNA showed intense staining in all sarcomas, congruent with the highly aggressive nature of this tumor type (Fig. 14). All sarcomas had microvessel formation determined by CD31 (Fig. 17).

TgPTTGp53<sup>+/-</sup> mice aged to 10 months included 8 females and 6 males. 5 of 8 (63%) females showed focal to severe cervical dysplasia resulting in carcinomas *in situ* (Fig. 17), and 3 of 8 (38%) showed dilation of the fallopian tube. 2 of 14 (14%) developed high grade leiomyosarcomas (Fig. 17). Comparatively, p53<sup>+/-</sup> mice developed sarcomas between 11 – 12 months of age (2 of 28, 7%).

The timeline of tumor development in p53<sup>mut</sup> and TgPTTG/p53<sup>mut</sup> mice is summarized in Fig. 18.

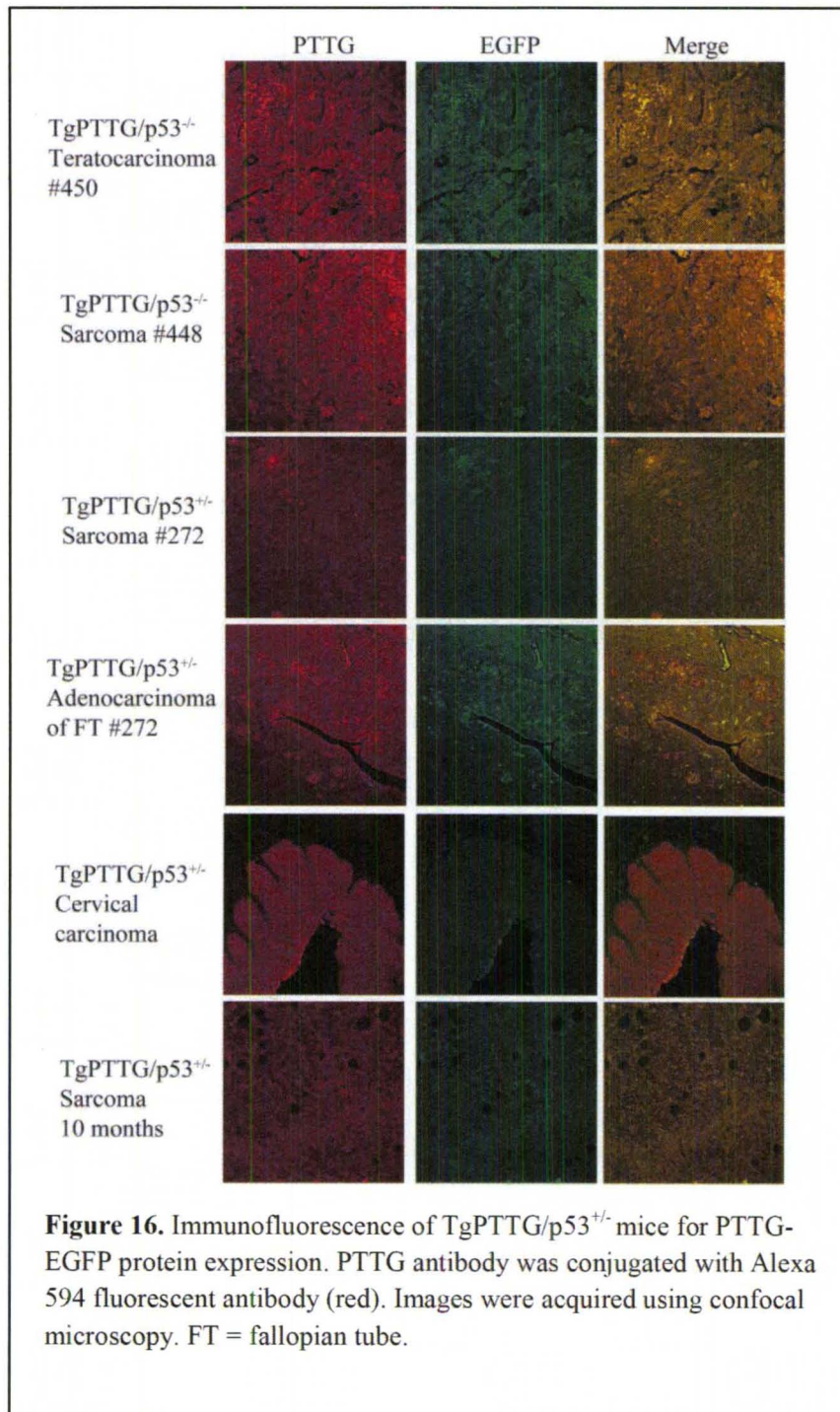




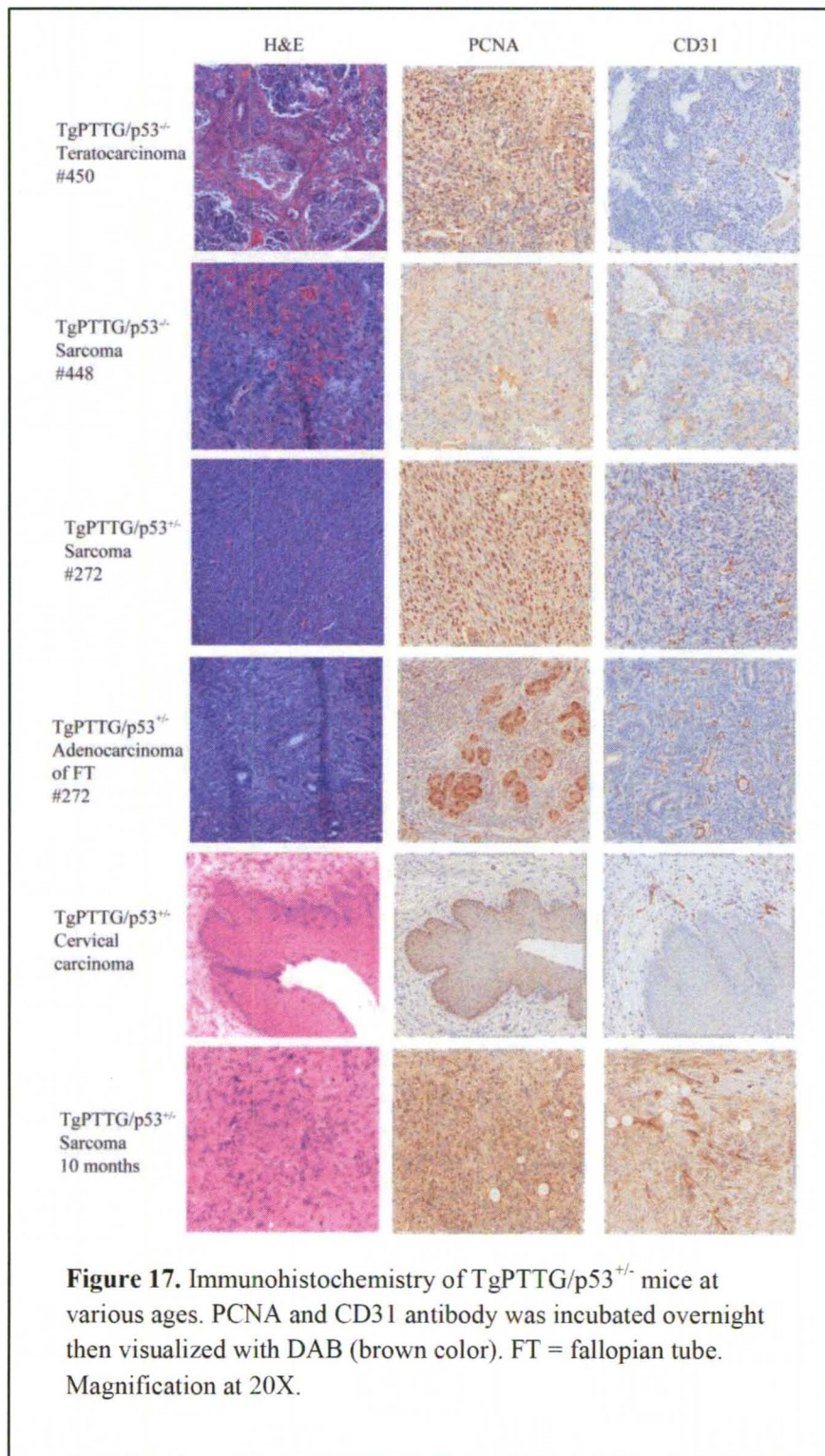
## Discussion

Ovarian cancer is a heterogeneous disease that is classified based on its tissue of origin: epithelial cells (90%), sex-cord stromal cells, and germ cells [135]. Epithelial ovarian cancer (EOC) can be further sub-classified as serous (70%), endometrioid (20%), mucinous (5-10%), and clear cell (5-10%) [5]. However, the most common type of ovarian cancer, high grade serous, often display p53 mutations [136]. Gene associated with spontaneous EOC are classified in 4 groups: 1) sex steroid hormone pathway genes, 2) cell cycle genes, 3) DNA repair genes, and 4) oncogenes and onco-suppressor genes [137]. Mutations of K-Ras, B-Raf, and PTEN have been reported in mucinous, endometrioid, and low grade serous. Additionally, approximately 10% of ovarian cancer cases have been linked to hereditary alteration of *BRCA1* or *BRCA2* [138], however, a majority of cases are sporadic in origin [135].

The pathogenesis of ovarian cancer has been unclear, not only genetic alterations but also concerning its site of origin. Traditionally, the epithelial cells of the ovary were thought to be the primary site of origin for high grade serous adenocarcinomas but recent studies suggest that these tumors may arise from fallopian tube fimbria or fallopian tube-peritoneal junction and subsequently metastasize to the ovary as ovarian adenocarcinomas, fallopian tube carcinomas, and peritoneal carcinomas are all embryonically derived from Müllerian ducts [139-142]. In our







TgPTTG model, we observed animals with ovarian adenocarcinomas without fallopian tube adenocarcinomas. Furthermore, we noted animals that developed adenomyosis of the uterus, suggesting the ovary was the site of origin. However, in TgPTTG/p53<sup>+/-</sup> mice we noted a female that developed fallopian tube adenocarcinoma without an ovarian precursor lesion.

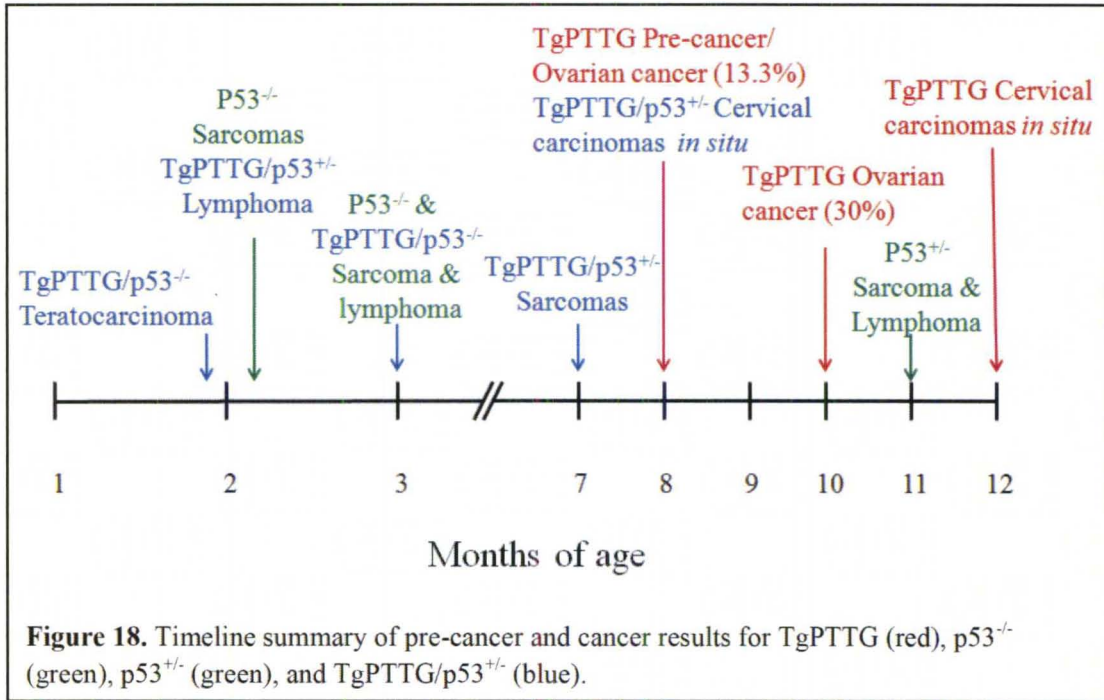
PTTG is an oncogene involved in pituitary carcinogenesis [115] and is overexpressed in ovarian cancer [116]. In a previous attempt to generate an ovarian cancer model representative of EOC, PTTG was placed under the control of MISIR in an effort to target it to the ovarian surface epithelium [130]. However, despite PTTG expression in the ovary and testes, these animals developed cystic glandular hyperplasia but failed to develop ovarian adenocarcinomas. However, abnormalities in the ovarian structure occurred resulting in an enlarged corpus luteum and corresponding hormone serum levels. This was possibly due to the weak promoter strength as the level of PTTG protein expression was crucial for tumor development [116]. Low levels of PTTG in the pituitary have been shown to cause senescence [100] rather than increase cell proliferation as seen in PTTG transfection of HEK 293 cells [102].

Due to the lack of specific ovarian promoter, we selected a strong non-specific CMV promoter, to induce the necessary level of PTTG to achieve this biological function, as the level of PTTG is critical for tumorigenesis [116, 120]. However, due to the nature of this promoter, it was necessary to analyze other tissues to determine if tumorigenesis has occurred. We found that the CMV promoter seems to target the ovary and fallopian tube and that PTTG expression caused the development of carcinomas. By using this approach, we were able to generate ovarian tumors as early as 8 months of age (Fig. 9) and continued to observe them at 10 months (Fig. 11). However, since our incidence of ovarian cancer was ~20%, we cross-bred our TgPTTG mice with p53<sup>+/-</sup> mice. Using this approach resulted in earlier tumor development than PTTG or p53<sup>+/-</sup> alone (Fig. 18) and increased our incidence of high grade leiomyosarcomas from 7% in p53<sup>+/-</sup> mice to 14% in TgPTTG/p53<sup>+/-</sup>. We also noted a significant incidence of cervical carcinomas of 63% in TgPTTG/p53<sup>+/-</sup>. Most cases of cervical cancer in women are due to human papilloma virus (HPV)

infections that cause inactivation of p53 and Rb, mutations that mainly affect the squamous epithelium along the transformation zone as HPV infections require cells that are proliferating [19]. In our TgPTTG mice, we noticed a reverse maturation of the basal squamous epithelium coupled to dysplasia. As PTTG increases cell proliferation as observed by PCNA staining, PTTG could serve to prime the basal epithelium, which could make these particular cells more susceptible to further neoplastic transformation due to alterations of additional genes, such as p53. We also noted a teratocarcinoma in TgPTTG/p53<sup>+/-</sup>. While little is known about the genetic contributions to teratocarcinomas, the field theory states that normal germ cells that are placed in an environment that allows expression of the cancer phenotype have the potential to become cancerous [143].

P53 has been shown to be an important oncogene in ovarian carcinomas. It is frequently mutated in 50-70% of ovarian carcinomas [144]. In combination with two other oncogenes *c-Myc*, *K-Ras*, and *Akt*, p53<sup>-/-</sup> mice developed ovarian tumors [59]. Contact mutant p53<sup>+/-</sup> mice cross-bred with *K-Ras* transgenic mice showed that contact mutant p53<sup>+/-</sup> acted in a dominant-negative fashion to promote K-Ras initiated lung adenocarcinomas with a subset developing sinonasal adenocarcinomas [145]. This was also the case in a p53<sup>+/-</sup>/K-Ras model of pancreatic cancer [146, 147] and pleomorphic rhabdomyosarcoma [148].

In conclusion, we show that PTTG is a functional oncogene that is capable of initiating transformation of normal tissue to dysplastic. Furthermore, a high expression level of PTTG was capable of tumorigenesis in the ovary and lead to tumorigenesis of the fallopian tube. Coupling PTTG overexpression with mutation of p53 led us to conclude that the early neoplastic events (normal to dysplastic) were independent of p53 as the additional mutation did not enhance our incidence of ovarian cancer. This suggests that p53 may not be the correct partner for PTTG, and further studies involving other potential oncogenes (K-Ras, B-Raf, c-Myc) and tumor suppressor genes (PTEN) in combination with PTTG may provide a better understanding of the transformation and tumorigenesis of ovarian cancer.



## CHAPTER 3

### WITHAFERIN A ENHANCES THE THERAPEUTIC EFFECT OF DOXORUBICIN THROUGH ROS-MEDIATED AUTOPHAGY IN OVARIAN CANCER CELLS

It is estimated that \$4.4 billion is spent annually in the US for the treatment of ovarian cancer [149]. While the mainline treatment of ovarian cancer is cytoreductive surgery followed by platinum-based chemotherapy (namely carboplatin and paclitaxel) [150-153], most patients relapse after achieving a complete response [154, 155]. If the relapse occurs less than 6 months after initial treatment, the carcinomas are considered platinum-resistant as is common in relapse, which accounts for approximately 70% of patients [155]. Due to the poor survival of women with platinum-resistant ovarian carcinomas, an alternative treatment strategy is desperately needed.

Doxorubicin (Dox) is a broad-spectrum anthracyclin isolated from *Streptomyces peucetius* that has been used for the treatment of several cancers, including ovarian, breast, and prostate [156]. In fact, anthracyclins are the most widely used USDA approved anticancer drugs [157]. Doxorubicin's effectiveness has been attributed to its ability to intercalate between the DNA strands to act as a topoisomerase II inhibitor and/or bind covalently to proteins involved in DNA replication and transcription [157]. However, despite side effects, patients treated with pegylated liposomal Dox (commercially known as Doxil) have a greater response rate (28.3%) than more conventional therapies [155] during clinical trials in the second-line setting [158-160]. Moreover, patients treated with Doxil have a reduction in death compared to patients on topotecan [159] or paclitaxel [161]. As such it remains a standard treatment option in patients that have platinum-resistant and recurrent ovarian cancer [162]. In a phase I clinical trial of 30 patients, Doxil was combined with bevacizumab in patients with recurrent or refractory ovarian cancer. Patients

achieved an overall response rate of 33% and a 6-months progression free survival of 47% with no treatment related deaths [162]. Additionally, in a multicenter phase III clinical trial of 976 patients with recurrent ovarian cancer, combination of Doxil with carboplatin vs. paclitaxel with carboplatin was statistically superior resulting in reduced severe nonhematologic toxicity, 28.4% vs. 36.8% respectively [161].

More recently combination therapy with Dox has garnered more attention. Combining Dox with sildenafil resulted in enhanced cell death through the down regulation of Bcl-2 coupled to an increase in caspase 3 and enhanced the Dox-induced generation of reactive oxygen species (ROS) while attenuating Dox-induced cardiac dysfunction [163]. Dox has also been combined with HO-3867, a synthetic curcumin analog, to achieve enhanced cell death and reduced cardiotoxicity through the use of lower doses of Dox [164]. Interestingly chebulagic acid, a COX-2/5-LOX dual inhibitor, lead to increased intracellular accumulation of Dox through modulation of multi-drug resistance transporter 1 (MDR1) to enhance Dox's cytotoxic effects [165]. MDR1 expression was down regulated in a Cox-2 dependent manner through inactivation of signal transduction pathways Akt, ERK, JNK, p38, and NF- $\kappa$ B [165]. However, some chemicals when combined have an antagonistic effect, such as sorafenib and Dox [166]. Dox requires that Raf/MEK/ERK signaling be intact for its mechanism of action to occur [167, 168], therefore the ERK inhibitor sorafenib acts counter to Dox, resulting in increased cell survival and reduced formation of autophagic vesicles [166].

Withaferin A (WFA) is bioactive steroidal lactone having withanolide skeleton as its basic structure. WFA is isolated from the plant *Withania somnifera*, which has been a part of Indian traditional medicine for centuries and is now available as an over-the-counter dietary supplement in the US. It was been used to treat various conditions due to its anti-inflammatory [169, 170] and anti-bacterial properties [171]. More recently, it has been suggested as a potential anti-cancer compound shown to inhibit tumor growth, angiogenesis, and metastasis [172, 173]. Several biological functions have been influenced by WFA including induction of apoptosis

through inactivation of Akt and NF- $\kappa$ B [174] as well as decrease of the pro-survival protein Bcl-2 [175, 176], G2/M cell cycle arrest [177], and generation of ROS [178, 179].

Autophagy is a dynamic process that is used to degrade large proteins and organelles, initiated by environmental stressors resulting in either adaptation and survival, or death [180]. This mode of cell death is characterized by the formation of a double membrane structure that encloses a portion of the cytoplasm as well as intracellular organelles known as an autophagosome [180]. These autophagosomes then fuse with lysosomes (to form an autolysosome) or late endosomes to degrade the contents [181, 182]. The Akt/mTOR/p70S6K signaling pathway acts as one gatekeeper of autophagy that exerts an inhibitory effect by activating anti-autophagic transcription and translation [183, 184]. DNA damaging agents lead to inactivation of mTOR evident by dephosphorylation of p70S6K and 4E-BP1 [185]. Conversely, Beclin-1 and the class III-type PI3K complex positively regulate autophagy [186].

A previous study has shown that WFA enhances the cytotoxic effect of Dox in an osteogenic sarcoma (U2OS) and breast cancer cell line (MCF-7) using a cell proliferation assay [187]. However, the combined effect of Dox and WFA has not been studied in ovarian cancer. We proposed that WFA will enhance Dox's cytotoxic effects so that a suboptimal dose of Dox can be used to achieve the same effects. We studied the combined effect of Dox and WFA on epithelial ovarian cancer cell lines A2780, A2780/CP70, and CAOV3. In addition, for the first time we show that cell death was induced by ROS production and DNA damage leading to the induction of autophagy and cell death in a caspase 3 dependent manner. We also show the effect of Dox and WFA on *in vitro* 3D tumors generated from A2780 cells on a human extracellular matrix. Furthermore, we examined for the first time the effect of this treatment *in vivo* on proliferation, angiogenesis, autophagy, cell death, and DNA damage using xenograft tumors produced from A2780 cells.

## Materials and Methods

### *Materials*

A2780 and A2780/CP70 cells were cultured in RPMI + 10% FBS + 1% Penicillin/Streptomycin + 0.05% (v/v) Insulin (Sigma) and maintained at humidified 37°C with 5% CO<sub>2</sub>. CAOV3 cells were cultured in DMEM + 10% FBS + 1% Penicillin/Streptomycin. Antibodies to phospho-Akt Ser<sup>473</sup>, Akt, phospho-p70S6K Thr<sup>389</sup>, p70S6K, phospho-BAD Ser<sup>136</sup>, Bcl-xL, cleaved caspase 3, and GAPDH were purchased from Cell Signaling Technology. Ki67 antibody was purchased from Santa Cruz Biotechnology, CD31 and LC3B from AbCam. Doxorubicin, withaferin A, N-acetyl-L-cysteine, catalase, superoxide dismutase, and DMSO were purchased from Sigma.

### *Cell treatments*

Cells were seeded overnight and treatments were performed in 5% FBS media by adding Dox (50, 100, 200, 300, 500, 1000 nM) and/or WFA (0.1, 0.5, 1, 1.5, 2, 3, 5 μM) and/or 0.1% DMSO as a vehicle control.

### *Cell proliferation assay*

A2780, A2780/CP70, and CAOV3 cells were seeded on 96-well plates and treated in triplicates for 24, 48, and 72 hr. Treatments were then replaced with MTT reagent (Promega) diluted in fresh 5% FBS media in a 1:5 ratio and incubated ~1 hr. Color was assessed by an ELISA scanner at 492 nM.

### *Flow cytometry for Annexin V*

Treated A2780 cells were dissociated with versene (Invitrogen), washed in PBS, and the pellet resuspended in Annexin Binding Buffer to a concentration of  $1 \times 10^6$  cells/mL. 2 μL of Annexin V-FITC (BD Biosciences) was incubated for 15 min in the dark in 100 μL of cells. Propidium iodide (PI) was then spiked in and 400 μL of Annexin Binding Buffer added and immediately run on a FACSCaliber (BD Biosciences) and analyzed with FlowJo software.



### *ROS assay*

A2780 cells were seeded on glass bottom 35 mm<sup>2</sup> dishes overnight prior to treatment. Treated cells were loaded with 2 μM 2',7'-dichlorodihydrofluorescein diacetate (H<sub>2</sub>DCFDA, Invitrogen) in growth media for 30 min at 37°C. Cells were then washed with PBS and viewed by confocal microscopy. Cells were counted from 3 representative fields at 20X magnification. ROS quantification was performed by seeding cells in a 96-well plate in triplicates, counterstaining live cells with 10 μg/mL Hoechst 33342 for 10 min for the total cell count, and reading with a multi-filter fluorometer.

### *TUNEL assay*

A2780 cells were seeded on chamber slides and treated cells as described for 24 hr. Cells were then assayed for DNA damage via DeadEnd Fluorometric TUNEL assay (Promega) according to the manufacturer's protocol. Briefly, cells were fixed with 4% formaldehyde in PBS for 25 min and permeabilized with 0.2% Triton X-100 in PBS for 5 min at RT. After equilibration, cells were incubated with dTdT reaction mix for 60 min at 37°C. Reaction was stopped with 2x SSC for 15 min. Cells were counterstained with PI to visualize nuclei.

TUNEL assay in tissue section was performed using an ApopTag Plus Peroxidase Apoptosis Detection Kit (Millipore) according to manufacturer's protocol.

### *Protein isolation and Western blotting*

A2780 cells were seeded on 6-well plates and treated with Dox (200 nM), WFA (0.5, 1.5, or 2 μM) in RPMI + 5% FBS + 0.5% penicillin/streptomycin + Insulin for 24 hr. Lysis buffer [1% (v/v) NP-40, 10% (v/v) glycerol, 137 mM NaCl, 20 mM Tris-HCl (pH 7.4), 4 mM PMSF, 1 mM Na<sub>3</sub>VO<sub>4</sub>, and 1% (v/v) Triton X-100 supplemented with proteinase inhibitor cocktail (Sigma) was added directly to the well and incubated on ice for 10 min then collected into a microcentrifuge tube and centrifuged at 14,000 rpm for 15 min at 4°C and the resulting supernatant collected. Samples were then quantitated using the Bradford method with a BSA standard. Proteins were resolved with SDS-PAGE and immunoblotted transferred to a nitrocellulose membrane (GE

Healthcare). Proteins were visualized by ECL or ECL plus (GE Healthcare). Blots were then re-probed with GAPDH to normalize differences in loading.

#### *Xenograft tumor formation*

A2780 cells were injected into 5-6 wk old nu/nu mice (Charles River) and tumors allowed to grow for 20 days until they reached 1 cm<sup>2</sup> in size. The mice were then randomized into 6 groups: 1) negative control with PBS, 2) control vehicle 10% DMSO, 3) Dox 9 mg/kg, 4) Dox 1 mg/kg, 5) WFA 2 mg/kg, and 6) Dox 1mg/kg + WFA 2mg/kg. Tumor measurements were taken every other day and treatments given i.p. in 100  $\mu$ L injections. Mice were sacrificed after 12 days of treatment. All treatments were approved by IACUC, University of Louisville.

#### *Immunohistochemistry*

Xenograft tumors were fixed in 10% neutral buffered formalin and embedded in paraffin for sectioning. Slides were deparaffinized in xylene and rehydrated in a graded series of ethanol. Antigen retrieval was conducted by incubating the slides in 10mM Sodium Citrate pH 6.0 for 20 min at 95°C. After washing in PBS, slides were incubated in 0.3% H<sub>2</sub>O<sub>2</sub> in methanol for 20 min. Following washing, slides were processed using the Vectastain ABC Elite Anti-Rabbit kit (Vector Labs) with overnight incubation of the primary antibody. Color was developed using DAB (Vector Labs) and counterstained with hematoxylin QS (Vector Labs) to stain nuclei. Primary antibodies used were Ki67 (diluted 1:50, Santa Cruz Biotechnology), CD31 (1:50, AbCam), LC3B (1:500, AbCam), and caspase 3 (1:200, Cell Signaling).

#### *3D in vitro tumor growth*

1.5 x 10<sup>4</sup> cells were combined with Hubiogel in a 1:4 ratio, dispensed into 10  $\mu$ L beads, allowed to polymerize, and then warm complete media was added to the cells. After two weeks, the cell beads were individually transferred to one well of a 96-well plate and treated twice weekly with 1) media control, 2) DMSO vehicle control, 3) Dox 0.2  $\mu$ M, 4) Dox 2  $\mu$ M, 5) WFA 0.5  $\mu$ M, 6) WFA 1.5  $\mu$ M, 7) Dox 0.2  $\mu$ M + WFA 0.5  $\mu$ M, and 8) Dox 0.2  $\mu$ M + WFA 1.5 $\mu$ M for 7 days.

### *MTT assay for 3D tumors*

MTT assay was performed by adding 20  $\mu$ L MTT stock solution (12 mM) to each cell bead in a 96-well plate and incubating for 2 hr until formazan crystals were visible. Then 150  $\mu$ L of 10% SDS solution was incubated overnight and read absorbance at 570 nm.

### *Microscopy of 3D tumors*

One cell bead was placed in a 96-well plate and volume corrected to 100  $\mu$ L. Calcein AM (0.5  $\mu$ M) was added to each well and incubated for 30 min. Images were acquired on Nikon B-2E/C FITC filter block ( $I_{ex}$  465-495nm,  $I_{em}$  515-555nm).

## **Results**

### *WFA enhances the anti-proliferative effect of doxorubicin of ovarian cancer cells*

Dox is typically used at 5  $\mu$ M to mimic the concentration found in plasma of patients undergoing Dox treatment [188]. However, at this dose, patients present with serious side effects as a concentration of 1  $\mu$ M needs to be maintained for the various mechanism of actions to occur [188]. The effect of Dox alone was first assessed in a dose-dependent manner. Cell death was assessed by MTT assay. After 24 hr of treatment, Dox alone produced an  $IC_{50}$  value of 2  $\mu$ M (Fig. 19a). To assess if WFA could enhance the effect of Dox, we combined a steady dose of WFA (1.5  $\mu$ M) with Dox. Combination reduced the  $IC_{50}$  to 0.3  $\mu$ M (Fig. 19a). Dose-dependent WFA treatment produced an  $IC_{50}$  value of 3  $\mu$ M, which was enhanced by the addition of Dox 200 nM to 1.7  $\mu$ M (Fig. 19b).

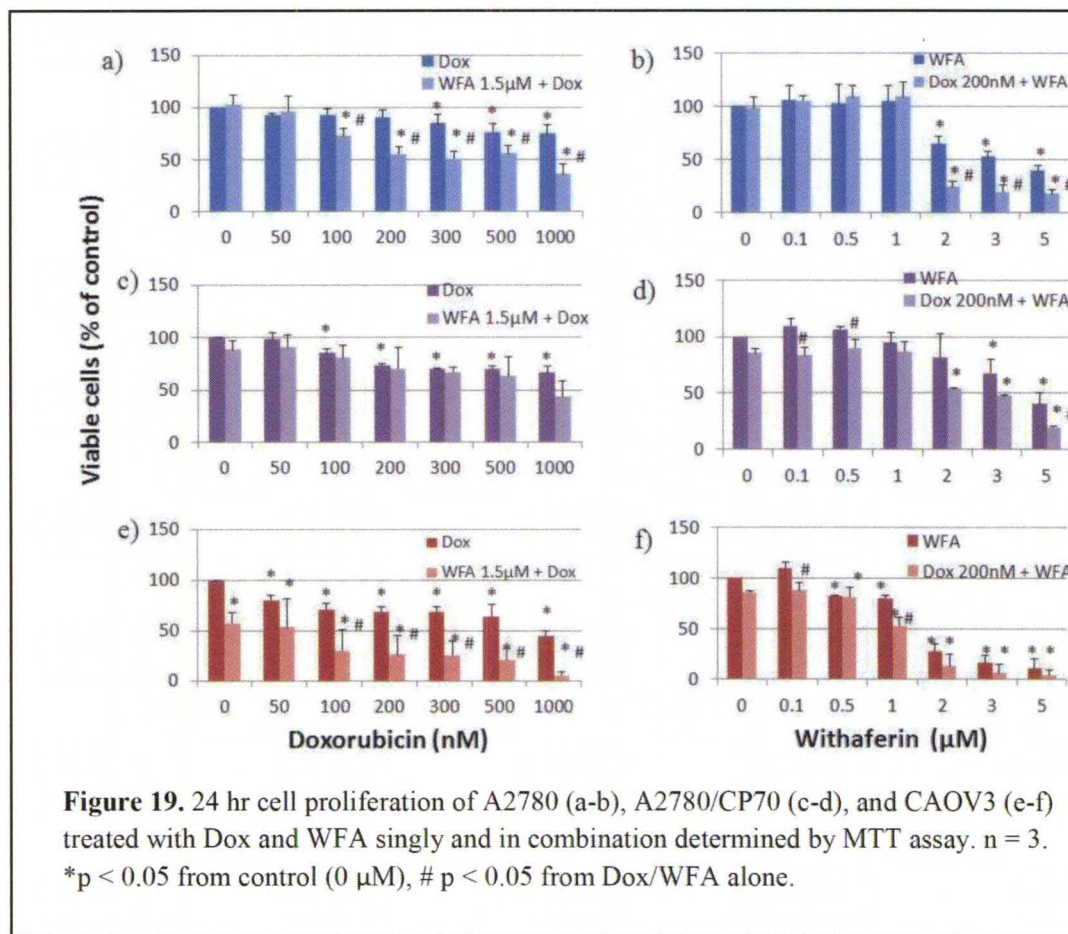
To assess the efficacy of combination therapy against cisplatin resistant ovarian cancer, we used the cisplatin-resistant cell line A2780/CP70. Dox alone produced an  $IC_{50}$  value of 1.5  $\mu$ M after 24 hr of treatment (Fig. 19c). Addition of WFA 1.5  $\mu$ M to Dox further enhanced cell death and reduced the  $IC_{50}$  value to 0.7  $\mu$ M (Fig. 19c). A2780/CP70 cells were less sensitive to WFA, requiring 4  $\mu$ M to achieve 50% cell death (Fig. 19d). Addition of Dox 200 nM enhanced this effect and resulted in an  $IC_{50}$  value of 2  $\mu$ M (Fig. 19d).

We also tested the effect of combination therapy on p53 mutant cell line CAOV3 as p53 mutations can be found in 50-70% of human ovarian carcinomas [144]. CAOV3 cells were more sensitive to Dox, since as little as 0.7  $\mu\text{M}$  was able to cause 50% of cell death after 24 hr (Fig. 19e). CAOV3 cells were also extremely sensitive to WFA as 1.6  $\mu\text{M}$  caused 50% cell death (Fig. 19f). Combination of Dox 200 nM with WFA reduced the  $\text{IC}_{50}$  value to 1.0  $\mu\text{M}$ .

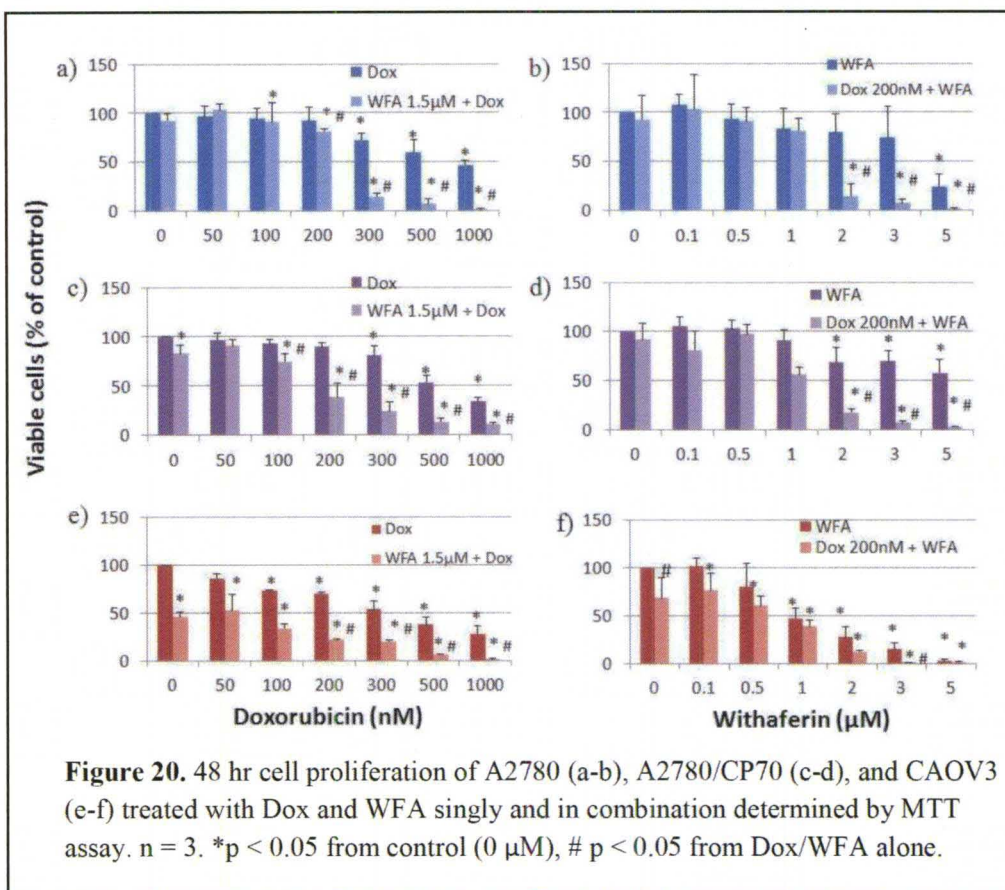
After 48 hr of treatment of A2780 cells, Dox 0.8  $\mu\text{M}$  produced 50% cell death (Fig. 20a). Combining a steady dose of WFA 1.5  $\mu\text{M}$  in a dose-dependent manner with Dox enhanced cell death and reduced the  $\text{IC}_{50}$  of Dox to 0.16  $\mu\text{M}$  (Fig. 20a). Dose-dependent concentrations of WFA alone resulted in 50% cell death 4.1  $\mu\text{M}$  (Fig. 20b). However, when combined with Dox 200 nM, the  $\text{IC}_{50}$  of WFA was reduced to 1.5  $\mu\text{M}$  (Fig. 20b). In A2780/CP70 cells the  $\text{IC}_{50}$  value for Dox was 0.65  $\mu\text{M}$ . However, combination with WFA 1.5  $\mu\text{M}$  enhanced the  $\text{IC}_{50}$  of Dox to 0.18  $\mu\text{M}$  (Fig. 20c). WFA alone required 6  $\mu\text{M}$  to achieve 50% cell death (Fig. 20d), but was reduced to 1.2  $\mu\text{M}$  with the addition of Dox 200 nM (Fig. 20d). CAOV3 cells were more sensitive to Dox and WFA requiring Dox 300 nM (Fig. 20e) and WFA 1  $\mu\text{M}$  (Fig. 20f) to achieve 50% inhibition. When Dox was combined with WFA 1.5  $\mu\text{M}$ , 50% inhibition was achieved with Dox 50 nM (Fig. 20e), while WFA was reduced to 0.7  $\mu\text{M}$  when combined with Dox 200 nM (Fig. 20f). A summary of  $\text{IC}_{50}$  values for each cell line in response to Dox, WFA, and in combination can be found in Table 1.

After 72 hr of treatment, the  $\text{IC}_{50}$  for Dox in A2780 was 0.4  $\mu\text{M}$ , while addition of WFA 1.5  $\mu\text{M}$  reduced the  $\text{IC}_{50}$  to 0.1  $\mu\text{M}$  (Fig. 21a). WFA 1.7  $\mu\text{M}$  resulted in 50% cells and was reduced to 1.3  $\mu\text{M}$  with the addition of WFA 1.5  $\mu\text{M}$  (Fig. 21b). In A2780/CP70, the  $\text{IC}_{50}$  for Dox was 0.5  $\mu\text{M}$ , while addition of WFA 1.5  $\mu\text{M}$  reduced the  $\text{IC}_{50}$  to 0.35  $\mu\text{M}$  (Fig. 21c). WFA 2  $\mu\text{M}$  resulted in 50% cells and was reduced to 1.3  $\mu\text{M}$  with the addition of WFA 1.5  $\mu\text{M}$  (Fig. 21d). In

CAOV3, the IC<sub>50</sub> for Dox was 0.3 μM (Fig. 21e) and for WFA 1 μM, which was reduced to WFA 0.75 μM with the addition of Dox 200 nM (Fig. 21f).



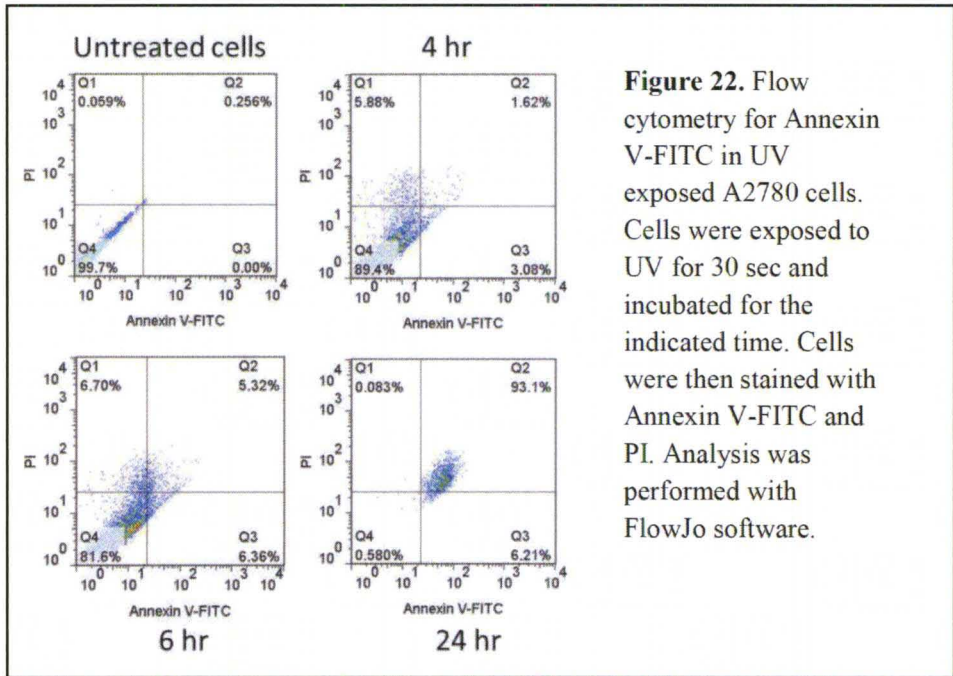
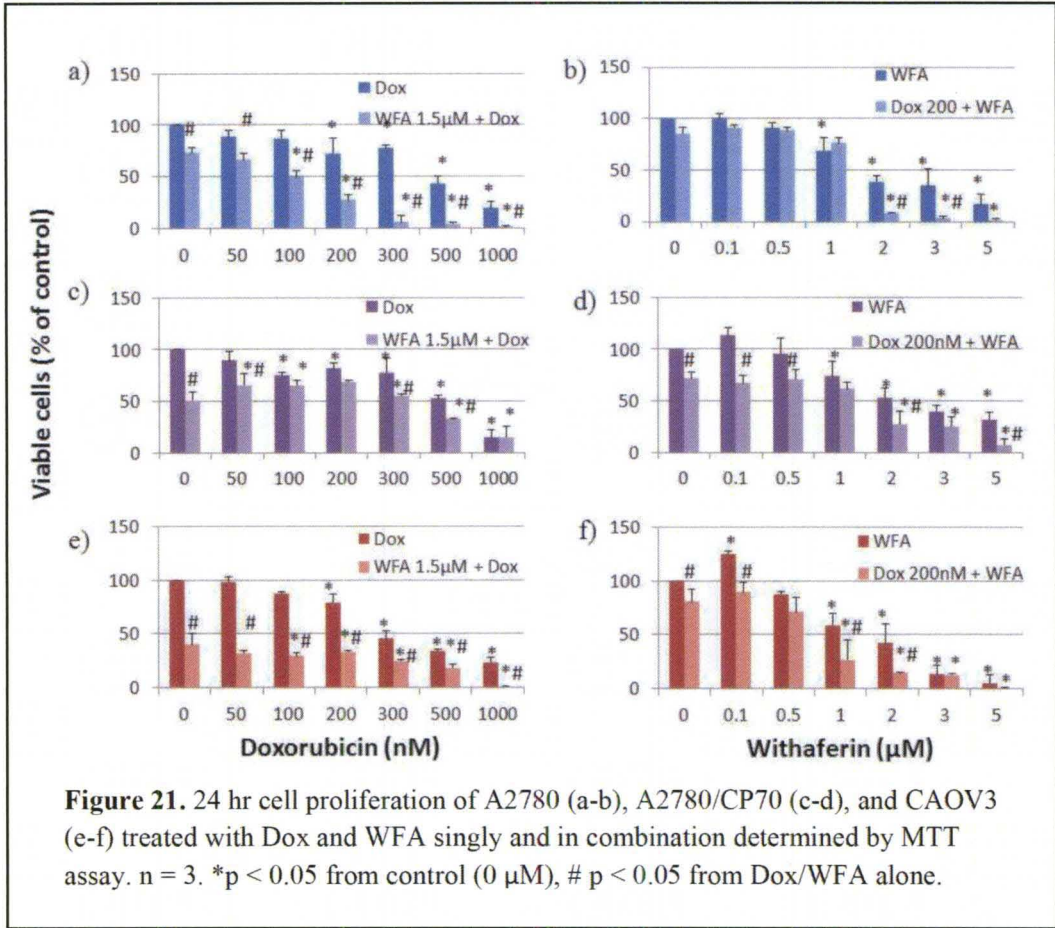
After 72 hr of treatment, addition of WFA 1.5 μM significantly reduced the cell viability when combined with various doses of Dox in A2780 (Fig. 21a), A2780/CP70 (Fig. 21c), and CAOV3 (Fig. 21e). In A2780, Dox 500 nM was necessary to achieve 50% inhibition, but when Dox was combined with WFA 1.5 μM, only 100 nM was needed (Fig. 21a). WFA alone significantly reduced cell viability in all three cells lines at 1 μM (Fig. 21b, d, f). Combination of Dox 200 nM with WFA significantly improved treatment in A2780/CP70 at nearly all concentrations of WFA (Fig. 21d).

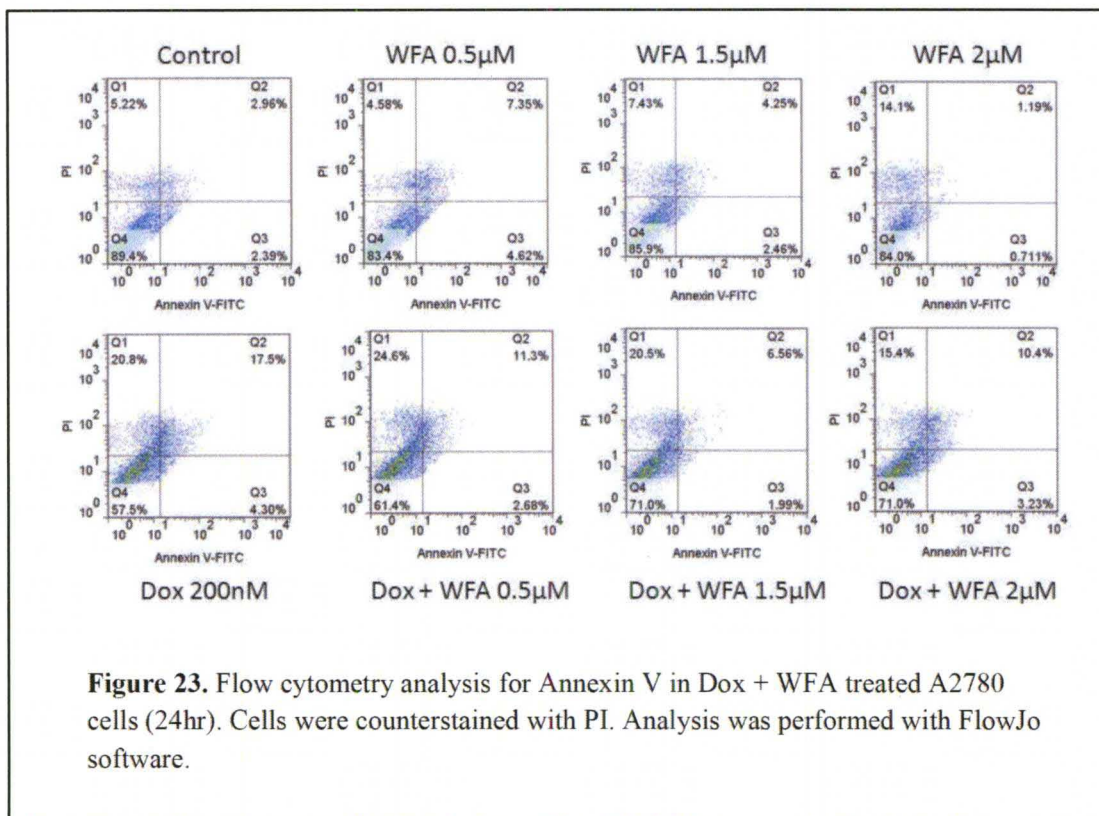


We performed Annexin V-FITC flow cytometry to determine if apoptosis was the cause of cell death in A2780 cells treated with Dox and WFA alone and in combination. Positive control samples were produced using UV exposure for 30 sec and analyzing cells after 4 hr, 6 hr, and 24 hr after exposure to ensure efficiency of staining (Fig. 22). Analysis of Dox, WFA, and Dox + WFA treated samples showed a non-significant increase over control for Annexin V (Fig. 23), indicating that an alternative pathway is being used to cause cell death.

*Dox enhances the WFA-induced inactivation of Akt pathway*

The effect of WFA on Akt inactivation has been well documented in numerous cell lines [174, 189, 190] including ovarian cancer cell lines CAOV3 and SKOV3 [191]. Using A2780, we examined the effect of Dox and WFA alone and in combination on Akt phosphorylation. After 24 hr of treatment, we found phospho-Akt<sup>473</sup> (p-Akt) increased with Dox treatment, while there were no significant changes in WFA treated cells (Fig. 24). Total Akt did not change significantly





with treatment (Fig. 24). One of the main downstream targets of Akt in mammalian cells is mammalian target of rapamycin (mTOR), which is responsible for protein synthesis and cell growth through activation by phosphorylation of p70 ribosomal subunit 6 kinase (p70S6K) [192-195]. We found that phospho-p70S6K<sup>389</sup> (p-p70S6K) increased in response to Dox treatment and more subtly with WFA alone and was further enhanced with combination treatment in a dose-dependent manner (Fig. 24). Interestingly, while p-p70S6K markedly increased, total p70S6K decreased accordingly (Fig. 24).

Akt phosphorylates BAD at Ser<sup>136</sup> (pBAD<sup>136</sup>) as a means to regulate apoptosis [196]. While investigating apoptosis in our system, we examined pBAD<sup>136</sup> as well as Bcl-xL. pBAD<sup>136</sup> was only significantly increased in Dox + WFA 1.5 µM, while the rest of the treatments did not alter expression (Fig. 24). Bcl-xL levels did not change (Fig. 24), suggesting that intrinsic apoptosis is not responsible for our observed cell death.



After 48 hr of treatment WFA led to the inactivation of Akt in a dose-dependent manner and addition of Dox enhanced this effect (Fig. 24). Total Akt was not affected until Dox was combined with WFA 2  $\mu$ M (Fig. 24). Interestingly, we found that Dox 200 nM, WFA 1.5  $\mu$ M, and WFA 2  $\mu$ M alone reduced the total amount of p70S6K which was more pronounced with combination Dox + WFA 1.5  $\mu$ M (Fig. 24). Combination treatment of Dox + WFA 2  $\mu$ M resulted in the complete down regulation of p70S6K (Fig. 24). pBAD<sup>136</sup> was significantly downregulated in all treatment groups with the most drastic effect noticed with Dox alone (Fig. 24).

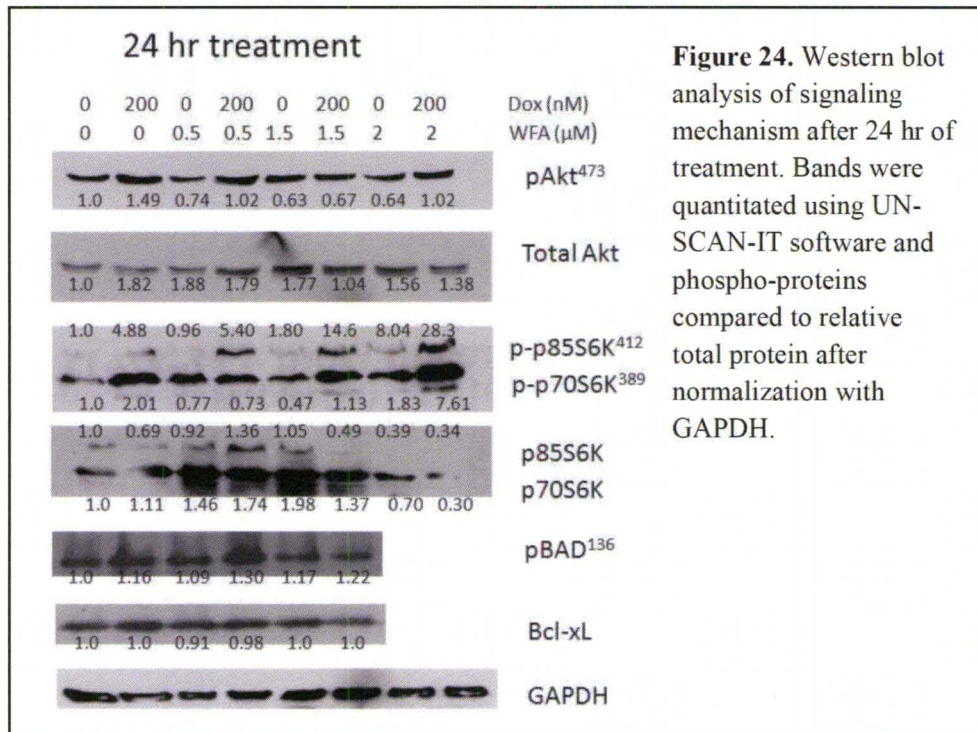
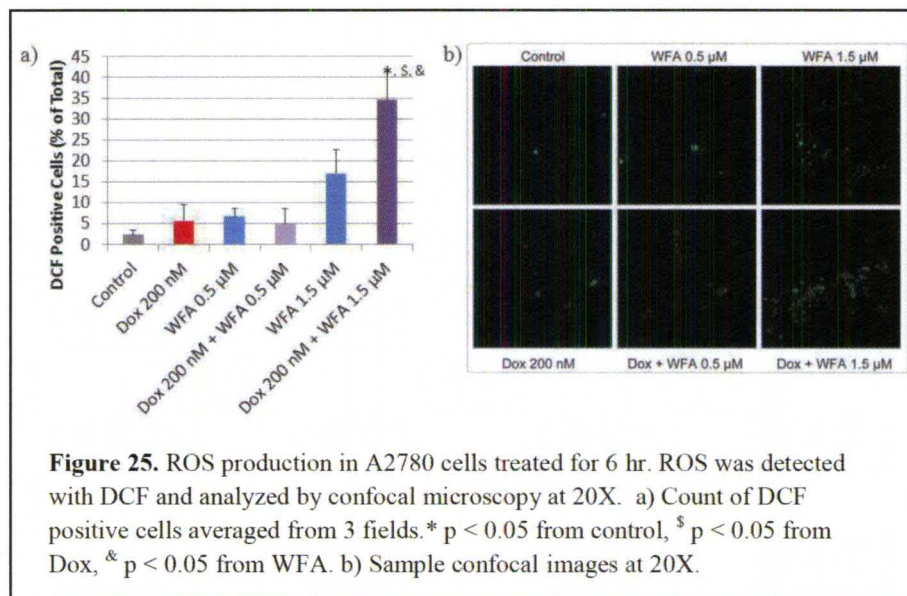


**Figure 24.** Western blot analysis of signaling mechanism after 24 hr of treatment. Bands were quantitated using UN-SCAN-IT software and phospho-proteins compared to relative total protein after normalization with GAPDH.

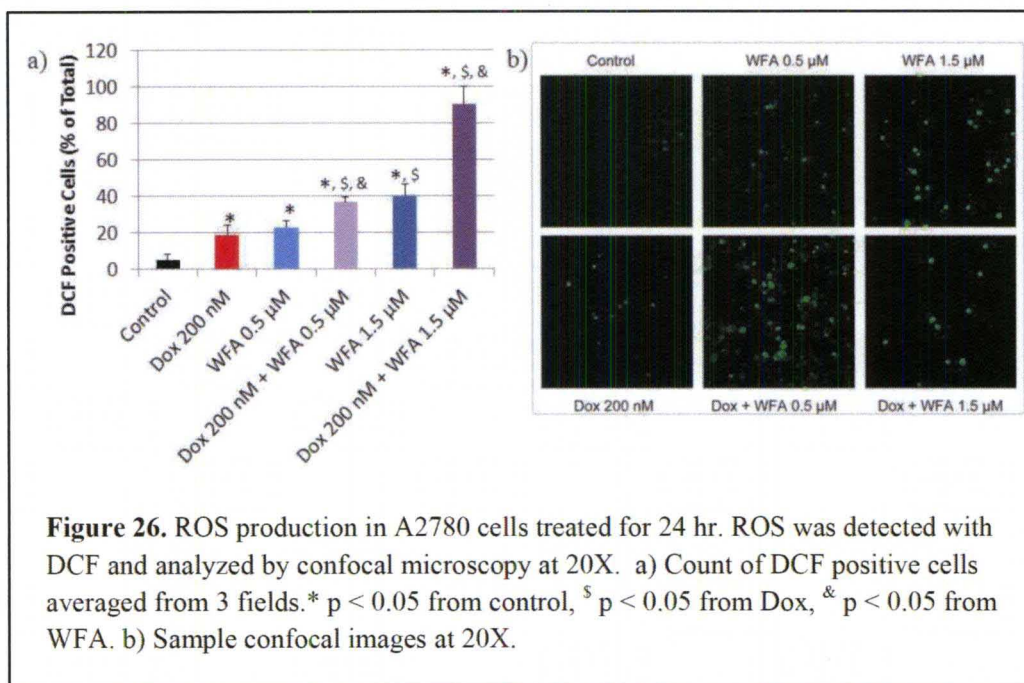
#### *ROS-induced cell death*

Dox is known to produce ROS as a part of its mechanism [156, 157]. There have also been numerous reports about WFA generating ROS production as a part of its apoptotic mechanism in various cancer types [175, 178, 179, 190]. Therefore, we asked whether WFA could enhance the effect of the low concentration of Dox after 24 hr of treatment using the detection agent H<sub>2</sub>DCFDA, which is a stable non-polar compound that is readily diffused into the

cells. This compound is then hydrolyzed by intracellular esterases to form DCFH, which in turn is oxidized by hydrogen peroxide to yield the highly fluorescent compound 2',7'-dichlorofluorescein (DCF) [190]. Consistent with reports [163, 197], after 6 hr of treatment WFA 1.5  $\mu\text{M}$  was significantly elevated over control cells from 2% to 17% (Fig. 25a-b). Combination of WFA 1.5  $\mu\text{M}$  + Dox 200 nM further increased ROS production to 59% (Fig. 25a-b). After 24 hr of treatment Dox 200 nM showed a low level of ROS positive cells, 18% (Fig. 26a-b). While WFA 0.5  $\mu\text{M}$  (23%) was not significantly different from Dox, combination of Dox + WFA 0.5  $\mu\text{M}$  increased ROS production to 37%. This effect was even more pronounced with Dox + WFA 1.5  $\mu\text{M}$ , which increased to 90% from 40% with WFA 1.5  $\mu\text{M}$  alone (Fig. 26a-b). However, after 24 hr of treatment, WFA 2  $\mu\text{M}$  caused a significant amount of cell death and damaged the cells too severely to produce ROS.

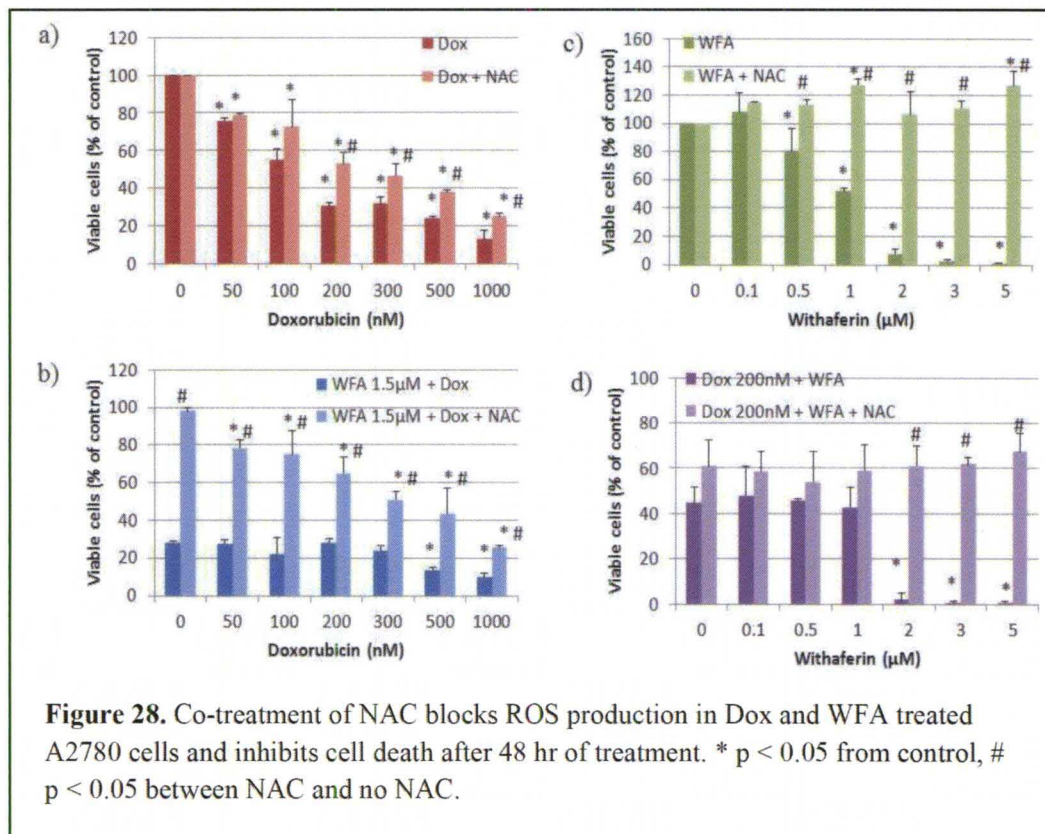
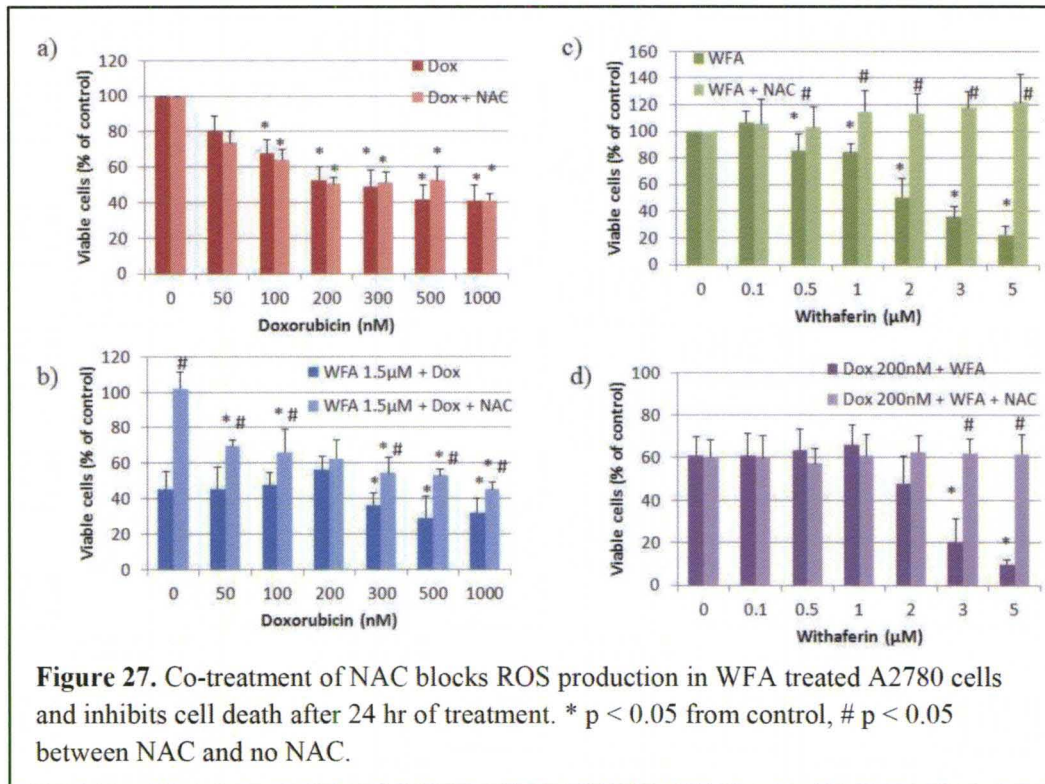


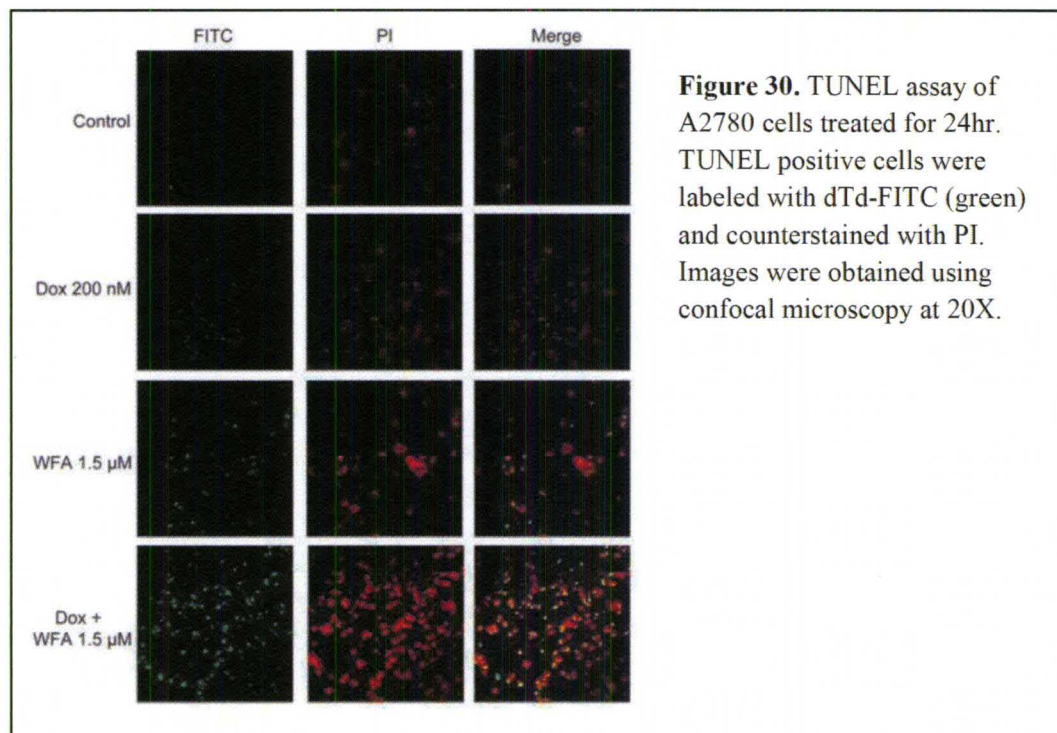
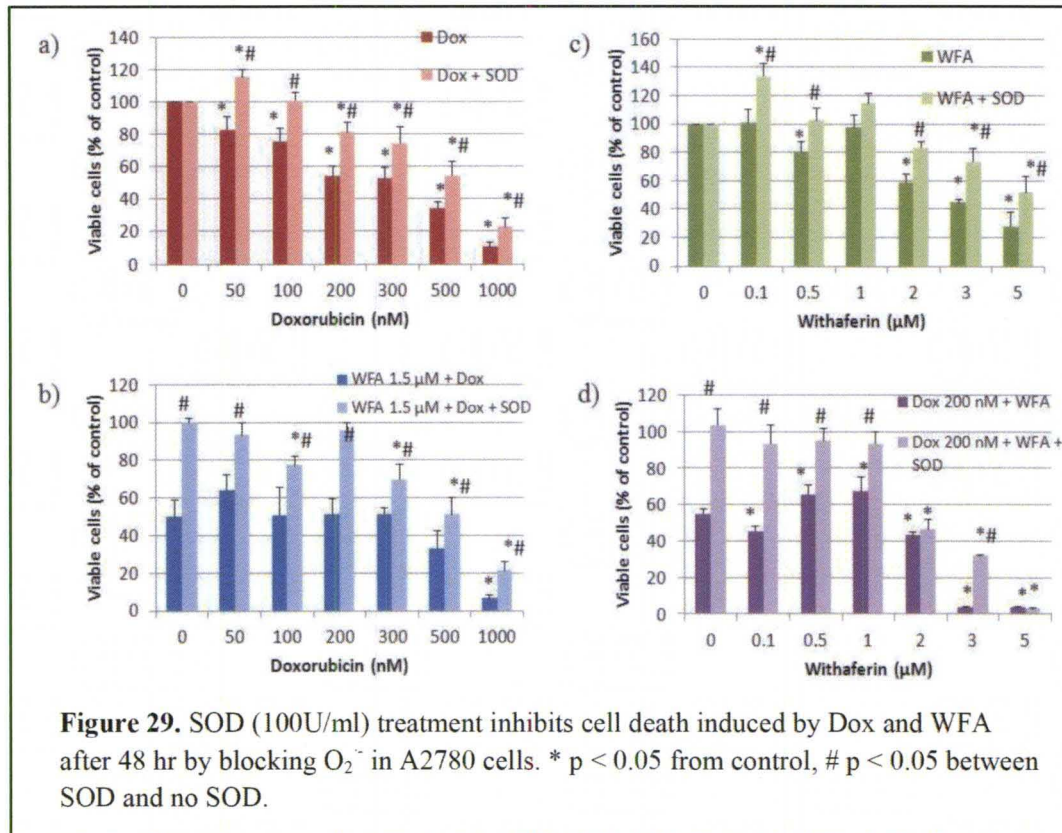
To confirm that ROS are responsible for cell death, we co-treated A2780 cells with 5 mM N-acetyl-L-cysteine (NAC), or with enzymatic inhibitors 500 U/ml catalase or 100 U/ml superoxide dismutase (SOD) with Dox and WFA treatments for 24 and 48 hr. While NAC did not block cell death induced by Dox (Fig. 27a-b), it was very effective in blocking cell death induced



by WFA (Fig. 27c-d) after 24 hr. However, after 48 hr NAC resulted in a partial blockage of Dox (Fig. 28a-b) while blocking the effect by WFA (Fig. 28c-d). SOD specifically catalyzes superoxide anions ( $O_2^-$ ) [198], while catalase is used by cells to degrade hydrogen peroxide ( $H_2O_2$ ) [199]. We saw no blockade of cell death in cells treated with catalase; however, SOD provided a significant reduction of cell death in Dox and WFA treated cells in monotherapy and combination therapy, demonstrating that  $O_2^-$  are the major ROS produced (Fig. 29a-d).

As ROS causes DNA damage, we performed the TUNEL assay to visualize the extent of DNA damage when treated with Dox and WFA alone and in combination. After 24 hr of treatment, Dox 200 nM resulted in a few positive cells while WFA 1.5 μM alone increased the number of positive cells (Fig. 30). Treatment with Dox 200 nM + WFA 1.5 μM significantly increased the number of positive cells causing DNA damage in nearly every cell (Fig. 30).

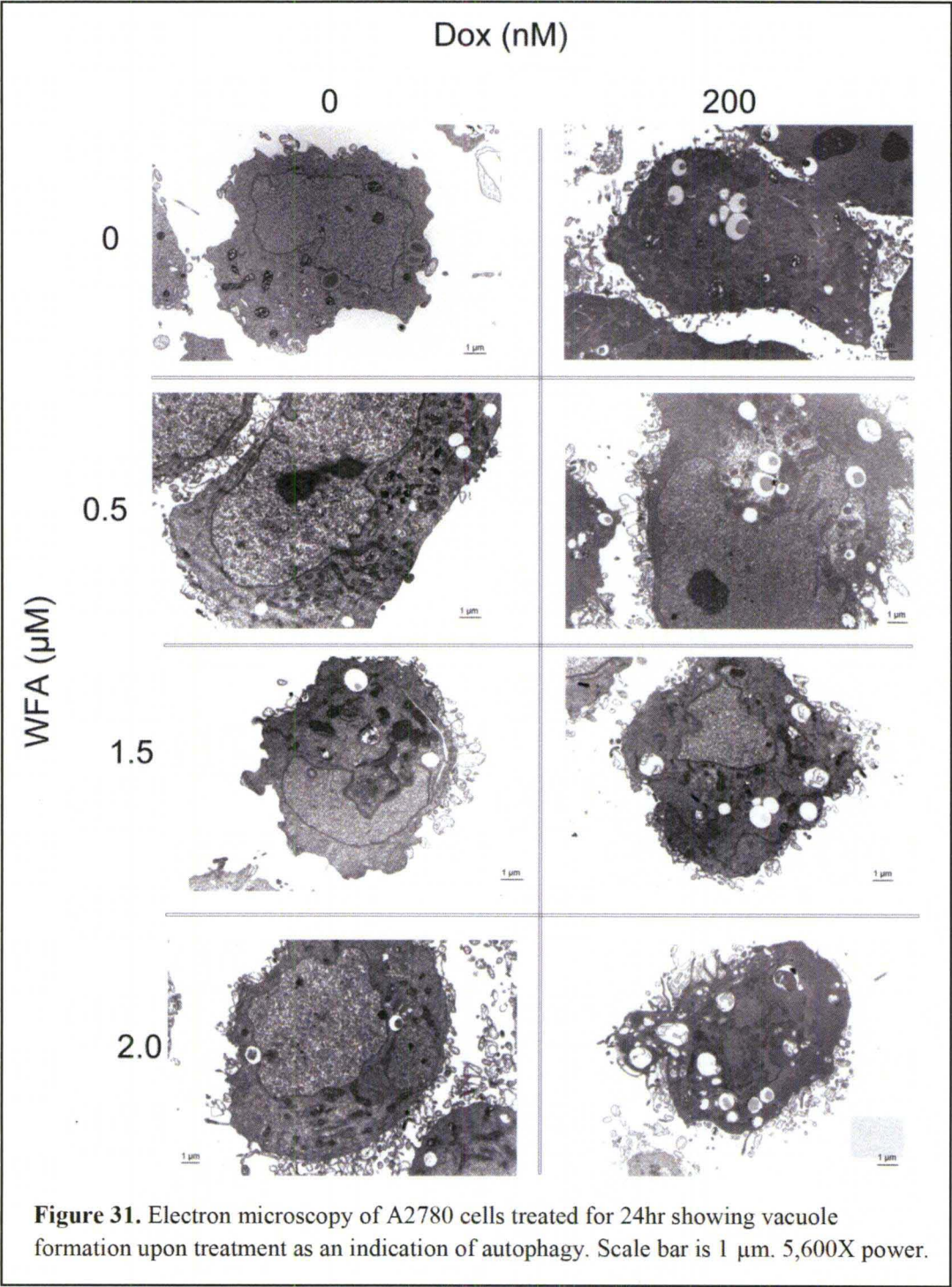


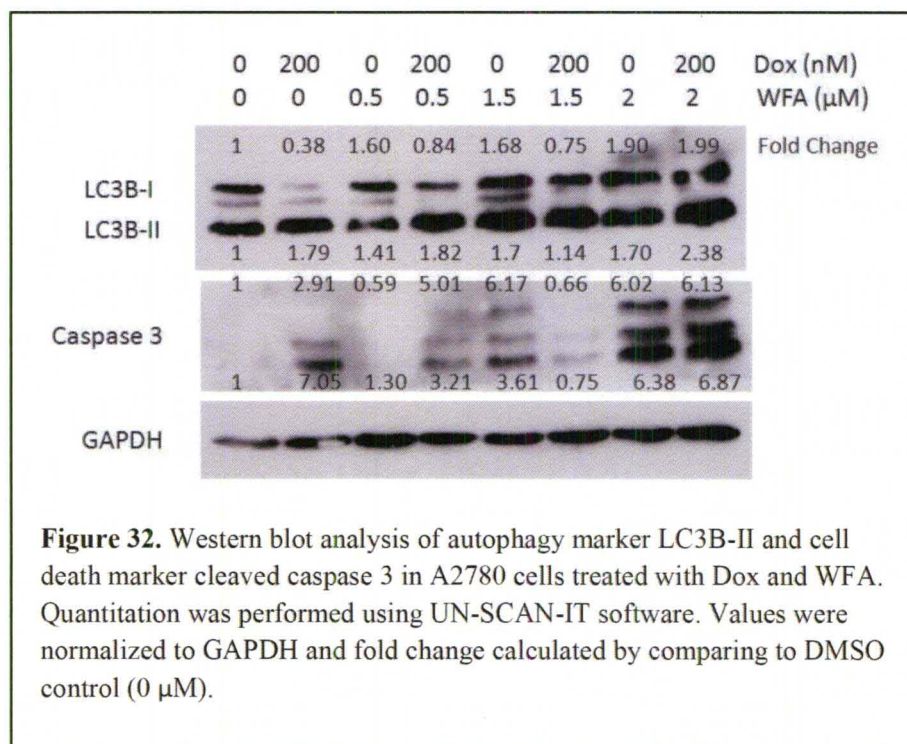


### *Dox and WFA induce cell death by autophagy*

The Akt/mTOR/p70S6 kinase signaling pathway acts as one gatekeeper of autophagy that exerts an inhibitory effect by activating anti-autophagic transcription and translation [183, 184]. DNA damaging agents lead to inactivation of mTOR evident by dephosphorylation of p70S6K and 4E-BP1 [185]. Therefore investigating the role of chemotherapy agent Dox combined with WFA in autophagy is an avenue of interest. Electron microscopy revealed control cells treated with DMSO have intact mitochondria (black arrows) and nuclear envelop (Fig. 29). While WFA 0.5  $\mu\text{M}$  alone had little to no effect, WFA 1.5 and 2  $\mu\text{M}$  showed some autophagosomes but left the mitochondria intact. Dox alone produce formation of autophagosomes containing cytoplasm with little mitochondria. Dox with WFA 0.5  $\mu\text{M}$  or 1.5  $\mu\text{M}$  produced an enhanced effect in a dose-dependent manner. Dox + WFA 2  $\mu\text{M}$  showed intense autophagic vacuoles, collapse of the nuclear envelop, and absence of mitochondria (Fig. 31).

To confirm that cells were undergoing autophagy, the canonical marker of autophagosome formation microtubule-associated protein-1 light chain 3B (LC3B) [166] was evaluated. Western blot analysis showed two specific bands: an upper band (18 kDa) representing LC3B-I and a lower band (16 kDa) corresponding to LC3B-II (Fig. 32). Cytosolic LC3B-I is converted to LC3B-II through lipidation and allows LC3B-II to become associated with autophagic vesicles [200]. Treatment with Dox induced production of LC3B-II (Fig. 32), while WFA alone stimulated production of the pre-cursor LC3B-I as well as LC3B-II (Fig. 32). Combination treatment enhanced LC3B-II in a dose-dependent manner with Dox + WFA 2  $\mu\text{M}$  showing the greatest intensity (Fig. 32). Furthermore, we investigated cleaved caspase 3 as a marker for cell death. Western blot analysis showed a modest increased in Dox 200nM treated cells. WFA 0.5  $\mu\text{M}$  showed no indication of cell death, while WFA alone showed a dose-dependent increase in the amount of cleaved caspase 3. Furthermore, combination treatment enhanced cell death in a dose dependent manner (Fig. 32).

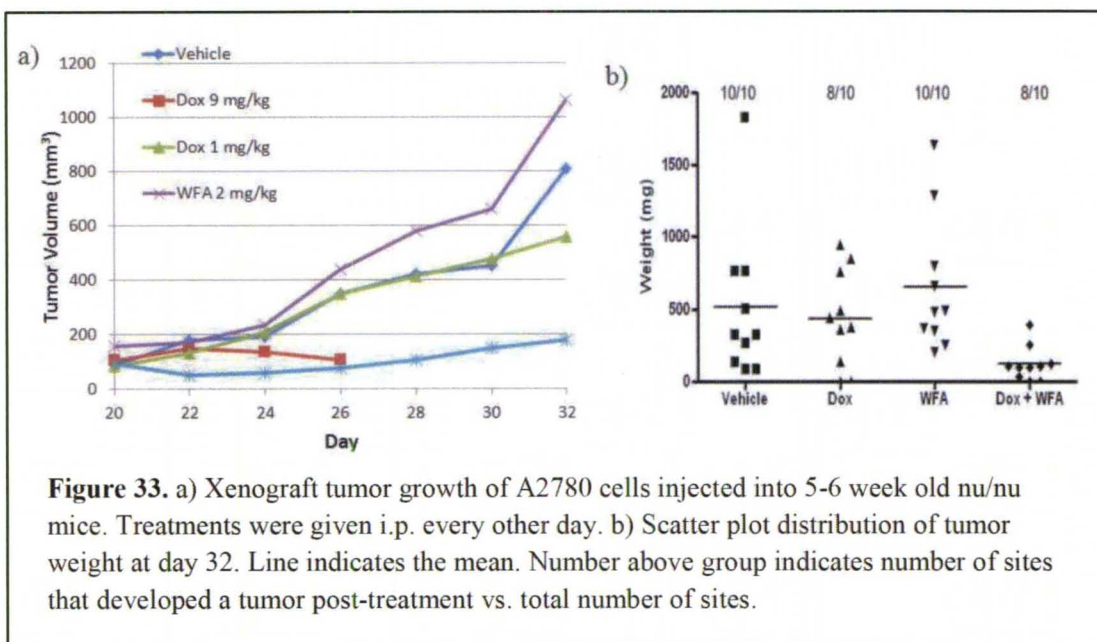




*Effect of Dox + WFA on xenograft tumorigenesis*

A2780 cells ( $2 \times 10^6$ ) were subcutaneously injected bilaterally in the ventral flank of 5-6 week old nu/nu mice. Tumors were allowed to grow until they reach  $1 \text{ cm}^2$  in size. At day 20 post-cell injection, mice were randomized into 6 treatment groups of 5 mice each: 1) negative control with PBS, 2) vehicle control of 10% DMSO, 3) Dox 9 mg/kg, 4) Dox 1 mg/kg, 5) WFA 2 mg/kg, and 6) Dox 1 mg/kg + WFA 2 mg/kg. Tumors were measured every other and mice given  $100 \mu\text{L}$  i.p treatment for 12 days for a total time of 32 days. Mice receiving Dox 9 mg/kg appeared uncomfortable after the first treatment and died after 4 treatments. Mice in the other treatment groups tolerated receiving the treatment. The tumor volume was not significantly different between vehicle, Dox 1 mg/kg, and WFA 2 mg/kg. However mice receiving Dox 1 mg/kg + WFA 2 mg/kg showed a significant reduction in tumor growth (Fig. 33a). Similarly, tumor weight measured at day 32 showed a drastic decrease in the Dox 1 mg/kg + WFA 2 mg/kg group (Fig. 33b).





H&E analysis identified the tumors as serous adenocarcinoma (Fig. 34). Vehicle group tumors were high grade with extensive necrosis. Dox 1 mg/kg group also had extensive necrosis. However, WFA 2 mg/kg and Dox 1 mg/kg + WFA 2 mg/kg were poorly differentiated with tumor necrosis. Immunohistochemistry for Ki67, a proliferation marker, showed intense staining in the vehicle group with less intense staining in Dox 1 mg/kg and WFA 2 mg/kg. Dox 1 mg/kg + WFA 2 mg/kg showed no staining for Ki67, showing that combination therapy effectively reduces tumor growth (Fig. 32). Microvessel marker CD31 has also stained. Vehicle control tumors showed a high amount of microvessel formation, which was reduced in Dox 1 mg/kg and WFA 2 mg/kg. Dox 1 mg/kg + WFA 2 mg/kg tumors were no significantly different from Dox or WFA alone (Fig. 34).

We also performed immunohistochemistry for autophagy marker LC3B. Tumors receiving vehicle control showed a nest of positive cells whereas tumors receiving Dox 1 mg/kg, WFA 2 mg/kg, or combination showed more dispersed staining (Fig 34). Staining for caspase 3 showed a low level of staining in DMSO and WFA 2 mg/kg treated tumors. Caspase 3 was

increased in Dox 1 mg/kg and further enhanced in Dox 1 mg/kg + WFA 2 mg/kg treated tumors (Fig. 34).

TUNEL assay in tumors revealed positive cells in animals receiving Dox 1 mg/kg with a lower amount in WFA 2 mg/kg (Fig. 32). However, combination of Dox 1mg/kg + WFA 2 mg/kg showed enhanced staining over monotherapy along (Fig. 34).

#### *Effect of Dox + WFA on 3-D tumors in vitro*

Hubiugel has been shown to represent the human matrix more accurately than Matrigel in order to predict preclinical endpoints [201]. A2780 cells were cultured to 70-80% confluency and 15,000 cells were mixed with Hubiugel in a 1:4 ratio to form 10  $\mu$ L beads that were suspended in warm complete media and given the following doses twice weekly: 1) Dox 0.2  $\mu$ M, 2) Dox 2.0  $\mu$ M, 3) WFA 0.5  $\mu$ M, 4) WFA 2.0  $\mu$ M, 5) Dox 0.2  $\mu$ M + WFA 0.5  $\mu$ M, and 6) Dox 0.2  $\mu$ M + WFA 2  $\mu$ M. Measurements were taken at day 1, 3, and 7 for MTT assay and microscopy. Media and DMSO treated cells continued to grow throughout treatment, whereas Dox 0.2  $\mu$ M had their growth halted at day 7 (Fig. 35a). Dox 2.0  $\mu$ M and WFA 2.0  $\mu$ M treated cells showed reduced tumor growth and showed a more pronounced effect with Dox 0.2  $\mu$ M + WFA 2.0  $\mu$ M (Fig 31a). Dox 0.2  $\mu$ M + WFA 0.5  $\mu$ M achieved a drastically reduced growth compared to monotherapy of either compound (Fig. 35a). Microscopy images from day 3 and day 7 are shown in Fig. 31c and 31c respectively.

#### **Discussion**

The cytotoxic activity of WFA was been established as an  $IC_{50}$  of  $\sim 5$   $\mu$ M after 72 hr in a panel of cancer cell lines and transformed fibroblast cell line [202], however this did not include an ovarian cancer cell line. WFA doses less than 500 nM did not affect cell proliferation [202]. However, in our study we noticed that as little as WFA 300 nM resulted in a noticeable decrease in cell proliferation in A2780 as well as CAOV3 cells (Fig. 19-21). Consistent with previous reports on Dox and WFA, we confirm that both agents produce ROS. Combination of Dox +

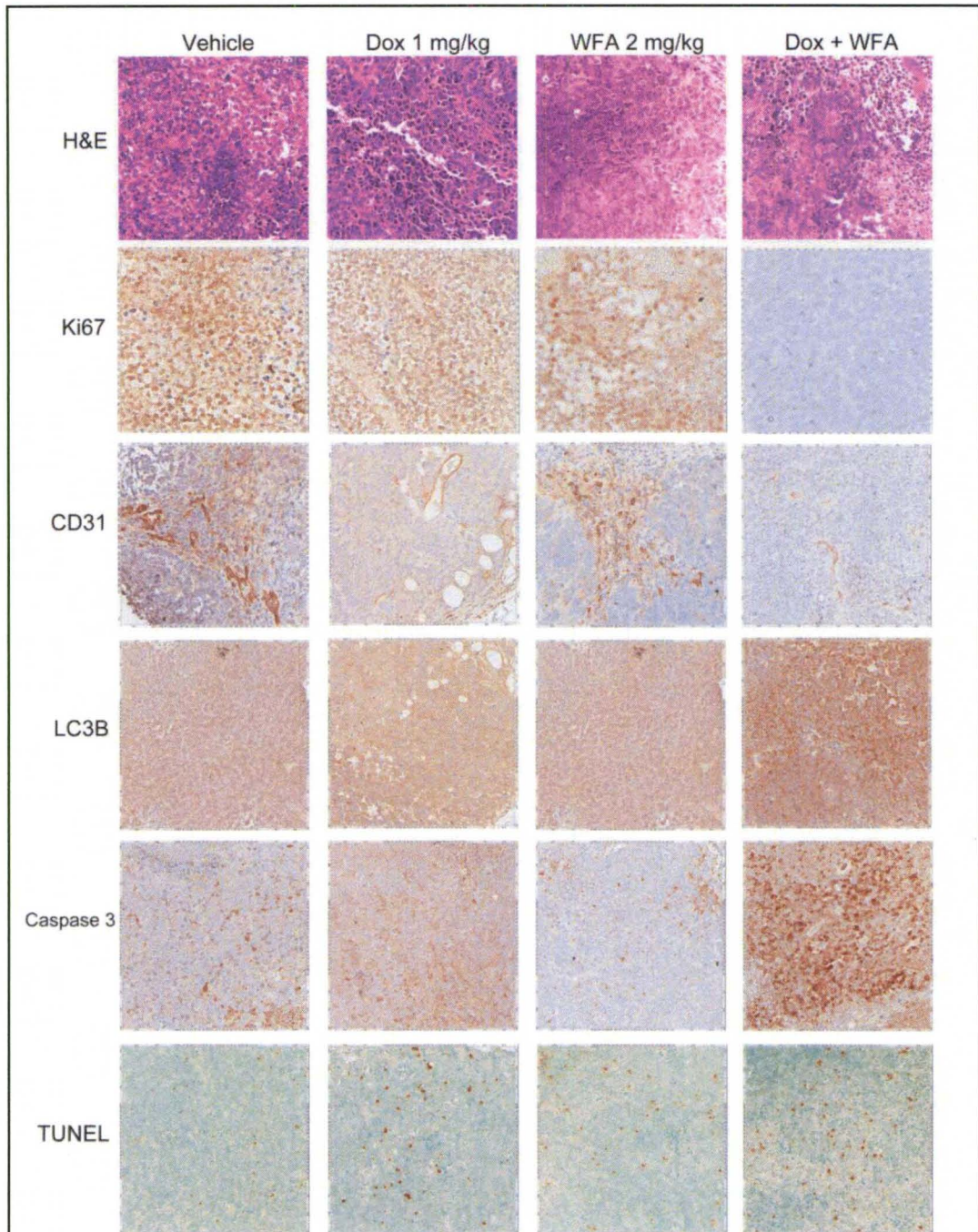


**Figure 34.** Immunohistochemistry of A2780 xenograft tumors. Tumors were fixed in formalin and paraffin embedded. Primary antibody was incubated overnight and developed with DAB (brown color). TUNEL was performed with ApopTag Plus Peroxidase Apoptosis Detection Kit. Images acquired at 20X power.

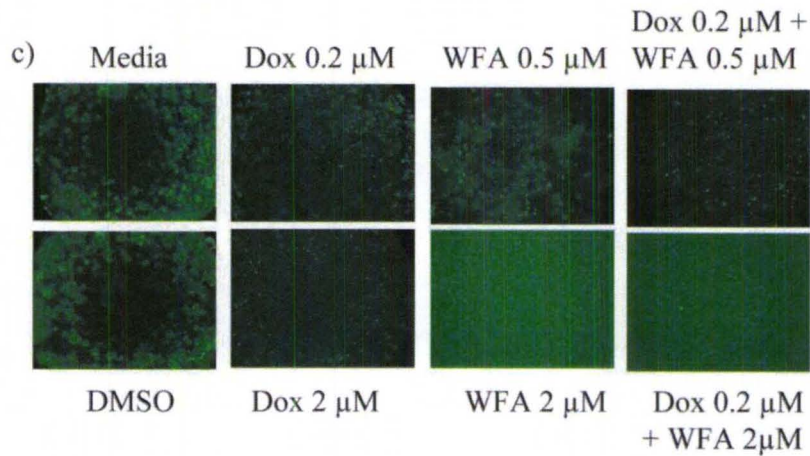
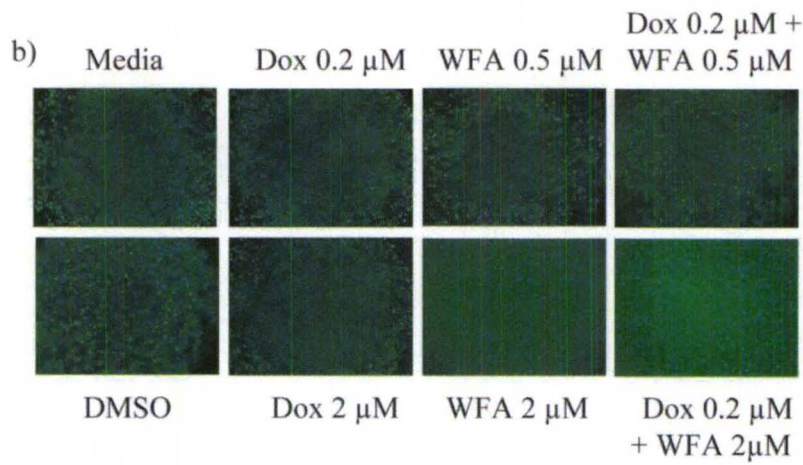
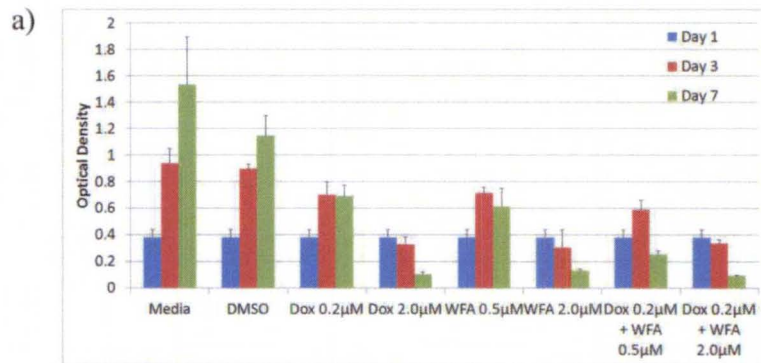


**Figure 35.** 3D tumor growth in HuBioGel generated from A2780 cells and treated with Dox and WFA. a) MTT assay of tumor growth measured at Day 1, 3, and 7 of treatment. Microscopy images of tumor growth at day 3 (b) and day 7 (c).

WFA further enhanced ROS production (Fig. 25-26). As a result of ROS production, DNA damage was increased as assessed by TUNEL assay (Fig. 30), resulting in autophagic cell death (Fig. 31, 32). WFA also reduces *in vivo* tumor growth of human pancreatic [203] and breast cancer cells [172]. Here we show a low dose of WFA alone did not affect *in vitro* or *in vivo* tumor growth, however combining a low dose of WFA with a low dose of Dox resulted in significant inhibition (Fig. 33, 34).

Akt functions as one of the main pro-survival pathways and is frequently dysregulated in cancer [204]. Furthermore, it has been reportedly over expressed in ovarian carcinomas [205]. Dox has been shown to inactivate Akt [165]. The effect of WFA on Akt phosphorylation and apoptosis intrinsic cascade has been well documented. WFA downregulates Notch-1 signaling resulting in the down regulation of p-Akt and subsequent downstream molecules IKK- $\alpha$ , NF- $\kappa$ B, p-p70S6 kinase, and 4E-BP *in vitro* in colon cancer [176]. In ovarian cancer cell lines CAOV3 and SKOV3, WFA resulted in dephosphorylation of Akt in a dose-dependent manner [191]. In our cell line A2780, we found that after 24 hr treatment with Dox increased pAkt while WFA did not (Fig 24). This discrepancy could be due to the p53 status of the cells. A2780 cells have WT p53, while CAOV3 have mutant p53 and SKOV3 are p53-null, which affects expression of *PIK3CA*, the gene that codes for the catalytic subunit p110 $\alpha$  of PI3K which in turn phosphorylates Akt [206]. Furthermore, WFA has been shown to directly affect the ability of NF- $\kappa$ B to bind to DNA [174, 207] and that in turn directly affects transcription of downstream target molecules such as c-FLIP [179], IL-6, IL-8, MCP1, A20, cyclin D, VEGF, MDR-1, and Bfl-1 [207]. In prostate cancer, NF- $\kappa$ B inhibition was dependent of proapoptotic protein prostate apoptosis response-4 (Par-4) [208]. Coupled with down regulation of Bcl-2, colon cancer cells were more sensitive to apoptosis [176]. WFA has also been shown to trigger the intrinsic apoptosis cascade in melanoma with generation of ROS and down regulation of Bcl-2, showing that WFA exhibits the properties of two pharmacological agents used in clinical trial (Disulfiram

and Oblimersen) [175]. In fact, Bcl-2 overexpression in leukemia cells was able to block the induction of apoptosis induced by WFA, demonstrating that Bcl-2 is important for WFA-induced apoptosis [189]. In ovarian cancer, we have been unable to detect endogenous amounts of Bcl-2 and perhaps because of the lack of Bcl-2, the action of WFA preferentially uses autophagy rather than apoptosis to achieve cell death.

Apoptosis was thought to be the principle mechanism by which chemotherapy agents kill cancer cells. Apoptosis is a highly conserved cellular program that eliminates damaged and infected cells and consists of two major pathways: the extrinsic pathway that is mediated by death receptors and the intrinsic pathway that is mediated by the mitochondria. Both pathways lead to activation of caspases, cysteine proteases that cleave different substrates and cause cellular breakdown [209]. However, more recent evidence suggests that anticancer agents also induce other forms of non-apoptotic cell death including necrosis, mitotic catastrophe, autophagy, and senescence [210-212]. Various anticancer chemotherapies have been shown to induce autophagy which cooperates with apoptosis to induce cell death [209, 213-216]. Autophagy enables cells to survive harsh conditions such as chemotherapy treatment and thus conferring resistance [209]. This adaptive response is signified by a high level of autophagy as inhibition of autophagy allows chemotherapy agents to more effectively kill cancer cells in various cell types exposed to various drugs [180]. As such, it is still unclear why autophagy participates in cell death in some instances while preventing it in other, especially since both effects can be observed with the same anticancer compound. However, autophagy can have tumor suppressive functions. One proposed pathway suggests that autophagy eliminates damaged organelles that may produce a high level of ROS and therefore limit chromosomal instability [217]. We found that treatment with Dox + WFA increased ROS production as early as 6 hr of treatment with continued increase production with 24 hr of treatment (Fig. 25, 26). This is consistent with previous reports that both Dox and WFA as a monotherapy both produce ROS [156, 157, 175, 178, 179, 190]. ROS-mediated autophagy has been observed in a number of different carcinoma cell lines [218-220].

Additionally, blocking ROS production with ROS scavengers and antioxidants reduced autophagic cell death in various solid tumors cell lines [220, 221]. Mitochondrial ROS damage the mitochondrial membrane and result in leakage of ROS to the cytosol where they can damage other organelles as well as cause DNA damage and oxidation of amino acids and polyunsaturated fatty acids [222, 223]. Electron microscopy revealed the presence of autophagic vacuoles which we confirmed with Western blot analysis of LC3B (Fig. 31, 32). In order to determine the major pathway of action for Dox + WFA, we analyzed p-Akt levels as well as p70S6K and observed a decrease of both proteins. Cell death was confirmed with Western blot analysis of caspase 3 (Fig. 32). However, we observed no change in the level of Bcl-xL (Fig. 24) or in Annexin-V flow cytometry (Fig. 23). Taken together this suggests that cell death is being mediated principally through autophagy and not apoptosis.

Dox or its derivative Doxil has been used in combination with several other compounds in various cancer types. Doxil used in combination with bevacizumab in patients with recurrent ovarian cancer achieved a 33% response rate [162]. In prostate cancer Dox has been combined with sildenafil, which promoted apoptosis through enhancement of the intrinsic pathway including down regulation of anti-apoptotic proteins Bcl-xL and reduced phosphorylation of pro-apoptotic protein BAD as well as induction of pro-apoptotic protein Bax [163]. This combination therapy resulted in the generation of reactive oxygen species (ROS), but attenuated the cardiotoxic action of doxorubicin. Here, we show that Dox alone affected pBAD<sup>136</sup>, an effect that was attenuated with the addition of WFA (Fig. 24). Chebulagic acid acts synergistically with Dox by increasing the Dox accumulation intracellularly through down regulation of MDR-1 transporter to enhance its cytotoxicity on hepatocellular carcinoma cell line HepG2 and thereby decreasing the necessary dosage of Dox to achieve a reduction in cell proliferation [165]. MDR-1 down regulation was achieved through inactivation of signaling pathways Akt, ERK, p38, JNK, and NF- $\kappa$ B in a COX-2 dependent manner. A synthetic analog of curcumin HO-3867 has also been used in the same manner to achieve a complementary outcome with Dox to increase cancer

cell toxicity without cardiotoxicity [164]. Using this combination therapy, they were able to decrease the concentration of Dox from 50 $\mu$ M to 2.5 $\mu$ M to achieve the same anti-proliferative effect in Dox-resistant breast cancer cell line MCF-7 MDR and showed decreased expression of Bcl-2 and pAkt. This lowered combination treatment resulted in better cardiac performance in treated mice. Combining arsenic trioxide with conventional therapies including Dox reduced cancer stem-like cells in hepatocellular carcinoma cell line and thereby sensitize the carcinoma to chemotherapy agents [224].

In our study, combination of Dox with WFA resulted in cell death not through apoptosis (Annexin V, pBAD<sup>136</sup>, and Bcl-xL), but through ROS-mediated autophagy (p70S6K, LC3B, caspase 3). We have also demonstrated the efficacy of Dox + WFA for the treatment of ovarian cancer *in vivo* using a xenograft tumor model and *in vitro* using a 3D tumor growth model on a human extracellular matrix. In both cases, Dox + WFA combination treatment resulted in inhibited tumor growth. In the case of xenograft tumors, we confirmed this with Ki67 and CD31 immunohistochemistry.



## CHAPTER 4

### CONCLUSIONS

One of the main barriers to developing an ovarian cancer mouse model is the genetic and epigenetic heterogeneous nature of this disease. At least 17 oncogenes (Appendix 1, Table 6), 16 tumor suppressor genes (Appendix 1, Table 7), and 7 signaling pathways have been implicated [225] to be involved in the pathogenesis of ovarian cancer. These pathways include aberrations in cell proliferation, apoptosis, autophagy, and cell adhesion and motility. Oncogene expression alterations utilize various mechanisms including gene amplification, mutation, and overexpression, while tumor suppressor genes are mutated or go through loss of heterozygosity for silencing protein functionality [144]. In addition, the expression of many genes is controlled through epigenetic alterations such as hypomethylation of DNA, promoter methylation, and histone modification [144, 225]. Furthermore, micro-RNAs (mi-RNAs) play a role in controlling RNA stability and thus protein translation, participating in vital pathways including development, differentiation, cell cycle, apoptosis, metabolism, and proliferation [226]. Similarly to genes, mi-RNAs can be classified as oncogenes or suppressor genes depending on the pattern of their alteration. The mi-RNA shown to be overexpressed in ovarian carcinomas are miR-200a, miR-141, miR-200c and miR-200b [225]. On the other hand, miR-199a, miR-140, miR-145 and miR-125b1 were among the most down-regulated mi-RNAs [225]. With so many genetic alterations present in a histologically diverse disease, the challenge of developing a spontaneous reliable model that accurately reflects human EOC becomes immense.

In our transgenic model, TgPPTG, we observed ~20% incidence of localized ovarian cancer in 8 month old mice (Fig. 7) and continued to observe them in 10 month old mice (Fig. 9)

as the CMV promoter seemed to target the ovary and fallopian tube. Since our incidence of ovarian cancer was low, we cross-bred our mice with p53<sup>+/-</sup> mice, as p53 is mutated in 50-70% of human ovarian carcinomas [2, 144]. Using this approach resulted in earlier tumor development than PTTG or p53<sup>+/-</sup> alone (Fig. 13) and increased our incidence of high grade leiomyosarcomas from 7% in p53<sup>+/-</sup> mice to 14% in TgPTTG/p53<sup>+/-</sup>. We also observed tetratocarcinomas in PTTG/p53<sup>-/-</sup> that were not present in p53<sup>-/-</sup> alone. We also noted a significant incidence of cervical carcinomas of 63% in TgPTTG/p53<sup>+/-</sup> at both 8 and 10 months, suggesting that this combination provides an attractive model for studying cervical cancer.

Having a reliable mouse model that accurately reflects the spontaneous human counterpart would provide a monumental amount of knowledge of the genetic alterations that occur during tumorigenesis as well as metastasis. In addition, the model would be a useful method of testing new chemotherapy treatment strategies. But in order for the model to be reliable, several criteria have been suggested: 1) mice must carry the same mutation that occurs in human tumors, 2) mutations should be engineered within the endogenous locus, 3) mutated genes should be silent during embryogenesis and early postnatal development, except in models of inherited pediatric tumors, 4) mutations should be within the specific target tissues in selected cell types, and 5) mutations must occur in a limited number of cells [227]. However, the advantage of using genetically altered mice is the tumor exists in the presence of a competent immune system. As it stands, it is not surprising that the most used model for testing treatment strategies is the xenograft tumor model generated in immune compromised nude mice in which human cancer cells are injected under the skin and form a tumor over time. Xenograft tumors provide a more accurate tumor response to a patient's response despite the lack of a functional immune system [227]. However, these human tumors are generated using a mouse extracellular matrix (ECM), and thus do not accurately reflect patient response. To address this concern, we generated human 3D tumors using human ECM (Hubiogel) to test tumor response to our combination Dox + WFA therapy. As such, we tested the tumor response to substandard dose of chemotherapy agent Dox

in combination with WFA to enhance cell death. 3D *in vitro* and xenograft *in vivo* tumors responded to treatment and showed delayed tumor progression when treated with suboptimal doses of Dox + WFA (Fig. 31, 33). We also demonstrated the mechanism of cell death in response to Dox and WFA was DNA damage and production of ROS (Fig. 23-27) leading to the induction of autophagy and leading to cell death in a caspase-3 dependent manner (Fig. 29, 30).

## REFERENCES

1. Fong MY, Kakar SS: **The role of cancer stem cells and the side population in epithelial ovarian cancer.** *Histol Histopathol* 2010, **25**:113-120.
2. Landen C, Jr, Birrer M, Sood A: **Early events in the pathogenesis of epithelial ovarian cancer.** *J. Clin. Oncol.* 2008, **26**:995-1005.
3. Low JJ, Ilancheran A, Ng JS: **Malignant ovarian germ-cell tumours.** *Best Pract Res Clin Obstet Gynaecol* 2012,
4. Gershenson DM: **Management of early ovarian cancer: germ cell and sex cord-stromal tumors.** *Gynecol Oncol* 1994, **55**:S62-72.
5. Neesham D: **Ovarian cancer screening.** *Austr. Fam. Physician* 2007, **36**:126-128.
6. McCluggage WG: **Morphological subtypes of ovarian carcinoma: a review with emphasis on new developments and pathogenesis.** *Pathology* 2011, **43**:420-32.
7. National Cancer Institute: **Stat Fact Sheet.**  
[\[http://seer.cancer.gov/statfacts/html/ovary.html\]](http://seer.cancer.gov/statfacts/html/ovary.html).
8. American Cancer Society: **What is ovarian cancer? Ovarian cancer overview** October 18, 2010.
9. Seidman JD, Yemelyanova A, Zaino RJ, Kurman RJ: **The fallopian tube-peritoneal junction: a potential site of carcinogenesis.** *Int J Gynecol Pathol* **30**:4-11.
10. Cibula D, Widschwendter M, Zikan M, Dusek L: **Underlying mechanisms of ovarian cancer risk reduction after tubal ligation.** *Acta Obstet Gynecol Scand*
11. Auersperg N, Wong A, Choi K, Kang S, Leung P: **Ovarian surface epithelium: Biology, endocrinology, and pathology.** *Endocr Rev.* 2001, **22**:255-288.
12. Bose C: **Follicle stimulating hormone receptor in ovarian surface epithelium and epithelial ovarian cancer.** *Oncol. Res.* 2008, **17**:231-238.
13. Ivarsson K, Sundfeldt K, Brannstrom M, Hellberg P, Janson PO: **Diverse effects of FSH and LH on proliferation of human ovarian surface epithelial cells.** *Hum Reprod* 2001, **16**:18-23.
14. Wimalasena J, Dostal R, Meehan D: **Gonadotropins, estradiol, and growth factors regulate epithelial ovarian cancer cell growth.** *Gynecol Oncol* 1992, **46**:345-50.
15. Chudecka-Glaz A, Rzepka-Gorska I, Kosmowska B: **Gonadotropin (LH, FSH) levels in serum and cyst fluid in epithelial tumors of the ovary.** *Arch Gynecol Obstet* 2004, **270**:151-6.
16. Irmer G, Burger C, Muller R, Ortmann O, Peter U, Kakar SS, Neill JD, Schulz KD, Emons G: **Expression of the messenger RNAs for luteinizing hormone-releasing hormone (LHRH) and its receptor in human ovarian epithelial carcinoma.** *Cancer Res* 1995, **55**:817-22.
17. Mandai M, Konishi I, Kuroda H, Fukumoto M, Komatsu T, Yamamoto S, Nanbu K, Rao CV, Mori T: **Messenger ribonucleic acid expression of LH/hCG receptor gene in human ovarian carcinomas.** *Eur J Cancer* 1997, **33**:1501-7.
18. Hold G, El-Omar M: **Genetic aspects of inflammation and cancer.** *Biochem. J* 2008, **410**:225-235.
19. Jayshree RS, Sreenivas A, Tessy M, Krishna S: **Cell intrinsic & extrinsic factors in cervical carcinogenesis.** *Indian J Med Res* 2009, **130**:286-95.

20. Grivennikov SI, Greten FR, Karin M: **Immunity, inflammation, and cancer.** *Cell* 140:883-99.
21. Ness R, Grisso J, Cottreau C, Klapper J, Vergona R, Wheeler J, Morgan M, Schlesselman J: **Factors related to inflammation of the ovarian epithelium and risk of ovarian cancer.** *Epidemiology* 2000, 11:111-117.
22. Condeelis J, Pollard JW: **Macrophages: obligate partners for tumor cell migration, invasion, and metastasis.** *Cell* 2006, 124:263-6.
23. Polyak K, Hahn WC: **Roots and stems: stem cells in cancer.** *Nat Med* 2006, 12:296-300.
24. Clarke MF, Dick JE, Dirks PB, Eaves CJ, Jamieson CH, Jones DL, Visvader J, Weissman IL, Wahl GM: **Cancer stem cells--perspectives on current status and future directions: AACR Workshop on cancer stem cells.** *Cancer Res* 2006, 66:9339-44.
25. Dalerba P, Cho RW, Clarke MF: **Cancer stem cells: models and concepts.** *Annu Rev Med* 2007, 58:267-84.
26. Olempska M, Eisenach P, Ammerpohl O, Ungefroren H, Fandrich F, Kalthoff H: **Detection of tumor stem cell markers in pancreatic carcinoma cell lines.** *Hepatobiliary Pancreat. Dis. Int.* 2007, 6:92-97.
27. Davidson B, Zhang Z, Kleinberg L, Li M, Florenes VA, Wang TL, Shih Ie M: **Gene expression signatures differentiate ovarian/peritoneal serous carcinoma from diffuse malignant peritoneal mesothelioma.** *Clin Cancer Res* 2006, 12:5944-50.
28. Zhang S, Balch C, Chan M, Lai H, Matei D, Schilder J, Yan P, Huang T-M, Nephew K: **Identification and characterization of ovarian cancer-initiating cells from primary human tumors.** *Cancer Res.* 2008, 68:4311-4320.
29. Dontu G, El-Ashry D, Wicha M: **Breast cancer, stem/progenitor cells and the estrogen receptor.** *Trends Endocrinol. Metab.* 2004, 15:193-197.
30. Bukovsky A, Caudle M, Svetlikova M, Upadhyaya N: **Origin of germ cells and formation of new primary follicles in adult human ovaries.** *Reprod. Biol. Endocrinol.* 2004, 2:20.
31. Johnson J, Bagley J, Skaznik-Wikiel M, Lee H, Adams G, Niikura Y, Tschudy K, Tilly J, Cortes M, Forkert R, Spitzer T, Iacomini J, Scadden D, Tilly J: **Oocyte generation in adult mammalian ovaries by putative germ cells in bone marrow and peripheral blood.** *Cell* 2005, 122:303-315.
32. Srivastava VK, Nalbantoglu J: **Flow cytometric characterization of the DAOY medulloblastoma cell line for the cancer stem-like phenotype.** *Cytometry A* 2008, 73:940-8.
33. Lapidot T, Sirard C, Vormoor J, Murdoch B, Hoang T, Caceres-Cortes J, Minden M, Paterson B, Caligiuri M, Dick J: **A cell initiating human acute myeloid leukaemia after transplantation into SCID mice.** *Nature* 1994, 367:645-648.
34. Odoux C, Fohrer H, Hoppe T, Guzik L, Stolz D, Lewis D, Gollin S, Gambelin T, Geller D, Lagasse E: **A stochastic model for cancer stem cell origin in metastatic colon cancer.** *Cancer Res.* 2008, 68:6932-6941.
35. Dome B, Timar J, Dobos J, Meszaros L, Raso E, Paku S, Kenessey I, Ostoros G, Magyar M, Ladanyi A, Bogos K, Tovari J: **Identification and clinical significance of circulating endothelial progenitor cells in human non-small cell lung cancer.** *Cancer Res* 2006, 66:7341-7.
36. Bapat S, Mali A, Koppikar C, Kurrey N: **Stem and progenitor-like cells contribute to the aggressive behavior of human epithelial ovarian cancer.** *Cancer Res.* 2005, 65:3025-3029.

37. Al-Hajj M, Wicha MS, Benito-Hernandez A, Morrison SJ, Clarke MF: **Prospective identification of tumorigenic breast cancer cells.** *Proc Natl Acad Sci U S A* 2003, **100**:3983-8.
38. Collins AT, Berry PA, Hyde C, Stower MJ, Maitland NJ: **Prospective identification of tumorigenic prostate cancer stem cells.** *Cancer Res* 2005, **65**:10946-51.
39. Chiba T, Kita K, Zheng YW, Yokosuka O, Saisho H, Iwama A, Nakauchi H, Taniguchi H: **Side population purified from hepatocellular carcinoma cells harbors cancer stem cell-like properties.** *Hepatology* 2006, **44**:240-51.
40. Suetsugu A, Nagaki M, Aoki H, Motohashi T, Kunisada T, Moriwaki H: **Characterization of CD133+ hepatocellular carcinoma cells as cancer stem/progenitor cells.** *Biochem Biophys Res Commun* 2006, **351**:820-4.
41. Singh SK, Clarke ID, Terasaki M, Bonn VE, Hawkins C, Squire J, Dirks PB: **Identification of a cancer stem cell in human brain tumors.** *Cancer Res* 2003, **63**:5821-8.
42. Grichnik JM, Burch JA, Schulteis RD, Shan S, Liu J, Darrow TL, Vervaert CE, Seigler HF: **Melanoma, a tumor based on a mutant stem cell?** *J Invest Dermatol* 2006, **126**:142-53.
43. O'Brien CA, Pollett A, Gallinger S, Dick JE: **A human colon cancer cell capable of initiating tumour growth in immunodeficient mice.** *Nature* 2007, **445**:106-10.
44. Baba T, Convery PA, Matsumura N, Whitaker RS, Kondoh E, Perry T, Huang Z, Bentley RC, Mori S, Fujii S, Marks JR, Berchuck A, Murphy SK: **Epigenetic regulation of CD133 and tumorigenicity of CD133+ ovarian cancer cells.** *Oncogene* 2009, **28**:209-218.
45. Ferrandina G, Bonanno G, Pierelli L, Perillo A, Procoli A, Mariotti A, Corallo M, Martinelli E, Rutella S, Paglia A, Zannoni G, Mancuso S, Scambia G: **Expression of CD133-1 and CD133-2 in ovarian cancer.** *Int. J. Gynecol. Cancer* 2008, **18**:506-514.
46. Bourguignon L, Peyrollier K, Xia W, Gilad E: **Hyaluronan-CD44 Interaction Activates Stem Cell Marker Nanog, Stat-3-mediated MDR1 Gene Expression, and Ankyrin-regulated Multidrug Efflux in Breast and Ovarian Tumor Cells.** *J. Biol. Chem.* 2008, **283**:17635-17651.
47. Alvero AB, Chen R, Fu HH, Montagna M, Schwartz PE, Rutherford T, Silasi DA, Steffensen KD, Waldstrom M, Visintin I, Mor G: **Molecular phenotyping of human ovarian cancer stem cells unravels the mechanisms for repair and chemoresistance.** *Cell Cycle* 2009, **8**:158-66.
48. Kurrey NK, K A, Bapat SA: **Snail and Slug are major determinants of ovarian cancer invasiveness at the transcription level.** *Gynecol Oncol* 2005, **97**:155-65.
49. Godwin AK, Testa JR, Handel LM, Liu Z, Vanderveer LA, Tracey PA, Hamilton TC: **Spontaneous transformation of rat ovarian surface epithelial cells: association with cytogenetic changes and implications of repeated ovulation in the etiology of ovarian cancer.** *J Natl Cancer Inst* 1992, **84**:592-601.
50. Testa JR, Getts LA, Salazar H, Liu Z, Handel LM, Godwin AK, Hamilton TC: **Spontaneous transformation of rat ovarian surface epithelial cells results in well to poorly differentiated tumors with a parallel range of cytogenetic complexity.** *Cancer Res* 1994, **54**:2778-84.
51. Roberts PC, Mottillo EP, Baxa AC, Heng HH, Doyon-Reale N, Gregoire L, Lancaster WD, Rabah R, Schmelz EM: **Sequential molecular and cellular events during neoplastic progression: a mouse syngeneic ovarian cancer model.** *Neoplasia* 2005, **7**:944-56.
52. Greenaway J, Moorehead R, Shaw P, Petrik J: **Epithelial-stromal interaction increases cell proliferation, survival and tumorigenicity in a mouse model of human epithelial ovarian cancer.** *Gynecol Oncol* 2008, **108**:385-94.

53. Urzua U, Frankenberger C, Gangi L, Mayer S, Burkett S, Munroe DJ: **Microarray comparative genomic hybridization profile of a murine model for epithelial ovarian cancer reveals genomic imbalances resembling human ovarian carcinomas.** *Tumour Biol* 2005, **26**:236-44.
54. Janat-Amsbury MM, Yockman JW, Anderson ML, Kieback DG, Kim SW: **Combination of local, non-viral IL12 gene therapy and systemic paclitaxel chemotherapy in a syngeneic ID8 mouse model for human ovarian cancer.** *Anticancer Res* 2006, **26**:3223-8.
55. Janat-Amsbury MM, Yockman JW, Anderson ML, Kieback DG, Kim SW: **Comparison of ID8 MOSE and VEGF-modified ID8 cell lines in an immunocompetent animal model for human ovarian cancer.** *Anticancer Res* 2006, **26**:2785-9.
56. Urzua U, Roby KF, Gangi LM, Cherry JM, Powell JI, Munroe DJ: **Transcriptomic analysis of an in vitro murine model of ovarian carcinoma: functional similarity to the human disease and identification of prospective tumoral markers and targets.** *J Cell Physiol* 2006, **206**:594-602.
57. Roby KF, Taylor CC, Sweetwood JP, Cheng Y, Pace JL, Tawfik O, Persons DL, Smith PG, Terranova PF: **Development of a syngeneic mouse model for events related to ovarian cancer.** *Carcinogenesis* 2000, **21**:585-91.
58. Su F, Kozak KR, Imaizumi S, Gao F, Amneus MW, Grijalva V, Ng C, Wagner A, Hough G, Farias-Eisner G, Anantharamaiah GM, Van Lenten BJ, Navab M, Fogelman AM, Reddy ST, Farias-Eisner R: **Apolipoprotein A-I (apoA-I) and apoA-I mimetic peptides inhibit tumor development in a mouse model of ovarian cancer.** *Proc Natl Acad Sci U S A* **107**:19997-20002.
59. Orsulic S, Li Y, Soslow RA, Vitale-Cross LA, Gutkind JS, Varmus HE: **Induction of ovarian cancer by defined multiple genetic changes in a mouse model system.** *Cancer Cell* 2002, **1**:53-62.
60. Marks F, Furstenberger G, Muller-Decker K: **Tumor promotion as a target of cancer prevention.** *Recent Results Cancer Res* 2007, **174**:37-47.
61. Connolly DC, Bao R, Nikitin AY, Stephens KC, Poole TW, Hua X, Harris SS, Vanderhyden BC, Hamilton TC: **Female mice chimeric for expression of the simian virus 40 TAg under control of the MISiIR promoter develop epithelial ovarian cancer.** *Cancer Res* 2003, **63**:1389-97.
62. Aunoble B, Sanches R, Didier E, Bignon YJ: **Major oncogenes and tumor suppressor genes involved in epithelial ovarian cancer (review).** *Int J Oncol* 2000, **16**:567-76.
63. Tammela J, Odunsi K: **Gene expression and prognostic significance in ovarian cancer.** *Minerva Ginecol.* 2004, **56**:495-502.
64. Hensley H, Quinn BA, Wolf RL, Litwin SL, Mabuchi S, Williams SJ, Williams C, Hamilton TC, Connolly DC: **Magnetic resonance imaging for detection and determination of tumor volume in a genetically engineered mouse model of ovarian cancer.** *Cancer Biol Ther* 2007, **6**:1717-25.
65. Mabuchi S, Altomare DA, Connolly DC, Klein-Szanto A, Litwin S, Hoelzle MK, Hensley HH, Hamilton TC, Testa JR: **RAD001 (Everolimus) delays tumor onset and progression in a transgenic mouse model of ovarian cancer.** *Cancer Res* 2007, **67**:2408-13.
66. Quinn BA, Xiao F, Bickel LE, Martin LP, Hua X, Klein-Szanto AJ, Connolly DC: **Development of a syngeneic mouse model of epithelial ovarian cancer.** *J Ovarian Res* 2010, **3**:24.
67. Flesken-Nikitin A, Choi KC, Eng JP, Shmidt EN, Nikitin AY: **Induction of carcinogenesis by concurrent inactivation of p53 and Rb1 in the mouse ovarian surface epithelium.** *Cancer Res* 2003, **63**:3459-63.

68. Marino S, Vooijs M, van Der Gulden H, Jonkers J, Berns A: **Induction of medulloblastomas in p53-null mutant mice by somatic inactivation of Rb in the external granular layer cells of the cerebellum.** *Genes Dev* 2000, **14**:994-1004.
69. Jonkers J, Meuwissen R, van der Gulden H, Peterse H, van der Valk M, Berns A: **Synergistic tumor suppressor activity of BRCA2 and p53 in a conditional mouse model for breast cancer.** *Nat Genet* 2001, **29**:418-25.
70. Dinulescu DM, Ince TA, Quade BJ, Shafer SA, Crowley D, Jacks T: **Role of K-ras and Pten in the development of mouse models of endometriosis and endometrioid ovarian cancer.** *Nat Med* 2005, **11**:63-70.
71. Johnson L, Mercer K, Greenbaum D, Bronson RT, Crowley D, Tuveson DA, Jacks T: **Somatic activation of the K-ras oncogene causes early onset lung cancer in mice.** *Nature* 2001, **410**:1111-6.
72. Jackson EL, Willis N, Mercer K, Bronson RT, Crowley D, Montoya R, Jacks T, Tuveson DA: **Analysis of lung tumor initiation and progression using conditional expression of oncogenic K-ras.** *Genes Dev* 2001, **15**:3243-8.
73. Tuveson DA, Shaw AT, Willis NA, Silver DP, Jackson EL, Chang S, Mercer KL, Grochow R, Hock H, Crowley D, Hingorani SR, Zaks T, King C, Jacobetz MA, Wang L, Bronson RT, Orkin SH, DePinho RA, Jacks T: **Endogenous oncogenic K-ras(G12D) stimulates proliferation and widespread neoplastic and developmental defects.** *Cancer Cell* 2004, **5**:375-87.
74. Iwanaga K, Yang Y, Raso MG, Ma L, Hanna AE, Thilaganathan N, Moghaddam S, Evans CM, Li H, Cai WW, Sato M, Minna JD, Wu H, Creighton CJ, Demayo FJ, Wistuba, II, Kurie JM: **Pten inactivation accelerates oncogenic K-ras-initiated tumorigenesis in a mouse model of lung cancer.** *Cancer Res* 2008, **68**:1119-27.
75. Podsypanina K, Ellenson LH, Nemes A, Gu J, Tamura M, Yamada KM, Cordon-Cardo C, Catoretto G, Fisher PE, Parsons R: **Mutation of Pten/Mmac1 in mice causes neoplasia in multiple organ systems.** *Proc Natl Acad Sci U S A* 1999, **96**:1563-8.
76. Dourdin N, Schade B, Lesurf R, Hallett M, Munn RJ, Cardiff RD, Muller WJ: **Phosphatase and tensin homologue deleted on chromosome 10 deficiency accelerates tumor induction in a mouse model of ErbB-2 mammary tumorigenesis.** *Cancer Res* 2008, **68**:2122-31.
77. Huang X, Wullschleger S, Shpiro N, McGuire VA, Sakamoto K, Woods YL, McBurnie W, Fleming S, Alessi DR: **Important role of the LKB1-AMPK pathway in suppressing tumorigenesis in PTEN-deficient mice.** *Biochem J* 2008, **412**:211-21.
78. Suzuki A, de la Pompa JL, Stambolic V, Elia AJ, Sasaki T, del Barco Barrantes I, Ho A, Wakeham A, Itie A, Khoo W, Fukumoto M, Mak TW: **High cancer susceptibility and embryonic lethality associated with mutation of the PTEN tumor suppressor gene in mice.** *Curr Biol* 1998, **8**:1169-78.
79. Brachtel EF, Sanchez-Estevéz C, Moreno-Bueno G, Prat J, Palacios J, Oliva E: **Distinct molecular alterations in complex endometrial hyperplasia (CEH) with and without immature squamous metaplasia (squamous morules).** *Am J Surg Pathol* 2005, **29**:1322-9.
80. Wu R, Hendrix-Lucas N, Kuick R, Zhai Y, Schwartz DR, Akyol A, Hanash S, Misek DE, Katabuchi H, Williams BO, Fearon ER, Cho KR: **Mouse model of human ovarian endometrioid adenocarcinoma based on somatic defects in the Wnt/beta-catenin and PI3K/Pten signaling pathways.** *Cancer Cell* 2007, **11**:321-33.
81. Garson K, Macdonald E, Dube M, Bao R, Hamilton TC, Vanderhyden BC: **Generation of tumors in transgenic mice expressing the SV40 T antigen under the control of ovarian-specific promoter 1.** *J Soc Gynecol Investig* 2003, **10**:244-50.
82. Brabletz T, Hlubek F, Spaderna S, Schmalhofer O, Hiendlmeyer E, Jung A, Kirchner T: **Invasion and metastasis in colorectal cancer: epithelial-mesenchymal transition,**



- mesenchymal-epithelial transition, stem cells and beta-catenin.** *Cells Tissues Organs* 2005, **179**:56-65.
83. Larue L, Bellacosa A: **Epithelial-mesenchymal transition in development and cancer: role of phosphatidylinositol 3' kinase/AKT pathways.** *Oncogene* 2005, **24**:7443-54.
  84. Clark-Knowles KV, Garson K, Jonkers J, Vanderhyden BC: **Conditional inactivation of Brcal in the mouse ovarian surface epithelium results in an increase in preneoplastic changes.** *Exp Cell Res* 2007, **313**:133-45.
  85. Hutson R, Ramsdale J, Wells M: **p53 protein expression in putative precursor lesions of epithelial ovarian cancer.** *Histopathology* 1995, **27**:367-71.
  86. Maines-Bandiera SL, Auersperg N: **Increased E-cadherin expression in ovarian surface epithelium: an early step in metaplasia and dysplasia?** *Int J Gynecol Pathol* 1997, **16**:250-5.
  87. Capo-Chichi CD, Smith ER, Yang DH, Roland IH, Vanderveer L, Cohen C, Hamilton TC, Godwin AK, Xu XX: **Dynamic alterations of the extracellular environment of ovarian surface epithelial cells in premalignant transformation, tumorigenicity, and metastasis.** *Cancer* 2002, **95**:1802-15.
  88. Liang S, Yang N, Pan Y, Deng S, Lin X, Yang X, Katsaros D, Roby KF, Hamilton TC, Connolly DC, Coukos G, Zhang L: **Expression of activated PIK3CA in ovarian surface epithelium results in hyperplasia but not tumor formation.** *PLoS ONE* 2009, **4**:e4295.
  89. Wang Z, Melmed S: **Characterization of the murine pituitary tumor transforming gene (PTTG) and its promoter.** *Endocrinology* 2000, **141**:763-71.
  90. Pei L, Melmed S: **Isolation and characterization of a pituitary tumor-transforming gene (PTTG).** *Mol Endocrinol* 1997, **11**:433-41.
  91. Zhang X, Horwitz GA, Prezant TR, Valentini A, Nakashima M, Bronstein MD, Melmed S: **Structure, expression, and function of human pituitary tumor-transforming gene (PTTG).** *Mol Endocrinol* 1999, **13**:156-66.
  92. Kakar SS, Jennes L: **Molecular cloning and characterization of the tumor transforming gene (TUTR1): a novel gene in human tumorigenesis.** *Cytogenet Cell Genet* 1999, **84**:211-6.
  93. Lee IA, Seong C, Choe IS: **Cloning and expression of human cDNA encoding human homologue of pituitary tumor transforming gene.** *Biochem Mol Biol Int* 1999, **47**:891-7.
  94. Zou H, McGarry TJ, Bernal T, Kirschner MW: **Identification of a vertebrate sister-chromatid separation inhibitor involved in transformation and tumorigenesis.** *Science* 1999, **285**:418-22.
  95. Kumada K, Nakamura T, Nagao K, Funabiki H, Nakagawa T, Yanagida M: **Cut1 is loaded onto the spindle by binding to Cut2 and promotes anaphase spindle movement upon Cut2 proteolysis.** *Curr Biol* 1998, **8**:633-41.
  96. Romero F, Multon MC, Ramos-Morales F, Dominguez A, Bernal JA, Pintor-Toro JA, Tortolero M: **Human securin, hPTTG, is associated with Ku heterodimer, the regulatory subunit of the DNA-dependent protein kinase.** *Nucleic Acids Res* 2001, **29**:1300-7.
  97. Hamid T, Kakar SS: **PTTG/securin activates expression of p53 and modulates its function.** *Mol Cancer* 2004, **3**:18.
  98. Yu R, Heaney AP, Lu W, Chen J, Melmed S: **Pituitary tumor transforming gene causes aneuploidy and p53-dependent and p53-independent apoptosis.** *J Biol Chem* 2000, **275**:36502-5.
  99. Cho-Rok J, Yoo J, Jang YJ, Kim S, Chu IS, Yeom YI, Choi JY, Im DS: **Adenovirus-mediated transfer of siRNA against PTTG1 inhibits liver cancer cell growth in vitro and in vivo.** *Hepatology* 2006, **43**:1042-52.

100. Chesnokova V, Zonis S, Rubinek T, Yu R, Ben-Shlomo A, Kovacs K, Wawrowsky K, Melmed S: **Senescence mediates pituitary hypoplasia and restrains pituitary tumor growth.** *Cancer Res* 2007, **67**:10564-72.
101. Chesnokova V, Wong C, Zonis S, Gruszka A, Wawrowsky K, Ren SG, Benschlomo A, Yu R: **Diminished pancreatic beta-cell mass in securin-null mice is caused by beta-cell apoptosis and senescence.** *Endocrinology* 2009, **150**:2603-10.
102. Hamid T, Malik MT, Kakar SS: **Ectopic expression of PTTG1/securin promotes tumorigenesis in human embryonic kidney cells.** *Mol Cancer* 2005, **4**:3.
103. Heaney AP, Horwitz GA, Wang Z, Singson R, Melmed S: **Early involvement of estrogen-induced pituitary tumor transforming gene and fibroblast growth factor expression in prolactinoma pathogenesis.** *Nat Med* 1999, **5**:1317-21.
104. McCabe CJ, Boelaert K, Tannahill LA, Heaney AP, Stratford AL, Khaira JS, Hussain S, Sheppard MC, Franklyn JA, Gittoes NJ: **Vascular endothelial growth factor, its receptor KDR/Flk-1, and pituitary tumor transforming gene in pituitary tumors.** *J Clin Endocrinol Metab* 2002, **87**:4238-44.
105. Kim CS, Ying H, Willingham MC, Cheng SY: **The pituitary tumor-transforming gene promotes angiogenesis in a mouse model of follicular thyroid cancer.** *Carcinogenesis* 2007, **28**:932-9.
106. Minematsu T, Suzuki M, Sanno N, Takekoshi S, Teramoto A, Osamura RY: **PTTG overexpression is correlated with angiogenesis in human pituitary adenomas.** *Endocr Pathol* 2006, **17**:143-53.
107. Kim DS, Franklyn JA, Boelaert K, Eggo MC, Watkinson JC, McCabe CJ: **Pituitary tumor transforming gene (PTTG) stimulates thyroid cell proliferation via a vascular endothelial growth factor/kinase insert domain receptor/inhibitor of DNA binding-3 autocrine pathway.** *J Clin Endocrinol Metab* 2006, **91**:4603-11.
108. Kim DS, Franklyn JA, Stratford AL, Boelaert K, Watkinson JC, Eggo MC, McCabe CJ: **Pituitary tumor-transforming gene regulates multiple downstream angiogenic genes in thyroid cancer.** *J Clin Endocrinol Metab* 2006, **91**:1119-28.
109. Dameron KM, Volpert OV, Tainsky MA, Bouck N: **Control of angiogenesis in fibroblasts by p53 regulation of thrombospondin-1.** *Science* 1994, **265**:1582-4.
110. Malik MT, Kakar SS: **Regulation of angiogenesis and invasion by human Pituitary tumor transforming gene (PTTG) through increased expression and secretion of matrix metalloproteinase-2 (MMP-2).** *Mol Cancer* 2006, **5**:61.
111. Lengauer C, Kinzler KW, Vogelstein B: **Genetic instabilities in human cancers.** *Nature* 1998, **396**:643-9.
112. Kim D, Pemberton H, Stratford AL, Boelaert K, Watkinson JC, Lopes V, Franklyn JA, McCabe CJ: **Pituitary tumour transforming gene (PTTG) induces genetic instability in thyroid cells.** *Oncogene* 2005, **24**:4861-6.
113. Tsai SJ, Lin SJ, Cheng YM, Chen HM, Wing LY: **Expression and functional analysis of pituitary tumor transforming gene-1 [corrected] in uterine leiomyomas.** *J Clin Endocrinol Metab* 2005, **90**:3715-23.
114. Tang MH, Tan J, Cui FL: **[Expression of pituitary tumor transforming gene in human renal clear cell carcinoma and its significance].** *Nan Fang Yi Ke Da Xue Xue Bao* **30**:1712-4.
115. Heaney AP, Melmed S: **Pituitary tumour transforming gene: a novel factor in pituitary tumour formation.** *Baillieres Best Pract Res Clin Endocrinol Metab* 1999, **13**:367-80.
116. El-Naggar SM, Malik MT, Kakar SS: **Small interfering RNA against PTTG: a novel therapy for ovarian cancer.** *Int J Oncol* 2007, **31**:137-43.

117. Honda S, Hayashi M, Kobayashi Y, Ishikawa Y, Nakagawa K, Tsuchiya E: **A role for the pituitary tumor-transforming gene in the genesis and progression of non-small cell lung carcinomas.** *Anticancer Res* 2003, **23**:3775-82.
118. Chamaon K, Kirches E, Kanakis D, Braeuninger S, Dietzmann K, Mawrin C: **Regulation of the pituitary tumor transforming gene by insulin-like-growth factor-I and insulin differs between malignant and non-neoplastic astrocytes.** *Biochem Biophys Res Commun* 2005, **331**:86-92.
119. Kanakis D, Kirches E, Mawrin C, Dietzmann K: **Promoter mutations are no major cause of PTTG overexpression in pituitary adenomas.** *Clin Endocrinol (Oxf)* 2003, **58**:151-5.
120. Kakar SS, Malik MT: **Suppression of lung cancer with siRNA targeting PTTG.** *Int J Oncol* 2006, **29**:387-95.
121. Wang Z, Yu R, Melmed S: **Mice lacking pituitary tumor transforming gene show testicular and splenic hypoplasia, thymic hyperplasia, thrombocytopenia, aberrant cell cycle progression, and premature centromere division.** *Mol Endocrinol* 2001, **15**:1870-9.
122. Fraenkel M, Caloyeras J, Ren SG, Melmed S: **Sex-steroid milieu determines diabetes rescue in pttg-null mice.** *J Endocrinol* 2006, **189**:519-28.
123. Yu R, Cruz-Soto M, Li Calzi S, Hui H, Melmed S: **Murine pituitary tumor-transforming gene functions as a securin protein in insulin-secreting cells.** *J Endocrinol* 2006, **191**:45-53.
124. Jacks T, Fazeli A, Schmitt EM, Bronson RT, Goodell MA, Weinberg RA: **Effects of an Rb mutation in the mouse.** *Nature* 1992, **359**:295-300.
125. Hu N, Gutschmann A, Herbert DC, Bradley A, Lee WH, Lee EY: **Heterozygous Rb-1 delta 20/+mice are predisposed to tumors of the pituitary gland with a nearly complete penetrance.** *Oncogene* 1994, **9**:1021-7.
126. Chesnokova V, Kovacs K, Castro AV, Zonis S, Melmed S: **Pituitary hypoplasia in Pttg-/- mice is protective for Rb+/- pituitary tumorigenesis.** *Mol Endocrinol* 2005, **19**:2371-9.
127. Kaneshige M, Kaneshige K, Zhu X, Dace A, Garrett L, Carter TA, Kazlauskaitė R, Pankratz DG, Wynshaw-Boris A, Refetoff S, Weintraub B, Willingham MC, Barlow C, Cheng S: **Mice with a targeted mutation in the thyroid hormone beta receptor gene exhibit impaired growth and resistance to thyroid hormone.** *Proc Natl Acad Sci U S A* 2000, **97**:13209-14.
128. Abbud RA, Takumi I, Barker EM, Ren SG, Chen DY, Wawrowsky K, Melmed S: **Early multipotential pituitary focal hyperplasia in the alpha-subunit of glycoprotein hormone-driven pituitary tumor-transforming gene transgenic mice.** *Mol Endocrinol* 2005, **19**:1383-91.
129. Donangelo I, Gutman S, Horvath E, Kovacs K, Wawrowsky K, Mount M, Melmed S: **Pituitary tumor transforming gene overexpression facilitates pituitary tumor development.** *Endocrinology* 2006, **147**:4781-91.
130. El-Naggar SM, Malik MT, Martin A, Moore JP, Proctor M, Hamid T, Kakar SS: **Development of cystic glandular hyperplasia of the endometrium in Mullerian inhibitory substance type II receptor-pituitary tumor transforming gene transgenic mice.** *J Endocrinol* 2007, **194**:179-91.
131. Aiba-Masago S, Baba S, Li RY, Shinmura Y, Kosugi I, Arai Y, Nishimura M, Tsutsui Y: **Murine cytomegalovirus immediate-early promoter directs astrocyte-specific expression in transgenic mice.** *Am J Pathol* 1999, **154**:735-43.
132. Joshi M, Keith Pittman H, Haisch C, Verbanac K: **Real-time PCR to determine transgene copy number and to quantitate the biolocalization of adoptively transferred cells from EGFP-transgenic mice.** *Biotechniques* 2008, **45**:247-58.

133. Jacks T, Remington L, Williams BO, Schmitt EM, Halachmi S, Bronson RT, Weinberg RA: **Tumor spectrum analysis in p53-mutant mice.** *Curr Biol* 1994, **4**:1-7.
134. The Jackson Laboratory: **FVB.129S2(B6)-Trp53<sup>tm1Tyj</sup>/J.**
135. Koutsaki M, Zaravinos A, Spandidos DA: **Modern Trends into the Epidemiology and Screening of Ovarian Cancer. Genetic Substrate of the Sporadic Form.** *Pathol Oncol Res* 2011,
136. Merritt MA, Cramer DW: **Molecular pathogenesis of endometrial and ovarian cancer.** *Cancer Biomark* 2011, **9**:287-305.
137. Braem MG, Schouten LJ, Peeters PH, den Brandt PA, Onland-Moret NC: **Genetic susceptibility to sporadic ovarian cancer: A systematic review.** *Biochim Biophys Acta* 2011, **1816**:132-46.
138. Carvalho J, Carvalho F: **Is Chlamydia-infected tubal fimbria the origin of ovarian cancer?** *Medical Hypotheses* 2008, **71**:690-693.
139. Karst AM, Drapkin R: **The new face of ovarian cancer modeling: better prospects for detection and treatment.** *F1000 Med Rep* 2011, **3**:22.
140. Levanon K, Crum C, Drapkin R: **New insights into the pathogenesis of serous ovarian cancer and its clinical impact.** *J Clin Oncol* 2008, **26**:5284-93.
141. Dubeau L: **The cell of origin of ovarian epithelial tumours.** *Lancet Oncol* 2008, **9**:1191-7.
142. Seidman JD, Yemelyanova A, Zaino RJ, Kurman RJ: **The fallopian tube-peritoneal junction: a potential site of carcinogenesis.** *Int J Gynecol Pathol* 2011, **30**:4-11.
143. Sell S: **On the stem cell origin of cancer.** *Am J Pathol* 2010, **176**:2584-494.
144. Bast RC, Jr., Hennessy B, Mills GB: **The biology of ovarian cancer: new opportunities for translation.** *Nat Rev Cancer* 2009, **9**:415-28.
145. Jackson EL, Olive KP, Tuveson DA, Bronson R, Crowley D, Brown M, Jacks T: **The differential effects of mutant p53 alleles on advanced murine lung cancer.** *Cancer Res* 2005, **65**:10280-8.
146. Morton JP, Timpson P, Karim SA, Ridgway RA, Athineos D, Doyle B, Jamieson NB, Oien KA, Lowy AM, Brunton VG, Frame MC, Evans TR, Sansom OJ: **Mutant p53 drives metastasis and overcomes growth arrest/senescence in pancreatic cancer.** *Proc Natl Acad Sci U S A* 2010, **107**:246-51.
147. Seidler B, Schmidt A, Mayr U, Nakhai H, Schmid RM, Schneider G, Saur D: **A Cre-loxP-based mouse model for conditional somatic gene expression and knockdown in vivo by using avian retroviral vectors.** *Proc Natl Acad Sci U S A* 2008, **105**:10137-42.
148. Doyle B, Morton JP, Delaney DW, Ridgway RA, Wilkins JA, Sansom OJ: **p53 mutation and loss have different effects on tumorigenesis in a novel mouse model of pleomorphic rhabdomyosarcoma.** *J Pathol* 2010, **222**:129-37.
149. National Cancer Institute: **A snapshot of ovarian cancer.** September 2010.
150. Mangioni C, Bolis G, Pecorelli S, Bragman K, Epis A, Favalli G, Gambino A, Landoni F, Presti M, Torri W, et al.: **Randomized trial in advanced ovarian cancer comparing cisplatin and carboplatin.** *J Natl Cancer Inst* 1989, **81**:1464-71.
151. Alberts DS, Green S, Hannigan EV, O'Toole R, Stock-Novack D, Anderson P, Surwit EA, Malvly VK, Nahhas WA, Jolles CJ: **Improved therapeutic index of carboplatin plus cyclophosphamide versus cisplatin plus cyclophosphamide: final report by the Southwest Oncology Group of a phase III randomized trial in stages III and IV ovarian cancer.** *J Clin Oncol* 1992, **10**:706-17.
152. Parmar MK, Ledermann JA, Colombo N, du Bois A, Delaloye JF, Kristensen GB, Wheeler S, Swart AM, Qian W, Torri V, Floriani I, Jayson G, Lamont A, Trope C: **Paclitaxel plus platinum-based chemotherapy versus conventional platinum-based chemotherapy in women with relapsed ovarian cancer: the ICON4/AGO-OVAR-2.2 trial.** *Lancet* 2003, **361**:2099-106.

153. Pfisterer J, Ledermann JA: **Management of platinum-sensitive recurrent ovarian cancer.** *Semin Oncol* 2006, **33**:S12-6.
154. Piccart MJ, Bertelsen K, Stuart G, Cassidy J, Mangioni C, Simonsen E, James K, Kaye S, Vergote I, Blom R, Grimshaw R, Atkinson R, Swenerton K, Trope C, Nardi M, Kaern J, Tumolo S, Timmers P, Roy JA, Lhoas F, Lidvall B, Bacon M, Birt A, Andersen J, Zee B, Paul J, Pecorelli S, Baron B, McGuire W: **Long-term follow-up confirms a survival advantage of the paclitaxel-cisplatin regimen over the cyclophosphamide-cisplatin combination in advanced ovarian cancer.** *Int J Gynecol Cancer* 2003, **13 Suppl 2**:144-8.
155. Matsuo K, Lin YG, Roman LD, Sood AK: **Overcoming platinum resistance in ovarian carcinoma.** *Expert Opin Investig Drugs* 2010, **19**:1339-54.
156. Singal PK, Li T, Kumar D, Danelisen I, Iliskovic N: **Adriamycin-induced heart failure: mechanism and modulation.** *Mol Cell Biochem* 2000, **207**:77-86.
157. Carvalho C, Santos RX, Cardoso S, Correia S, Oliveira PJ, Santos MS, Moreira PI: **Doxorubicin: the good, the bad and the ugly effect.** *Curr Med Chem* 2009, **16**:3267-85.
158. Gordon AN, Fleagle JT, Guthrie D, Parkin DE, Gore ME, Lacave AJ: **Recurrent epithelial ovarian carcinoma: a randomized phase III study of pegylated liposomal doxorubicin versus topotecan.** *J Clin Oncol* 2001, **19**:3312-22.
159. Gordon AN, Tonda M, Sun S, Rackoff W: **Long-term survival advantage for women treated with pegylated liposomal doxorubicin compared with topotecan in a phase 3 randomized study of recurrent and refractory epithelial ovarian cancer.** *Gynecol Oncol* 2004, **95**:1-8.
160. Ferrandina G, Ludovisi M, Lorusso D, Pignata S, Breda E, Savarese A, Del Medico P, Scaltriti L, Katsaros D, Priolo D, Scambia G: **Phase III trial of gemcitabine compared with pegylated liposomal doxorubicin in progressive or recurrent ovarian cancer.** *J Clin Oncol* 2008, **26**:890-6.
161. Pujade-Lauraine E, Wagner U, Aavall-Lundqvist E, GebSKI V, Heywood M, Vasey PA, Volgger B, Vergote I, Pignata S, Ferrero A, Sehouli J, Lortholary A, Kristensen G, Jackisch C, Joly F, Brown C, Le Fur N, du Bois A: **Pegylated liposomal Doxorubicin and Carboplatin compared with Paclitaxel and Carboplatin for patients with platinum-sensitive ovarian cancer in late relapse.** *J Clin Oncol* **28**:3323-9.
162. Kudoh K, Takano M, Kouta H, Kikuchi R, Kita T, Miyamoto M, Watanabe A, Kato M, Goto T, Kikuchi Y: **Effects of bevacizumab and pegylated liposomal doxorubicin for the patients with recurrent or refractory ovarian cancers.** *Gynecol Oncol* 2011, **122**:233-7.
163. Das A, Durrant D, Mitchell C, Mayton E, Hoke NN, Salloum FN, Park MA, Qureshi I, Lee R, Dent P, Kukreja RC: **Sildenafil increases chemotherapeutic efficacy of doxorubicin in prostate cancer and ameliorates cardiac dysfunction.** *Proc Natl Acad Sci U S A* 2010, **107**:18202-7.
164. Dayton A, Selvendiran K, Meduru S, Khan M, Kuppusamy M, Naidu S, Kalai T, Hideg K, Kuppusamy P: **Amelioration of doxorubicin-induced cardiotoxicity by an anticancer-antioxidant dual-function compound, HO-3867.** *J Pharmacol Exp Ther* 2011,
165. Achari C, Reddy GV, Reddy TC, Reddanna P: **Chebulagic Acid Synergizes the Cytotoxicity of Doxorubicin in Human Hepatocellular Carcinoma Through COX-2 Dependant Modulation of MDR-1.** *Med Chem* 2011,
166. Manov I, Pollak Y, Broneshter R, Iancu TC: **Inhibition of doxorubicin-induced autophagy in hepatocellular carcinoma Hep3B cells by sorafenib - the role of extracellular signal-regulated kinase counteraction.** *FEBS J* 2011, **278**:3494-507.

167. Cagnol S, Chambard JC: **ERK and cell death: mechanisms of ERK-induced cell death--apoptosis, autophagy and senescence.** *FEBS J* 277:2-21.
168. Manov I, Bashenko Y, Eliaz-Wolkowicz A, Mizrahi M, Liran O, Iancu TC: **High-dose acetaminophen inhibits the lethal effect of doxorubicin in HepG2 cells: the role of P-glycoprotein and mitogen-activated protein kinase p44/42 pathway.** *J Pharmacol Exp Ther* 2007, **322**:1013-22.
169. Fugner A: **[Inhibition of immunologically induced inflammation by the plant steroid withaferin A].** *Arzneimittelforschung* 1973, **23**:932-5.
170. Rasool M, Varalakshmi P: **Immunomodulatory role of Withania somnifera root powder on experimental induced inflammation: An in vivo and in vitro study.** *Vascul Pharmacol* 2006, **44**:406-10.
171. Scartezzini P, Speroni E: **Review on some plants of Indian traditional medicine with antioxidant activity.** *J Ethnopharmacol* 2000, **71**:23-43.
172. Stan SD, Hahm ER, Warin R, Singh SV: **Withaferin A causes FOXO3a- and Bim-dependent apoptosis and inhibits growth of human breast cancer cells in vivo.** *Cancer Res* 2008, **68**:7661-9.
173. Mohan R, Hammers HJ, Bargagna-Mohan P, Zhan XH, Herbstritt CJ, Ruiz A, Zhang L, Hanson AD, Conner BP, Rougas J, Pribluda VS: **Withaferin A is a potent inhibitor of angiogenesis.** *Angiogenesis* 2004, **7**:115-22.
174. Oh JH, Kwon TK: **Withaferin A inhibits tumor necrosis factor-alpha-induced expression of cell adhesion molecules by inactivation of Akt and NF-kappaB in human pulmonary epithelial cells.** *Int Immunopharmacol* 2009, **9**:614-9.
175. Mayola E, Gallerne C, Esposti DD, Martel C, Pervaiz S, Larue L, Debuire B, Lemoine A, Brenner C, Lemaire C: **Withaferin A induces apoptosis in human melanoma cells through generation of reactive oxygen species and down-regulation of Bcl-2.** *Apoptosis* 2011,
176. Koduru S, Kumar R, Srinivasan S, Evers MB, Damodaran C: **Notch-1 inhibition by Withaferin-A: a therapeutic target against colon carcinogenesis.** *Mol Cancer Ther* 9:202-10.
177. Stan SD, Zeng Y, Singh SV: **Ayurvedic medicine constituent withaferin a causes G2 and M phase cell cycle arrest in human breast cancer cells.** *Nutr Cancer* 2008, **60 Suppl 1**:51-60.
178. Malik F, Kumar A, Bhushan S, Khan S, Bhatia A, Suri KA, Qazi GN, Singh J: **Reactive oxygen species generation and mitochondrial dysfunction in the apoptotic cell death of human myeloid leukemia HL-60 cells by a dietary compound withaferin A with concomitant protection by N-acetyl cysteine.** *Apoptosis* 2007, **12**:2115-33.
179. Lee TJ, Um HJ, Min do S, Park JW, Choi KS, Kwon TK: **Withaferin A sensitizes TRAIL-induced apoptosis through reactive oxygen species-mediated up-regulation of death receptor 5 and down-regulation of c-FLIP.** *Free Radic Biol Med* 2009, **46**:1639-49.
180. Kondo Y, Kanzawa T, Sawaya R, Kondo S: **The role of autophagy in cancer development and response to therapy.** *Nat Rev Cancer* 2005, **5**:726-34.
181. Mortimore GE, Miotto G, Venerando R, Kadowaki M: **Autophagy.** *Subcell Biochem* 1996, **27**:93-135.
182. Seglen PO, Berg TO, Blankson H, Fengsrud M, Holen I, Stromhaug PE: **Structural aspects of autophagy.** *Adv Exp Med Biol* 1996, **389**:103-11.
183. Paglin S, Lee NY, Nakar C, Fitzgerald M, Plotkin J, Deuel B, Hackett N, McMahill M, Sphicas E, Lampen N, Yahalom J: **Rapamycin-sensitive pathway regulates mitochondrial membrane potential, autophagy, and survival in irradiated MCF-7 cells.** *Cancer Res* 2005, **65**:11061-70.

184. Sini P, James D, Chresta C, Guichard S: **Simultaneous inhibition of mTORC1 and mTORC2 by mTOR kinase inhibitor AZD8055 induces autophagy and cell death in cancer cells.** *Autophagy* 2010, **6**:
185. Tee AR, Proud CG: **DNA-damaging agents cause inactivation of translational regulators linked to mTOR signalling.** *Oncogene* 2000, **19**:3021-31.
186. Funderburk SF, Wang QJ, Yue Z: **The Beclin 1-VPS34 complex--at the crossroads of autophagy and beyond.** *Trends Cell Biol* 2010, **20**:355-62.
187. Kaur K, Widodo N, Nagpal A, Kaul SC, Wadhwa R: **Sensitization of human cancer cells to anti-cancer drugs of leaf extract of Ashwagandha (Lash).** *Tiss Cult Res Commun* 2007, **26**:193-199.
188. Gewirtz DA: **A critical evaluation of the mechanisms of action proposed for the antitumor effects of the anthracycline antibiotics adriamycin and daunorubicin.** *Biochem Pharmacol* 1999, **57**:727-41.
189. Oh JH, Lee TJ, Kim SH, Choi YH, Lee SH, Lee JM, Kim YH, Park JW, Kwon TK: **Induction of apoptosis by withaferin A in human leukemia U937 cells through down-regulation of Akt phosphorylation.** *Apoptosis* 2008, **13**:1494-504.
190. Yang ES, Choi MJ, Kim JH, Choi KS, Kwon TK: **Withaferin A enhances radiation-induced apoptosis in Caki cells through induction of reactive oxygen species, Bcl-2 downregulation and Akt inhibition.** *Chem Biol Interact* 2011, **190**:9-15.
191. Zhang X, Samadi AK, Roby KF, Timmermann B, Cohen MS: **Inhibition of cell growth and induction of apoptosis in ovarian carcinoma cell lines CaOV3 and SKOV3 by natural withanolide Withaferin A.** *Gynecol Oncol* 2012, **124**:606-12.
192. Plas DR, Thompson CB: **Akt activation promotes degradation of tuberin and FOXO3a via the proteasome.** *J Biol Chem* 2003, **278**:12361-6.
193. Pene F, Claessens YE, Muller O, Viguie F, Mayeux P, Dreyfus F, Lacombe C, Bouscary D: **Role of the phosphatidylinositol 3-kinase/Akt and mTOR/P70S6-kinase pathways in the proliferation and apoptosis in multiple myeloma.** *Oncogene* 2002, **21**:6587-97.
194. Burgering BM, Coffey PJ: **Protein kinase B (c-Akt) in phosphatidylinositol-3-OH kinase signal transduction.** *Nature* 1995, **376**:599-602.
195. Johnson SM, Gulhati P, Rampy BA, Han Y, Rychahou PG, Doan HQ, Weiss HL, Evers BM: **Novel expression patterns of PI3K/Akt/mTOR signaling pathway components in colorectal cancer.** *J Am Coll Surg* **210**:767-76, 776-8.
196. Fan J, Xu G, Nagel DJ, Hua Z, Zhang N, Yin G: **A model of ischemia and reperfusion increases JNK activity, inhibits the association of BAD and 14-3-3, and induces apoptosis of rabbit spinal neurocytes.** *Neurosci Lett* 2010, **473**:196-201.
197. Tsang WP, Chau SP, Kong SK, Fung KP, Kwok TT: **Reactive oxygen species mediate doxorubicin induced p53-independent apoptosis.** *Life Sci* 2003, **73**:2047-58.
198. McCord JM, Fridovich I: **Superoxide dismutase. An enzymic function for erythrocyte hemocuprein (hemocuprein).** *J Biol Chem* 1969, **244**:6049-55.
199. Gaetani GF, Ferraris AM, Rolfo M, Mangerini R, Arena S, Kirkman HN: **Predominant role of catalase in the disposal of hydrogen peroxide within human erythrocytes.** *Blood* 1996, **87**:1595-9.
200. Kabeya Y, Mizushima N, Ueno T, Yamamoto A, Kirisako T, Noda T, Kominami E, Ohsumi Y, Yoshimori T: **LC3, a mammalian homologue of yeast Apg8p, is localized in autophagosomal membranes after processing.** *EMBO J* 2000, **19**:5720-8.
201. Seales EC, Belousova R, Singh R: **3D tumorigenesis and angiogenesis assay models: predicting better functional and preclinical endpoints.** *Drug discovery+ international* 2007, **16**-19.
202. Thaiparambil JT, Bender L, Ganesh T, Kline E, Patel P, Liu Y, Tighiouart M, Vertino PM, Harvey RD, Garcia A, Marcus AI: **Withaferin A inhibits breast cancer invasion**

- and metastasis at sub-cytotoxic doses by inducing vimentin disassembly and serine 56 phosphorylation. *Int J Cancer***
203. Yu Y, Hamza A, Zhang T, Gu M, Zou P, Newman B, Li Y, Gunatilaka AA, Zhan CG, Sun D: **Withaferin A targets heat shock protein 90 in pancreatic cancer cells.** *Biochem Pharmacol* 2010, **79**:542-51.
  204. Dillon RL, Muller WJ: **Distinct biological roles for the akt family in mammary tumor progression.** *Cancer Res* 70:4260-4.
  205. Sun M, Wang G, Paciga JE, Feldman RI, Yuan ZQ, Ma XL, Shelley SA, Jove R, Tsiichlis PN, Nicosia SV, Cheng JQ: **AKT1/PKBalpha kinase is frequently elevated in human cancers and its constitutive activation is required for oncogenic transformation in NIH3T3 cells.** *Am J Pathol* 2001, **159**:431-7.
  206. Astanache A, Arenillas D, Wasserman WW, Leung PC, Dunn SE, Davies BR, Mills GB, Auersperg N: **Mechanisms underlying p53 regulation of PIK3CA transcription in ovarian surface epithelium and in ovarian cancer.** *J Cell Sci* 2008, **121**:664-74.
  207. Suttana W, Mankhetkorn S, Poompimon W, Palagani A, Zhokhov S, Gerlo S, Haegeman G, Berghe WV: **Differential chemosensitization of P-glycoprotein overexpressing K562/Adr cells by withaferin A and Siamois polyphenols.** *Mol Cancer* 9:99.
  208. Srinivasan S, Ranga RS, Burikhanov R, Han SS, Chendil D: **Par-4-dependent apoptosis by the dietary compound withaferin A in prostate cancer cells.** *Cancer Res* 2007, **67**:246-53.
  209. Notte A, Leclere L, Michiels C: **Autophagy as a mediator of chemotherapy-induced cell death in cancer.** *Biochem Pharmacol* 2011, **82**:427-34.
  210. Ricci MS, Zong WX: **Chemotherapeutic approaches for targeting cell death pathways.** *Oncologist* 2006, **11**:342-57.
  211. Portugal J, Bataller M, Mansilla S: **Cell death pathways in response to antitumor therapy.** *Tumori* 2009, **95**:409-21.
  212. Al-Ejeh F, Kumar R, Wiegman A, Lakhani SR, Brown MP, Khanna KK: **Harnessing the complexity of DNA-damage response pathways to improve cancer treatment outcomes.** *Oncogene* 2010, **29**:6085-98.
  213. Cosse JP, Rommelaere G, Ninane N, Arnould T, Michiels C: **BNIP3 protects HepG2 cells against etoposide-induced cell death under hypoxia by an autophagy-independent pathway.** *Biochem Pharmacol* 2010, **80**:1160-9.
  214. Lee SB, Tong SY, Kim JJ, Um SJ, Park JS: **Caspase-independent autophagic cytotoxicity in etoposide-treated CaSki cervical carcinoma cells.** *DNA Cell Biol* 2007, **26**:713-20.
  215. Lin CI, Whang EE, Donner DB, Du J, Lorch J, He F, Jiang X, Price BD, Moore FD, Jr., Ruan DT: **Autophagy induction with RAD001 enhances chemosensitivity and radiosensitivity through Met inhibition in papillary thyroid cancer.** *Mol Cancer Res* 2010, **8**:1217-26.
  216. Lambert LA, Qiao N, Hunt KK, Lambert DH, Mills GB, Meijer L, Keyomarsi K: **Autophagy: a novel mechanism of synergistic cytotoxicity between doxorubicin and roscovitine in a sarcoma model.** *Cancer Res* 2008, **68**:7966-74.
  217. Mathew R, Kongara S, Beaudoin B, Karp CM, Bray K, Degenhardt K, Chen G, Jin S, White E: **Autophagy suppresses tumor progression by limiting chromosomal instability.** *Genes Dev* 2007, **21**:1367-81.
  218. Hatchi E, Rodier G, Sardet C, Le Cam LO: **E4F1 dysfunction results in autophagic cell death in myeloid leukemic cells.** *Autophagy* 2011, **7**:
  219. Donadelli M, Dando I, Zaniboni T, Costanzo C, Dalla Pozza E, Scupoli MT, Scarpa A, Zappavigna S, Marra M, Abbruzzese A, Bifulco M, Caraglia M, Palmieri M: **Gemcitabine/cannabinoid combination triggers autophagy in pancreatic cancer cells through a ROS-mediated mechanism.** *Cell Death Dis* 2011, **2**:e152.



220. Lee YJ, Kim NY, Suh YA, Lee C: **Involvement of ROS in Curcumin-induced Autophagic Cell Death.** *Korean J Physiol Pharmacol* 2011, **15**:1-7.
221. Kuo CC, Liu TW, Chen LT, Shiah HS, Wu CM, Cheng YT, Pan WY, Liu JF, Chen KL, Yang YN, Chen SN, Chang JY: **Combination of arsenic trioxide and BCNU synergistically triggers redox-mediated autophagic cell death in human solid tumors.** *Free Radic Biol Med* 2011,
222. Ravikumar B, Sarkar S, Davies JE, Futter M, Garcia-Arencibia M, Green-Thompson ZW, Jimenez-Sanchez M, Korolchuk VI, Lichtenberg M, Luo S, Massey DC, Menzies FM, Moreau K, Narayanan U, Renna M, Siddiqi FH, Underwood BR, Winslow AR, Rubinsztein DC: **Regulation of mammalian autophagy in physiology and pathophysiology.** *Physiol Rev* 2010, **90**:1383-435.
223. Mazure NM, Pouyssegur J: **Hypoxia-induced autophagy: cell death or cell survival?** *Curr Opin Cell Biol* 2010, **22**:177-80.
224. Tomuleasa C, Soritau O, Fischer-Fodor E, Pop T, Susman S, Mosteanu O, Petrushev B, Aldea M, Acalovschi M, Irimie A, Kacso G: **Arsenic trioxide plus cisplatin/interferon alpha-2b/doxorubicin/capecitabine combination chemotherapy for unresectable hepatocellular carcinoma.** *Hematol Oncol Stem Cell Ther* **4**:60-66.
225. Asadollahi R, Hyde CA, Zhong XY: **Epigenetics of ovarian cancer: from the lab to the clinic.** *Gynecol Oncol* 2010, **118**:81-7.
226. Flynt AS, Lai EC: **Biological principles of microRNA-mediated regulation: shared themes amid diversity.** *Nat Rev Genet* 2008, **9**:831-42.
227. Richmond A, Su Y: **Mouse xenograft models vs GEM models for human cancer therapeutics.** *Dis Model Mech* 2008, **1**:78-82.
228. Fong MY, Kakar SS: **Ovarian cancer mouse models: A summary of current models and their limitations.** *J Ovarian Res* 2009, **2**:12.
229. Lee MH, Surh YJ: **eEF1A2 as a putative oncogene.** *Ann N Y Acad Sci* 2009, **1171**:87-93.

## APPENDIX I

**Table 1.** Summary of promoters and targeted genes in epithelial ovarian cancer transgenic mouse models. Adapted from [228]. RCAS = replication-competent avian leukosis viral-derived vectors, MISIIR = Müllerian Inhibitory Substance Type II Receptor, AdCre = adenovirus carrying Cre recombinase, FSHR = follicle stimulating hormone receptor.

<b>Authors</b>	<b>Promoter</b>	<b>Targeted gene</b>	<b>Tumorigenesis</b>
Orsulic et al. (2002)	keratin-5, RCAS	TVA, p53 <sup>-/-</sup> , oncogenes	Yes
Connolly et al. (2003)	MISIIR	SV40 TAg	Yes
Flesken-Nikkita et al. (2003)	AdCre	p53 <sup>-/-</sup> & Rb <sup>-/-</sup>	Yes
Dinulescu et al. (2005)	AdCre	K-Ras & PTEN <sup>-/-</sup>	Yes
Wu et al. (2007)	AdCre	PTEN <sup>-/-</sup> & APC <sup>-/-</sup>	Yes
Chondankar et al. (2005)	FSHR	Cre, BRCA1 <sup>-/-</sup>	No
Clark-Knowles et al. (2007)	AdCre	BRCA1 <sup>Δ5-13</sup>	No
El-Naggar et al. (2007)	MISIIR	PTTG	No
Liang et al. (2009)	MISIIR	PIK3CA	No

**Table 2.** Breeding summary of TgPTTG founders. WT = wildtype

<b>Founder</b>	<b>Number of breedings</b>	<b>Total number of offspring</b>	<b>Number of positive mice in F1</b>
71282	5 (WT)	37	None
71288	5 (WT)	43	None
71305	5 (WT)	42	16
71309	4 (WT)	36	19

**Table 3.** PTTG transgenic (TgPTTG) mice group assignments. Number in columns indicate number of mice assigned to each group.

Age	Female Control	Male Control	Female TgPTTG	Male TgPTTG	TgPTTG Died
1 month					1
3 months					1
4 months	2	1	2	2	1
6 months	1	1	3	3	3
8 months	4	7	15	9	1
10 months	6	7	10	10	
12 months	10	10	11	11	

**Table 4.** p53<sup>mut</sup> mice group assignments. Number in columns indicate number of mice assigned to each group. Genotype of mice as indicated in parentheses next to numbers.

Age	Female p53 <sup>mut</sup>	Male p53 <sup>mut</sup>	Died
9 weeks		2 (-/-)	2
3 months	2 (-/-)	9 (-/-), 2 (+/-)	11
4 months		1 (-/-)	1
5 months	1 (+/-)		1
7 months	2 (+/-)	1 (+/-)	1
8 months	6 (+/-)	6 (+/-)	
10 months	2 (+/-)	3 (+/-)	
11 months	9 (+/-)	14 (+/-)	

**Table 5.** Group assignments of TgPTTG/p53<sup>mut</sup> crossbred mice. Number in columns indicate number of mice assigned to each group. Genotype of mice as indicated in parentheses next to numbers.

Age	Female TgPTTG/p53 <sup>mut</sup>	Male TgPTTG/p53 <sup>mut</sup>	Died
7 weeks		1 (-/-)	1
9 weeks		1 (+/-)	1
3 months	1 (-/-)		1
4 months	1 (+/-)		1
8 months	9 (+/-)	8 (+/-)	
10 months	8 (+/-)	6 (+/-)	

**Table 6.** Oncogenes involved in the pathogenesis of ovarian cancer, adapted from [2, 144] with contributions from [229]. AURKA, aurora kinase A; CCNE1, cyclin E1; eEF1A, eukaryotic elongation factor 1- $\alpha$ ; EGFR, epidermal growth factor receptor; FGF1, fibroblast growth factor 1; IGFR, insulin-like growth factor receptor; PIK3CA, PI3K catalytic subunit; PRKCI, protein kinase C.

Oncogene	% Gene Amplification	% Overexpressed	% Mutated	Function
<i>AKT1</i>	NA	12-18%		Inhibits apoptosis
<i>AKT2</i>	12-27%	12%		Cytoplasmic serine–threonine protein kinase
<i>AURKA</i>	10-15%	48%		Nuclear serine–threonine protein kinase
<i>B-RAF</i>			30-50%	Promotes growth through MAPK
<i>CCNE1</i>	12-36%	42-63%		Cyclin
<i>eEF1A</i>		30%		Protein elongation factor
<i>EGFR1</i>	11-20%	9-28%	<1%	Protein tyrosine kinase growth factor receptor
<i>ERBB2</i>	6-11%	4-12%		Protein tyrosine kinase growth factor receptor
<i>FGF1</i>		51%		Growth factor for cancer and angiogenesis
<i>IGFR</i>		21-25%		Promotes growth
<i>K-RAS</i>	5%	30-52%	2-24%	Cytoplasmic GTPase
<i>MYC</i>	20%	41-66%		Transcription factor
<i>NOTCH3</i>	20-21%	62%		Cell surface growth factor receptor
<i>PIK3CA</i>	9-11%	32%	8-12%	Cytoplasmic lipid kinase
<i>PRKCI</i>	44%	78%		Cytoplasmic serine–threonine protein kinase
<i>RAB25</i>	54%	80-89%		Cytoplasmic GTPase and apical vesicle trafficking
<i>Src</i>		80-90%		Promotes growth, angiogenesis, and survival

**Table 7.** Tumor suppressor genes dysregulated in ovarian cancer, adapted from [144]. ARL11, ADP-ribosylation factor-like 11; DAB2, disabled homologue 2; DLEC1, deleted in lung and esophageal cancer 1; DSB, double strand break; EGF, epidermal growth factor; GPI, glycosylphosphatidylinositol; GRB2, growth factor receptor-bound 2; ILK, integrin-linked kinase; JNK, JUN N-terminal kinase; LOH, loss of heterozygosity; OPCML, opioid-binding protein/cell adhesion molecule- like; PEG3, paternally expressed 3; PLAGL1, pleiomorphic adenoma gene-like 1; RPS6KA2; ribosomal protein S6 kinase 2; SPARC, secreted protein, acidic, cysteine-rich; STAT3, signal transducer and activator of transcription 3; TNF, tumour necrosis factor-; TPA, tissue plasminogen activator.

Gene	% of cancers downregulated or inactivated	Mechanism of downregulation	Function
<i>ARHI(DIRAS3)</i>	60%	Imprinting; LOH; promoter methylation; transcription downregulated by E2F1 and E2F4	26 kDa GTPase; inhibits proliferation and motility; induces autophagy and dormancy; upregulates p21; inhibits cyclin D1, PI3K, Ras–Mapk signalling and STAT3
<i>ARL11</i>	62%	Promoter methylation	ADP ribosylation factor; induces apoptosis
<i>BRCA1</i>	6-8%	Mutation; LOH	E3 ubiquitin ligase that participates directly in repair of DNA DSBs through homologous recombination; regulates ABL1; induces p53, androgen receptor, oestrogen receptor and MYC
<i>BRCA2</i>	3-6%	Mutation; LOH	Binds RAD51 during repair of DNA double strand breaks
<i>DAB2 (DOC2)</i>	58-85%	Transcription	Binds GRB2, preventing Ras and MAPK activation; prevents FOS induction and decreases ILK activity; contributes to anoikis; inhibits proliferation; inhibits anchorage-independent growth and tumorigenicity
<i>DLEC1</i>	73%	Promoter hypermethylation and histone hypoacetylation	Inhibits anchorage-dependent growth
<i>OPCML</i>	56-83%	Promoter methylation; LOH; mutation	GPI-anchored IgLON family member; induces aggregation;

			inhibits proliferation and tumorigenicity
<i>PEG3</i>	75%	Imprinting; LOH; promoter methylation; transcription	Induces p53-dependent apoptosis
<i>PLAGL1 (LOT1)</i>	39%	Imprinting; LOH; transcription downregulated by EGF and TPA	Inhibits proliferation and tumorigenicity
<i>PTEN</i>	20%	Promoter methylation; LOH; mutation	decreases proliferation, migration, and survival through Akt; decreases cyclin D; increases p27
<i>RASSF1A</i>	60%	Hypermethylation	Inhibits proliferation and tumorigenicity; interacts with Ras inhibiting and downregulating cyclin D and signaling through JNK; stabilizes microtubules; regulates spindle checkpoint; regulates CD95- and TNF -induced apoptosis
<i>RPS6KA2</i>	64%	Monoallelic expression in ovary; LOH	Inhibits growth; induces apoptosis; decreases Erk phosphorylation and cyclin D1; increases p21 and p27
<i>SPARC</i>	70-90%	Transcription	Binds GRB2, preventing Ras and MAPK activation; prevents FOS induction and decreases ILK activity; contributes to anoikis; inhibits proliferation; inhibits anchorage-independent growth and tumorigenicity
<i>TP53</i>	50-70%	Mutation	Induces p21 leading to cell cycle arrest and promotion of DNA stability; induces apoptosis
<i>WWOX</i>	30-49%	LOH; mutation	Decreases anchorage-independent growth and tumorigenicity; mouse homologue required for apoptosis

## CURRICULUM VITAE

**Miranda Yen Fong**  
[eurynome\\_13@yahoo.com](mailto:eurynome_13@yahoo.com)  
[mvfong01@exchange.louisville.edu](mailto:mvfong01@exchange.louisville.edu)

**Contact Information:** 123 E. Tenny Ave., Apt 2  
Louisville, KY 40214  
(775) 342-3265

**DOB:** Reno, NV – January 13, 1982

### EDUCATION:

- Bachelor of Science – University of Nevada, Reno  
Enrollment Dates: 8/2000 – 5/2004  
Duel Major: Veterinary Medicine and Animal Science  
GPA: 3.94
- University of Louisville, Department of Physiology and Biophysics  
Enrollment Dates: 8/2007 – 5/2012  
Degree: PhD  
GPA: 3.966

### PUBLICATIONS

#### Research Articles

1. Cobine CA, **Fong M**, Hamilton R, Keef KD. 2007. Species dependent differences in the actions of sympathetic nerves and noradrenaline in the internal anal sphincter. *Neurogastroenterol Motil* 19: 937-945.
2. McDonnell B, Hamilton R, **Fong M**, Ward SM, Keef KD. 2008. Functional evidence for purinergic inhibitory neuromuscular transmission in the mouse internal anal sphincter. *Am J Physiol Gastrointest Liver Physiol* 294: G1041-1051.
3. **Fong MY**, McDunn J, Kakar SS. 2011. Identification of metabolites in the normal ovary and their transformation in primary and metastatic ovarian cancer. *PLoS ONE* 6(5): e19963. Epub 2011 May 19.

4. Shah PP, **Fong MY**, and Kakar SS. 2011. PTTG induces EMT through integrin  $\alpha_3\beta_1$  focal adhesion kinase signaling in lung cancer cells. *Oncogene*. doi: 10.1038/nc.2011.488. [Epub ahead of print]
5. **Fong MY**, Farghaly H, and Kakar SS. 2012. PTTG transgenic mice develop adenocarcinoma of the ovary and fallopian tube. *PLoS ONE*. Submitted.
6. **Fong MY**, Jin S, Gupta R, Rane M, and Kakar SS. 2012. Withaferin A enhances the therapeutic effect of doxorubicin through ROS-mediated autophagy in ovarian cancer. *Lancet Oncology*. Submitted.

### Review Articles

7. **Fong MY** and Kakar SS. 2009. Ovarian cancer mouse models: a summary of current models and their limitations. Review. *J Ovarian Res* 2: 12.
8. **Fong MY** and Kakar SS. 2010. The role of cancer stem cells and the side population in epithelial ovarian cancer. Review. *Histol Histopathol* 25: 113-120.

### Abstracts

9. **Fong MY**, Rane MJ, and Kakar SS. PTTG-induced Akt1 activation in epithelial ovarian cancer. Research! Louisville, University of Louisville, 2009.
10. **Fong MY**, Shah PP, Farghaly HI, and Kakar SS. Pituitary tumor-transforming gene (PTTG) transgenic mice as a model for epithelial ovarian cancer. Institute for Molecular Diversity and Drug Design (IMD<sup>3</sup>) Symposium, University of Louisville, 2010.
11. **Fong MY**, Shah PP, Farghaly HI, and Kakar SS. Pituitary tumor-transforming gene (PTTG) transgenic mice as a model for epithelial ovarian cancer. Research! Louisville, University of Louisville, 2010.
12. **Fong MY** and Kakar SS. Identification of metabolites in the normal ovary and its transformation in primary and metastatic ovarian cancer. American Association of Cancer Research (AACR), 2011.
13. **Fong MY**, Gupta R, and Kakar SS. Withaferin A enhances the killing effect of doxorubicin through autophagy in ovarian cancer. Brown Cancer Center Retreat, University of Louisville, 2011.
14. **Fong MY**, Jin S, Gupta R, Rane M, and Kakar SS. Withaferin A enhances the therapeutic effect of doxorubin through autophagy in ovarian cancer. IMD<sup>3</sup> Spring Symposium, University of Louisville, 2012.
15. Kakar SS, Gupta R, and **Fong MY**. Withaferin A enhances the therapeutic effect of doxorubicin through autophagy in ovarian cancer. AACR, 2012.



## **Book Chapter**

16. **Fong MY**, McDunn J, Kakar SS. 2012. Mass spectrometry for the identification of global metabolomics in ovarian carcinomas. In: Malek AM, Tchernitsa O (eds) *Ovarian Cancer: Methods and Protocols*. Humana Press.

## **SEMINARS**

1. PTTG-induced Akt1 activation in epithelial ovarian cancer. Department of Physiology and Biophysics, University of Louisville, 2009.
2. PTTG in the tumorigenesis of ovarian cancer. Department of Physiology and Biophysics, University of Louisville, 2010.
3. Identification of metabolites in the normal ovary and their transformation in primary and metastatic ovarian cancer. Department of Medicine, Endocrinology, University of Louisville, 2011; 1<sup>st</sup> Annual Houston Workshop at Texas Medical Center, Metabolon, Inc., 2011; Institute for Molecular Diversity and Drug Design (IMD<sup>3</sup>) Fall Fest, University of Louisville, 2011.
4. Withaferin A enhances the killing effect of doxorubicin in ovarian cancer. Department of Physiology and Biophysics, University of Louisville, 2011.

## **PATENTS**

U. S. Provisional Patent Application Serial No. 61/478,333. Methods For Primary And Metastatic Cancer Diagnosis And Treatment. ULRF Ref. No. 11008. C/M Code: UN024/UN182

## **SERVICES**

Referee for *Journal of Ovarian Research*, 2009-2010  
Referee for *Cellular and Molecular Life Sciences*, 2010  
Referee for *PLoS ONE*, 2011

Chair for Institute for Molecular Diversity and Drug Design (IMD<sup>3</sup>) Fall Fest, 2009

## **ACADEMIC AND PROFESSIONAL HONORS:**

Silver Scholar, 1999  
Millennium Scholarship, 2000-2004  
Alumni Association Class of '42 Scholarship, 2002  
Clara Field Stadtmuller Scholarship, 2002  
MacMillian Agriculture Scholarship, 2002-2003  
Wiegand, E.L. Agriculture Scholarship, 2002-2003  
Dust Case Scholarship, 2002  
Knights Templar Education Scholarship, 2003  
General Undergrad Grant in Aid, 2003  
University of Louisville, Fellowship, 2007-2009  
Sponsored Research Tuition Award, 2011

Travel Award, IMD<sup>3</sup> and Department of Physiology, 2011  
Dissertation Completion Award, 2012

Memberships in professional societies:  
Golden Key International Honor Society